analytical chemistry

pubs.acs.org/ac

Article

A Selective, Class-Specific Aptamer for Fentanyl Analog Screening

Linlin Wang,‖ Gabriel Castro,‖ Obtin Alkhamis, Madhu Sudhana Reddy Gangireddy, Konstantin V. Bukhryakov, Nelson R. Vinueza, and Yi Xiao*

Cite This: https://doi.org/10.1021/acs.analchem.6c03173

Read Online

ACCESS | Metrics & More | Article Recommendations | Supporting Information

ABSTRACT: Fentanyl and its analogs pose considerable dangers to public health and safety, and the development of simple tests that can detect these harmful substances accurately and rapidly could control their currently unchecked spread and thereby safeguard lives. Here, we use systematic evolution of ligands by exponential enrichment (SELEX) to isolate an aptamer that displays a rare blend of high affinity and broad cross-reactivity to 139 fentanyl analogs, alongside excellent specificity against nontarget interferents, including cutting agents, adulterants, and other drugs of abuse. We demonstrate the utility of this aptamer by developing a single-step colorimetric dye-displacement assay that can detect diverse fentanyl analogs within seconds with a simple mix-and-read format. The analog coverage of our assay rivals that of commercial immunoassay-based fentanyl tests while offering better specificity against substances that commonly trigger false positives in those tests, such as diphenhydramine, lidocaine, and methamphetamine. Our findings indicate that aptamers may be fundamentally better suited for achieving broad but specific detection of structurally related classes of molecules relative to other commonly used receptors, such as antibodies, due to their excellent and controllable binding properties, among other benefits, including low cost and high stability.

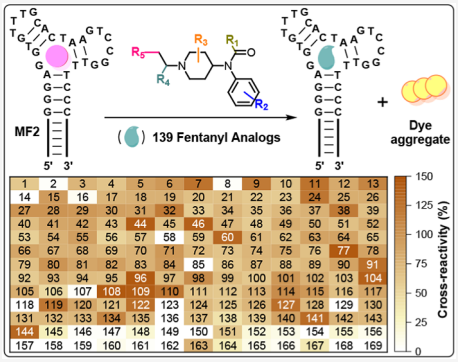

INTRODUCTION

Fentanyl is a potent synthetic opioid that is currently at the center of one of the most severe drug crises in US history.[1] As a primary contributor to the nearly 80,000 opioid overdose deaths in 2023,[2] fentanyl poses a major threat to public health and safety. However, there are also potent analogs of this drug that are even more dangerous, with lethal dosages that are one to two orders of magnitude lower than fentanyl.[3] As such, there is an urgent need for a testing platform that can effectively screen for fentanyl and its analogs in a cost-effective, rapid, and effective manner. Lateral-flow immunoassay test strips have been used to detect fentanyl and several analogs with excellent sensitivity,[4] and one commercialized fentanyl test strip achieves particularly broad coverage for fentanyl analogs, with the capacity to detect 134 out of 169 known analogs.[5] However, this test often yields false positives in response to innocuous substances such as lidocaine and diphenhydramine as well as drugs of abuse like methamphetamine.[6,7] Therefore, there is room for the development of tests that can deliver broad cross-reactivity to fentanyl analogs while also achieving greater specificity against interferent molecules.

Aptamers could potentially achieve the appropriate balance of promiscuity and specificity in this context. These are single-stranded nucleic acid oligonucleotides that are selected from randomized libraries via systematic evolution of ligands by exponential enrichment (SELEX) to bind specific targets with high affinity.[8,9] Because aptamer selection is performed *in vitro*, one can exercise precise control over the selection process to enrich aptamers with bespoke binding properties. For instance, aptamers can be generated that have high affinity for a single target and reject interferents that differ even by a single functional group,[10] or which achieve broad cross-reactivity to an entire class of targets with similar structures.[11] Indeed, one can even select aptamers that balance both characteristics, as we have demonstrated recently by isolating aptamers that recognize a variety of synthetic cathinones, another family of structurally related psychoactive substances, but do not respond to structurally similar interferents.[12]

We here utilized library-immobilized SELEX to isolate a new DNA aptamer that pairs high affinity and broad cross-reactivity to fentanyl and its analogs with exquisite specificity against interferents—even those that are similar in structure to fentanyl. Using this new aptamer, we develop a colorimetric dye-displacement assay that can detect fentanyl and its analogs in a rapid (seconds), simple, specific, and sensitive manner. The analog coverage of this aptamer rivals that of the commercial lateral-flow immunoassay, recognizing 139 out of 169 fentanyl analogs, while also achieving superior specificity, with minimal response to various structurally similar

Received: May 12, 2026
Revised: July 15, 2026
Accepted: July 16, 2026

interferents including diphenhydramine, lidocaine, or methamphetamine. Such a test will be valuable in several real-world contexts, including the detection of these drugs in field settings for forensic analysis as well as for harm reduction purposes, hence improving public health and safety.

MATERIALS AND METHODS

Chemicals

(±)-cis-3-Methyl fentanyl HCl, morphine sulfate hydrate, codeine phosphate hydrate, heroin HCl, (+)-pseudoephedrine HCl, methadone HCl, cis-tramadol HCl, lorazepam, and (+)-methamphetamine HCl were purchased as drug standards from Cayman Chemicals. Acetaminophen, benzocaine, caffeine, cocaine HCl, chlorpromazine HCl, diphenhydramine HCl, D-lactose, D-mannitol, lidocaine HCl monoydrate, procaine HCl, metamizole sodium salt, sodium dodecyl sulfate (SDS), Triton X-100, quinine hemisulfate monohydrate, and xylazine HCl were sourced from Sigma-Aldrich. Noscapine HCl was obtained from Tokyo Chemical Industry, and papaverine HCl from Acros Organics. Molecular biology-grade water was obtained from Corning, while ultrapure water (18.2 MΩ·cm resistivity) was produced from a Milli-Q EQ 7000 water purification system. Exonuclease I (Exo I, *E. coli*, 20 U/μL) and T5 exonuclease (T5 Exo, 10 U/μL) were purchased from New England Biolabs. GoTaq Hot Start Colorless Master Mix was purchased from Promega. The QIAquick PCR purification kit was obtained from Qiagen. SYBR Gold, streptavidin-coated agarose resin (capacity: 1−3 mg biotinylated BSA/mL resin), 0.5 M EDTA solution (pH 8.0), and formamide were purchased from Thermo Fisher Scientific. Fentanyl Analog Screening Kits (Item Nos. 9003237 and 9003380) were obtained from Cayman Chemicals. Unless otherwise specified, all other fentanyl analogs were purchased from Cayman Chemicals and other chemicals were obtained from Sigma-Aldrich.

Oligonucleotides

All DNA oligonucleotides were purchased from Integrated DNA Technologies (IDT) (see Supporting Information (SI), Table S1 for sequences). DNA sequences used for SELEX were HPLC purified, whereas high-throughput sequencing primers were purchased in PAGE-purified form. Other oligonucleotides were purchased at standard desalt purity. All oligonucleotides were dissolved in molecular biology-grade water and their concentration was determined using a NanoDrop 2000 spectrophotometer (Thermo Fisher Scientific).

Isolation of Aptamers for (±)-cis-3-Methyl Fentanyl via Library-Immobilized SELEX

We followed a previously reported protocol for aptamer isolation,[13] with detailed steps outlined in SI, Table S2. Briefly, the library was mixed with a biotinylated complementary DNA (cDNA15-bio) at a molar ratio of 1:5 in 250 μL of selection buffer (10 mM Tris-HCl (pH 7.4), 20 mM NaCl, 0.5 mM $MgCl_2$). The mixture was heated to 95 °C for 10 min and then slowly cooled to room temperature over 20 min to facilitate DNA hybridization. A 800 μL microgravity column was prepared by filling it with 300 μL of molecular biology-grade water, followed by vacuum degassing for 1 min. 250 μL of streptavidin-coated agarose resin was then loaded into the column and washed five times with 250 μL of selection buffer. The hybridized library-cDNA complex solution was added to the column to immobilize the library onto the agarose resin. To maximize library loading, the eluate was collected and passed through the column three times. The bead column was then washed 10−30 times with 250 μL of selection buffer to remove nonspecifically or weakly bound sequences. For target elution, 250 μL of (±)-cis-3-methyl fentanyl dissolved in selection buffer was introduced into the column; the target-binding sequences were displaced from the bead-attached biotinylated cDNA and collected. This target elution step was repeated three times, and the eluates were combined and purified using a 3 kDa MWCO filter (Millipore) to remove (±)-cis-3-methyl fentanyl and salts and concentrate the solution to <100 μL. The enriched library was then PCR-amplified using Promega GoTaq Hot Start Colorless Master Mix (2×) with 1 μM forward primer (FP) and 1 μM biotinylated reverse primer (RP-bio) utilizing a Bio-Rad C1000 thermal cycler with the following conditions: 2 min at 95 °C; 9−13 cycles of 95 °C for 15 s, 58 °C for 30 s, and 72 °C for 45 s; 5 min at 72 °C. The resulting amplicons were converted to single-stranded DNA using streptavidin-agarose resin and 0.2 M NaOH as a denaturant. The obtained DNA concentration was measured with a NanoDrop 2000 spectrophotometer. From Round 2 onward, Counter-SELEX was introduced to eliminate sequences that were bound to interfering molecules; after the initial selection buffer wash, 250 μL of counter-targets dissolved in selection buffer was added to the column three times, and the eluates were discarded. Following counter-SELEX, the column was washed 10−40 times with selection buffer to remove residual counter-targets and nonspecific binders. Positive selection with (±)-cis-3-methyl fentanyl was then performed as described above. The affinity and specificity of the final-round SELEX pool for (±)-cis-3-methyl fentanyl were determined using a gel elution assay.[12]

High-Throughput Sequencing (HTS)

Rounds 7 and 13 were subjected to Illumina-based high-throughput sequencing by Azenta Life Sciences. To prepare SELEX pools for sequencing, 100 nM of each pool was PCR-amplified using 1 μM of customized forward and reverse primers containing partial Illumina adapters. The PCR conditions were as follows: 95 °C for 2 min; 10 cycles of 95 °C for 15 s, 58 °C for 30 s, and 72 °C for 45 s; followed by a final extension at 72 °C for 5 min. The PCR products were purified using the QIAquick PCR purification kit, and the successful addition of adapters was confirmed via denaturing polyacrylamide gel electrophoresis. Twenty-five μL of each purified pool (concentration = 20 ng/μL) was submitted for sequencing, yielding approximately 400,000−900,000 reads per pool. Prior to analysis, complementary sequences were converted to their reverse complements using the FASTX-Toolkit and merged with the forward reads. The constant region was removed using Cutadapt,[14] and sequences containing "N" nucleotides within the random region were discarded. Finally, FASTAptamer[15] was used to determine the abundance of each unique sequence and its enrichment fold between Rounds 7 and 13. Summary HTS statistics are provided in SI, Table S3.

Dye-Displacement Experiments Utilizing X-732−91C and MF2-Mut

All dye-displacement experiments were performed in selection buffer containing 2% (v/v) DMSO, 0.01% (w/v) SDS, and 0.001% (v/v) Triton X-100. We began by optimizing the aptamer-dye ratio for the dye-displacement assay. First, 99 μL of varying concentrations of MF2-mut (final concentrations: 0−18 μM) were prepared in 1.01× buffer and incubated for 5 min. Next, 1 μL of 100× X-732−91C dissolved in DMSO (final concentration: 3 μM) was added to the aptamer solution and mixed by inverting rapidly to form dye-aptamer complexes. 75 μL of the mixed solution was transferred to a 384-well transparent plate, and the absorbance spectra between 300−900 nm (5 nm step size) were measured using a Tecan Spark microplate reader.

To generate a calibration curve for (±)-cis-3-methyl fentanyl and fentanyl, we first prepared MF2-mut in selection buffer (final concentration: 9 μM) and incubated for 5 min. Next, 100× X-732−91C dissolved in pure DMSO (final concentration: 3 μM dye) was added to solution and mixed by vortexing at low speed to form aptamer-dye complexes. Then, 99 μL of the dye-aptamer complex solution was mixed with 1 μL of 100× (±)-cis-3-methyl fentanyl or 100× fentanyl in DMSO (final concentrations: 0, 0.25, 0.5, 1.0, 1.5, 2.0, 5.0, 10, 25, 50, 100, or 200 μM). A series of aptamer-free control samples were prepared in the same manner. 75 μL of each sample was transferred to a 384-well flat-bottom transparent plate and absorbance spectra were measured as above using a Tecan Spark microplate reader. For data analysis, the area under the curve of the monomer peak (500−650 nm) and aggregate peak (400−500 nm) were determined using OriginPro software. R, the ratio between the areas

https://doi.org/10.1021/acs.analchem.6c03173
Anal. Chem. XXXX, XXX, XXX−XXX

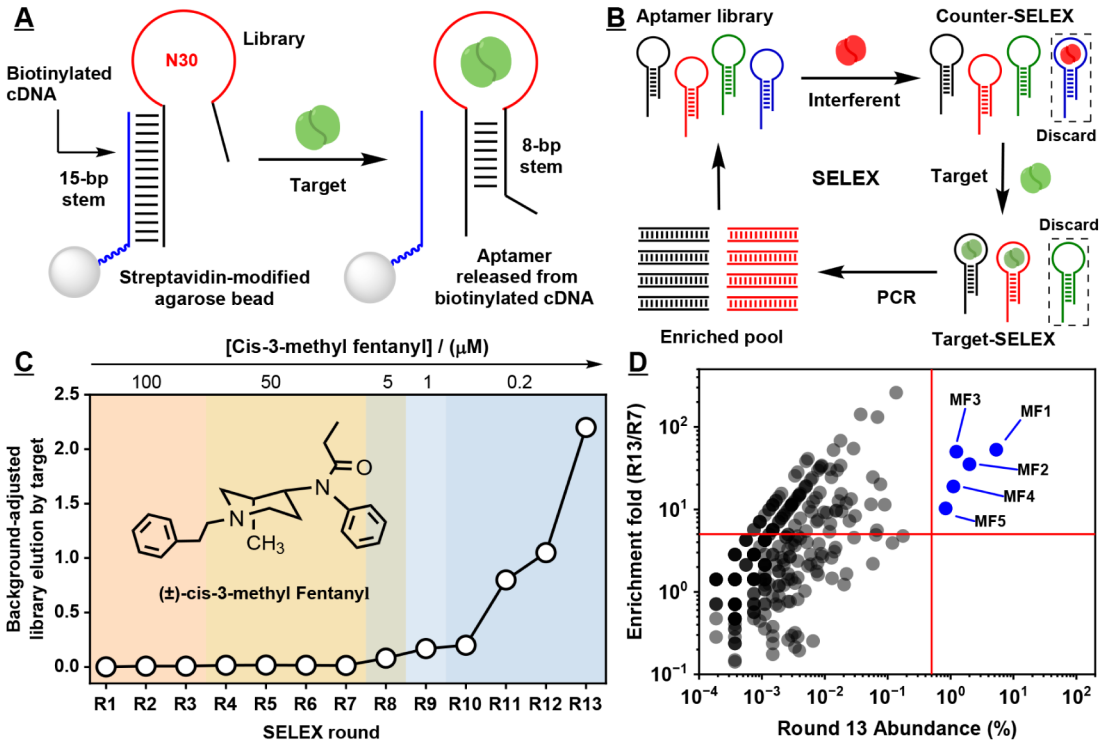

Figure 1. Discovery of class-specific aptamers for fentanyl analogs via *in vitro* selection. (**A**) Scheme of library-immobilized SELEX. (**B**) Workflow of SELEX. (**C**) Elution of library by (±)-cis-3-methyl fentanyl every SELEX round, adjusted for background elution. (**D**) Analysis of high-throughput sequencing (HTS) data from aptamer selection, with the abundance of sequences in Round 13 plotted against their enrichment fold between Rounds 7 and 13. Sequences chosen for further characterization are highlighted blue and labeled.

under the curves of the aggregate and monomer peaks was then calculated for each target concentration. Signal gain was determined using the formula $(R/R_0) - 1$, where R and R_0 represent the aggregate-to-monomer ratio for the target-containing sample and blank, respectively. Detection of fentanyl analogs, specificity testing against interferents, and detection of fentanyl in binary mixtures was performed in a similar fashion. 99 μL of dye-aptamer complex solution was mixed with 1 μL of 100× fentanyl analog, interferent, or fentanyl-interferent binary mixture in DMSO. For the detection of fentanyl analogs, final concentrations were 12.5 μM for analogs 138, 139, and 169; 25 μM for analogs 44, 46, 77, 92, 96, 108, 109, 149, 150, 153−155, 158−161, 165, 166, and 168; 50 μM for analogs 3, 4, 26, 40, 45, 49, 60, 68, 70, 98, 100, 104, 114, 122, 126, 127, 132, 133, 141−148, 152, 156, 157, 164, and 167; and 100 μM for analogs 1, 2, 5−25, 27−39, 41−43, 47, 48, 50−59, 61−67, 69, 71−76, 78−91, 93−95, 97, 99, 101−103, 105−107, 110−113, 115−121, 123−125, 128−131, 134−137, 140, 151, 162, and 163. For specificity testing, the following final concentrations of interferents were used: 250 μM lidocaine, acetaminophen, cis-tramadol, methadone, benzocaine, diphenhydramine, heroin, metamizole, caffeine, codeine, morphine, lactose, and mannitol; 125 μM methamphetamine, procaine, cocaine, and pseudoephedrine; 50 μM quinine, noscapine, papaverine, and lorazepam; and 10 μM chlorpromazine. For the detection of fentanyl in binary mixtures, final concentration for fentanyl was 12.5 μM fentanyl and interferent concentration was 125 μM or 250 μM. To calculate cross-reactivity, the following formula was used: $(SG_{analog}/SG_{3MF}) \times 100\%$, where SG_{analog} and SG_{3MF} are signal gains produced by the analog in question and (±)-cis-3 methyl fentanyl in the dye displacement assay, respectively. For binary mixture experiments, the cross reactivity was calculated relative to 12.5 μM fentanyl.

Isothermal Titration Calorimetry

Binding affinities were determined by isothermal titration calorimetry (ITC) at 23 °C using a MicroCal PEAQ ITC instrument (SI, Table S4). For aptamers MF1, MF2, MF2-mut, MF3, MF4, and MF5 a forward titration protocol was used in which the aptamer solution was loaded into the instrument sample cell with the target, (±)-cis-3-methyl fentanyl, loaded into the injection syringe. First, 300 μL of aptamer solution was prepared (final concentration: 20 μM) in selection buffer without salts, heated at 95 °C for 10 min, and then cooled in a water bath, after which the salts were added and the solution was loaded in the instrument sample cell. The target was prepared in selection buffer (specific concentrations detailed in Table S4) and 65 μL loaded in the injection syringe. Titrations consisted of an initial 0.4 μL purge injection followed by 19 successive 2 μL injections. To determine the binding affinity of MF2-mut to fentanyl analogs, 2% DMSO (v/v) was included in the selection buffer and a reverse titration protocol was used due to limited analog solubility. For the reverse titrations, the aptamer (final concentration: 300 μM) was prepared as described above in aqueous buffer with 2% DMSO (v/v) added after cooling and 65 μL was loaded into the injection syringe. Fentanyl analogs were prepared by drying methanolic stock solutions, then reconstituting to 1 mM in DMSO, sonicating for 10 min, and finally diluting to 20 μM with selection buffer. 300 μL of the analog was loaded into the sample cell. Titrations were conducted with an initial 0.4 μL purge followed by a series of 19 successive 2 μL injections. For 4-ANPP and benzyl carfentanil, a double titration was required to reach saturation, which was performed by reloading the injection syringe with aptamer solution upon the completion of a first titration and starting a second titration without removing the target solution from the sample cell. ITC data was analyzed using the MicroCal ITC Analysis software, in which the heat generated from each titration was plotted versus time and a plot of the integrated area of each injection peak used to construct a binding isotherm corrected for the background heat of dilution of aptamer or target. Data were fit with a single-site binding model.

https://doi.org/10.1021/acs.analchem.6c03173
Anal. Chem. XXXX, XXX, XXX−XXX

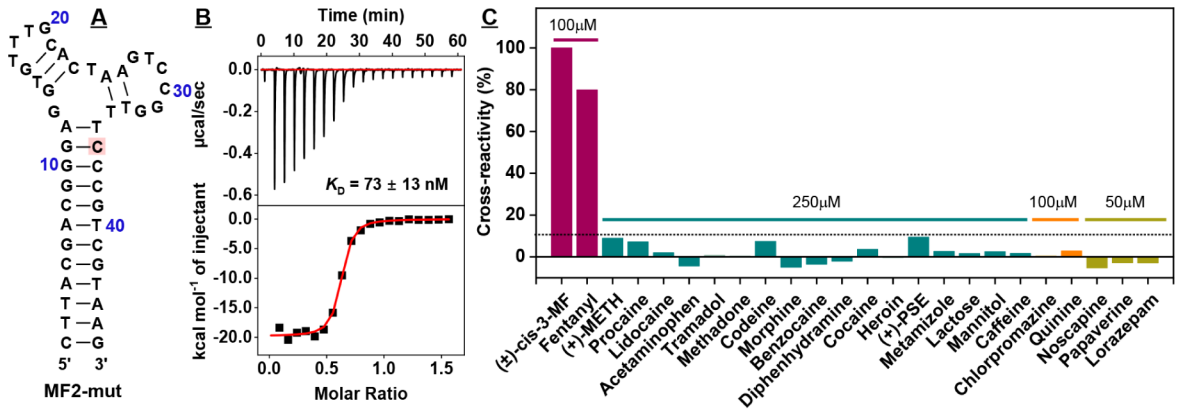

Figure 2. Determining the binding affinity and specificity of the aptamer MF2-mut. (**A**) Secondary structure of MF2-mut as predicted by NUPACK.[19] (**B**) Binding affinity of MF2-mut to (±)-cis-3-methyl fentanyl ((±)-cis-3-MF) as determined using ITC. (**C**) Specificity of MF2-mut to a variety of interferent molecules determined using an exonuclease-based fluorescence assay. Cross-reactivity is calculated using signal produced by 100 μM (±)-cis-3-methyl fentanyl. Dashed line shows a threshold of 10% cross-reactivity relative to the target. METH: methamphetamine, (+)-PSE: (+)-pseudoephedrine.

RESULTS AND DISCUSSION

Isolation of a Cross-Reactive DNA Aptamer for Fentanyl and Its Analogs

We performed library-immobilized SELEX[13,16] with the fentanyl analog (±)-cis-3-methyl fentanyl as the target. We employed a 73-nucleotide (nt) stem-loop-structured DNA library with an 8-base-pair (bp) stem, 30 nt random loop, and flanking PCR primer sites (see Supporting Information (SI), Table S1 for oligonucleotide sequences). We first hybridized the library with a 3′ biotinylated complementary DNA (cDNA) strand, resulting in the formation of a 15 bp duplex that we then immobilized onto streptavidin-modified agarose resin (Figure 1A, left). Library strands that bind to the target dissociate from the cDNA (Figure 1A, right) and are collected and amplified by polymerase chain reaction (PCR). As the number of target-binding sequences in the library is initially extremely low, the entire process of binding, partitioning, and amplification is performed for several rounds until the pool of oligonucleotides is highly enriched with target binders (Figure 1B). To enhance aptamer specificity, we perform counter-SELEX[10] against structurally similar interferents and discard interferent-binding sequences before challenging the remaining library with the target.

For the first round of SELEX, we used 1 nmol of library and 100 μM (±)-cis-3-methyl fentanyl (Figure 1C). Starting from Round 2, we preceded positive selection against the target with a counter-SELEX process with interferents including alkaloids from the poppy plant, other drugs of abuse, adulterants, and cutting agents commonly identified in seized drug material (selection process detailed in SI, Table S2). To increase selection stringency, we reduced the target concentration to 50 μM in Rounds 4−7, 5 μM in Round 8, 1 μM in Round 9, and finally, 0.2 μM in Rounds 10−13. For the first seven rounds, we generally observed relatively low levels of library elution by the target that did not meaningfully differ in magnitude compared to the elution of library by buffer alone (i.e., background elution) (Figure 1C). In Round 8, however, we observed a small increase in library elution by the target versus background elution, which continued to rise in Rounds 9 and 10. In Round 11, target-specific library elution rose sharply, peaking in Round 13. We measured the pool binding affinity of the Round 13 pool to (±)-cis-3-methyl fentanyl and determined a K_D of 31 μM (SI, Figure S1).

HTS Analysis of SELEX and Aptamer Characterization

We subjected the Round 7 and 13 pools to high-throughput sequencing (HTS) and obtained 767,622 and 538,626 complete reads, respectively, with 37% and 27% unique sequences in each pool (SI, Table S3). To identify promising aptamer candidates, we plotted the abundance of each sequence in the Round 13 pool against their change in abundance (i.e., enrichment fold) between Rounds 7 and 13 (Figure 1D). Almost every sequence in the Round 13 pool had an abundance of ≤0.1%, implying that the pool was not thoroughly enriched—possibly because we employed relatively low target concentrations in the last few rounds of SELEX. We characterized five sequences (MF1, MF2, MF3, MF4, MF5) that had abundances > 0.5% and enrichment fold > 5 using isothermal titration calorimetry (ITC), and obtained K_Ds of 1,200 ± 200, 309 ± 9, 1,100 ± 100, 341 ± 25, and 158 ± 20 nM, respectively (SI, Figure S2). Interestingly, while the binding stoichiometry of MF1 and MF3 was nearly 1, implying 1:1 aptamer-ligand binding, MF2, MF4, and MF5 displayed a binding stoichiometry of ∼0.5. Since we used a racemic mixture of cis-3-methyl fentanyl for the ITC experiment, we rationalized that MF1 and MF3 may bind both enantiomers of cis-3-methyl fentanyl with similar affinity, while MF2, MF4, and MF5 bind one enantiomer much more strongly than the other. We next determined the specificity of these five aptamers against the 22 interferents used for counter-SELEX (SI, Figures S3 and S4) using an exonuclease digestion fluorescence assay,[17] which we have previously used to extensively screen the specificity of a variety of aptamers.[18] MF2 displayed the best specificity of the five aptamers, with <10% cross-reactivity to interferents present at a concentration of 50−250 μM (depending on solubility limitations of certain compounds) relative to 100 μM (±)-cis-3-methyl fentanyl; notably, this included diphenhydramine and methamphetamine, two interferents which are known to generate false-positives in other assays.[6,7] In contrast, all other aptamers had moderate (10−40%) cross-reactivity to several compounds, including heroin, cocaine, benzocaine, quinine, methadone, and methamphetamine. Given the high affinity and specificity

https://doi.org/10.1021/acs.analchem.6c03173
Anal. Chem. XXXX, XXX, XXX−XXX

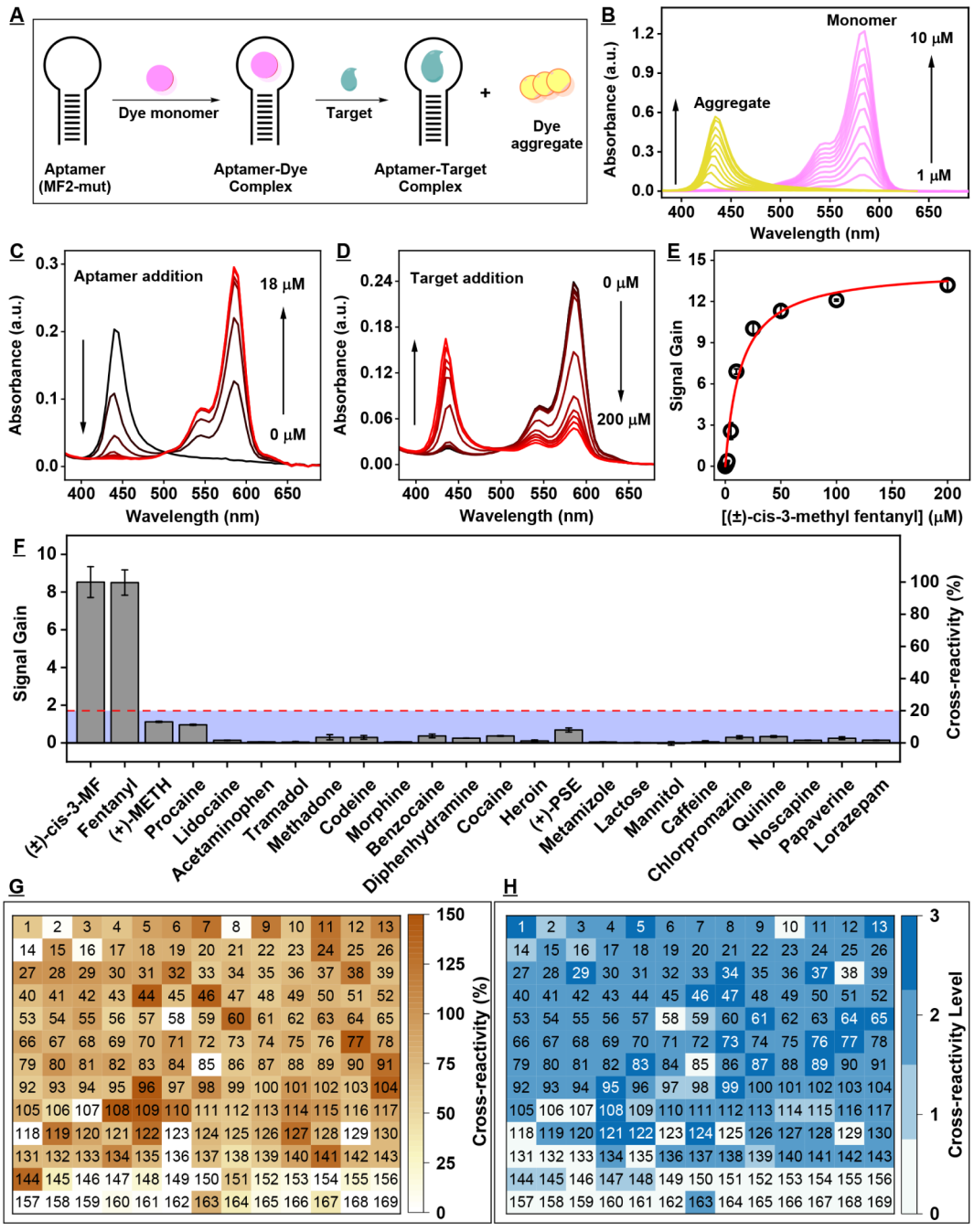

Figure 3. Sensing performance of a dye-displacement assay utilizing the MF2-mut aptamer and X-732−91C dye. (**A**) Working principle of the assay. (**B**) Absorbance spectra of X-732−91C monomer in 100% DMSO (pink) or aggregates in selection buffer (10 mM Tris-HCl, pH 7.4, 20 mM NaCl, 0.5 mM $MgCl_2$) containing 2% DMSO, 0.01% SDS, and 0.001% Triton X-100 (yellow). (**C**) Absorbance spectra of solutions containing 3 μM X-732−91C with 0, 3, 6, 9, 12, 15, or 18 μM MF2-mut, with increasing concentrations shown by a black-to-red color gradient. (**D**) Absorbance spectra of solutions containing 3 μM X-732−91C and 9 μM MF2-mut challenged with 0, 0.25, 0.5, 1.0, 1.5, 2.0, 5.0, 10, 25, 50, 100, or 200 μM of (±)-cis-3-methyl fentanyl, where the black-to-red color gradient reflects increasing concentration. (**E**) Calibration curve for target detection. (**F**) Sensor response to 100 μM (±)-cis-3-methyl fentanyl; 100 μM fentanyl; 125 μM (+)-methamphetamine, procaine, cocaine, or (+)-pseudoephedrine; 50 μM quinine, noscapine, papaverine, or lorazepam; and 10 μM chlorpromazine. The remaining 13 interferents were tested at 250 μM. Cross-reactivity is calculated using signal produced by (±)-cis-3-methyl fentanyl at each respective concentration of analog tested. (**G, H**) Cross-reactivity heatmap of **G**, the MF2-mut-based X-732−91C displacement assay and **H**, the BTNX lateral-flow immunoassay to fentanyl and 168 fentanyl analogs. The data in **H** are based on published results.[5] Cross-reactivity levels 0−3 indicate no detection, 20,000 ng/mL, 2,000 ng/mL, and 200 ng/mL limits of detection, respectively.

of MF2, we focused on this aptamer for subsequent experiments.

Through mutation studies, we identified a mutant of MF2, MF2-mut (Figure 2A), that had notably improved affinity for (±)-cis-3-methyl fentanyl. MF2 contains a 12 bp stem with a G11-T36 mismatch. We hypothesized that changing this mismatch to a canonical G11-C36 pair (i.e., MF2-mut) would improve the affinity of the aptamer due to increase stability in the stem (SI, Figure S5). Indeed, the MF2-mut has a ∼4-fold lower K_D of 73 ± 13 nM (Figure 2B). The binding enthalpy

https://doi.org/10.1021/acs.analchem.6c03173
Anal. Chem. XXXX, XXX, XXX−XXX

decreased slightly for MF2-mut relative to MF2 (−20.9 vs −19.8 kcal/mol), but the binding entropy cost was lower for the mutant (−40.9 vs −34.2 cal/mol·K). Structural analysis with NUPACK[19] indicates that the mutation in MF2-mut results in a perfectly matched 12 bp stem, yielding a more stable structure and accounting for the lower binding entropy cost. Importantly, the specificity of MF2-mut remained excellent, and in some cases even improved, for instance, for chlorpromazine (Figure 2C).

Development of Dye-Displacement Assay for Target Detection

Having identified MF2-mut as a potentially suitable aptamer for sensing purposes, we developed a colorimetric dye-displacement assay[20,21] with this aptamer and the cyanine dye X-732−91C selected from the Max Weaver Dye Library at NC State University,[22] which offers high color contrast relative to conventional dyes such as Cy7.[20,21] In this assay, an aptamer is initially noncovalently bound to the dye in a monomeric form; target binding to the aptamer displaces the dye into solution, causing it to form aggregates (Figure 3A). The aptamer-bound monomeric and aggregate forms of the dye have differing optical properties, such that the presence of the target can be detected based on a color change in the solution. We synthesized X-732−91C based on a previously reported protocol[23,24] and verified its structure using nuclear magnetic resonance spectroscopy (SI, see **synthesis protocol** and Figures S6 and S7) and mass spectrometry (SI, Figure S8). In pure dimethyl sulfoxide (DMSO), the dye absorbs maximally at 585 nm with a shoulder at 545 nm, corresponding to the dye in its monomer and H-dimer form, respectively. In aqueous buffer, however, the dye forms H-aggregates with an absorbance maximum at 445 nm (Figure 3B). The high color contrast arises from the large peak separation of 140 nm, and both forms of the dye have minimal spectral overlap. We determined the molar absorptivity (ε) of the monomer and aggregate forms of the dye, obtaining values of 173,623 $M^{-1}cm^{-1}$ and 74,368 $M^{-1}cm^{-1}$, respectively (SI, Figure S9).

We first optimized the concentration of aptamer in the assay by mixing a fixed concentration of dye (3 μM, the lowest concentration of dye visible to the naked eye) with varying concentrations of MF2-mut (0−18 μM). The dye alone in solution was predominantly in the form of H-aggregates absorbing at 445 nm. At increasing aptamer concentrations, the H-aggregate peak diminished, and new peaks formed at 545 and 585 nm, respectively corresponding to dye H-dimers and monomers (Figure 3C). We found that 9 μM aptamer was sufficient to deplete H-aggregate absorbance and achieve 90% monomerization of the dye (SI, Figure S10). To perform target detection, we challenged aptamer-dye complexes with various concentrations of (±)-cis-3-methyl fentanyl. We observed that the addition of (±)-cis-3-methyl fentanyl resulted in the rapid (within 1 min) depletion of dye monomer absorbance and an increase in H-aggregate absorbance in a concentration-dependent manner (Figure 3D), with a dynamic range of 0−25 μM and a limit of detection by plate reader of 0.5 μM (Figure 3E). With the naked eye, we were able to observe a red to yellow color change that is detectable at as low as 10 μM (±)-cis-3-methyl fentanyl (SI, Figure S11). Thus, even with a heavily adulterated sample (e.g., 10 mg of 1% w/w fentanyl analog dissolved in 1 mL buffer), this detection limit is sufficient to confidently identify the analyte. As a control, we performed the same assay with dye alone and did not observe any significant change in dye absorbance at any target concentration (SI, Figure S12), indicating that signals in the assay are specifically generated by target binding to the aptamer-dye complex. The assay is also highly specific and minimally responded to the 21 interferent molecules (SI, Figure S13) commonly found in seized drug material, except for (+)-methamphetamine (Figure 3F and SI, Figures S14 and S15).[25] We also confirmed that the assay can sensitively detect fentanyl, with an instrumental limit of detection of 0.5 μM and a visual detection limit of 10 μM (SI, Figure S16). Since our aptamer assay involves a color change, we anticipate potential difficulties in testing samples that are dark or deeply colored. However, this issue could most likely be overcome by using relatively low quantities of sample (e.g., ≤1 mg), which is feasible given the high sensitivity of our assay. For instance, 1 mg of material containing 1% fentanyl (by weight) dissolved in 1 mL of buffer represents a concentration of ∼30 μM, which should yield an easily identifiable color change with the naked eye.

Given that the average purity of fentanyl in powdered samples is 10% by weight,[26] we evaluated our assay's ability to detect fentanyl in binary mixtures containing a large proportion of various interferents (i.e., diphenhydramine, lidocaine, xylazine, acetaminophen, caffeine, (+)-methamphetamine, heroin, or cocaine) with either 5% or 10% (by molarity) fentanyl. The assay was able to respond to fentanyl in all mixtures with a signal similar to fentanyl alone (SI, Figure S17), demonstrating that these interferents did not suppress signals induced by the target (SI, Figure S17A and Figures S18 and S19). To assess specificity under realistic conditions, we compared assay response at 12.5 μM fentanyl (the lowest visually discernible result) versus interferents at 10- or 20-fold higher concentrations. We observed low cross-reactivity (<5%) to all interferents except for (+)-methamphetamine, which had cross-reactivity of 20−30% (SI, Figure S17B and Figures S20 and S21). To more closely examine the specificity of our assay, we challenged our aptamer-based dye-displacement assay with various concentrations of (+)-methamphetamine, diphenhydramine, or cocaine up to 200 μM. We observed <5% cross-reactivity to cocaine and diphenhydramine and <20% cross-reactivity to (+)-methamphetamine at all concentrations tested relative to fentanyl (SI, Figure S22). These results indicate that our assay should be capable of detecting fentanyl in authentic seized drug material with reasonable sensitivity and specificity.

We next tested the cross-reactivity of the dye-displacement assay against a panel of fentanyl analogs. We used the FAS Kit and Emergent Panels 2 and 3 developed by Cayman Chemical, which respectively contain 120 and 62 different opioids. Of these 182 substances, 169 are either analogs of fentanyl or metabolites (for structures see SI, Figures S23−S28), while the remaining compounds are structural derivatives of another opioid family represented by U-47700 (SI, Figure S29). Our assay responded to 139 of the 169 fentanyl analogs (82%) with a cross-reactivity >20% relative to (±)-cis-3-methyl fentanyl, with most compounds tested at a concentration of 100 μM (some analogs were tested at 50, 25, or 12.5 μM due to solubility limitations) (Figure 3G and SI, Figures S30−S45). In contrast, the assay minimally responded to any of the 13 U-47700-derived opioids (SI, Figures S46−S48), indicating strong specificity for fentanyl and its analogs. Notably, the cross-reactivity and specificity of our assay is superior to that of a recently reported sensor using the organic host cucurbit[7]-uril, which responded to 58 fentanyl analogs but also cross-

https://doi.org/10.1021/acs.analchem.6c03173
Anal. Chem. XXXX, XXX, XXX−XXX

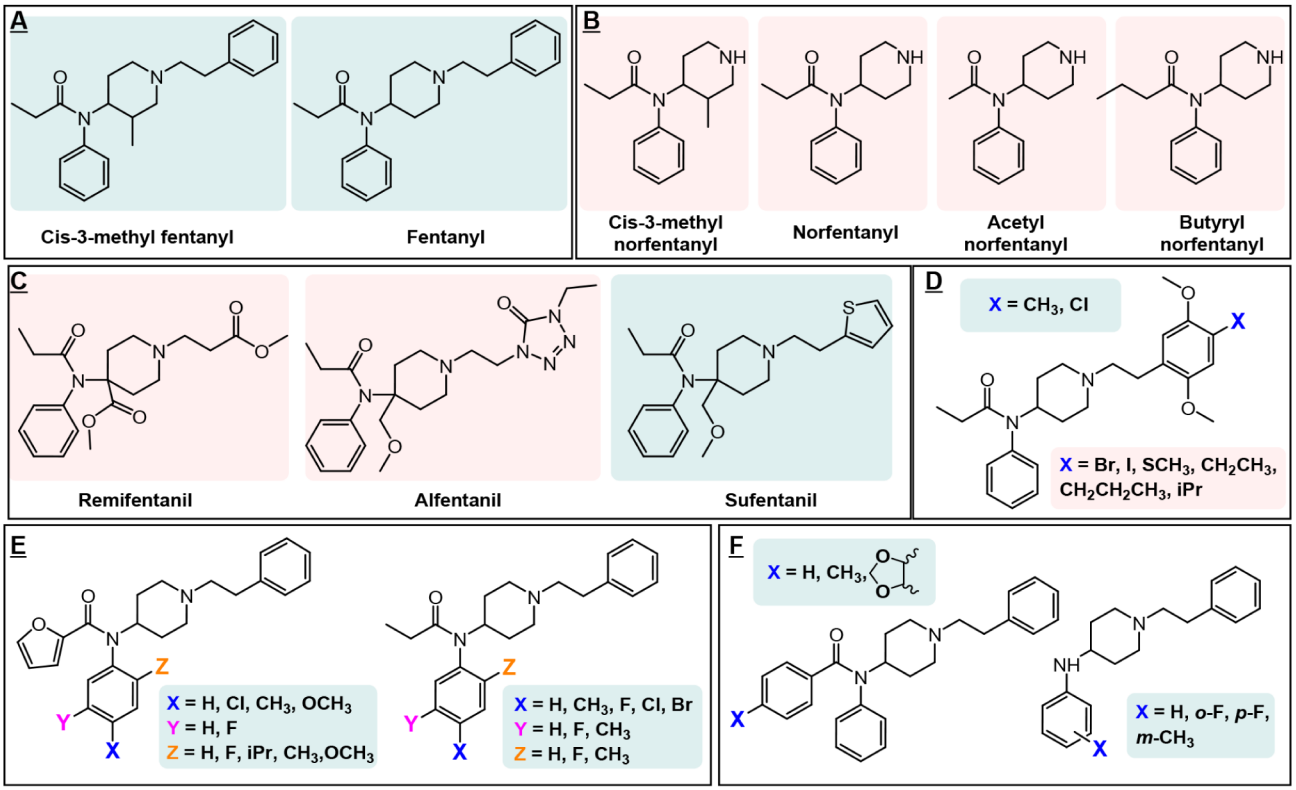

Figure 4. Analyzing structural determinants of detectability with the MF2-mut-based dye-displacement assay. Analogs that the assay responds with at least 20% cross-reactivity relative to (±)-cis-3-methyl fentanyl are labeled green, while analogs that yield a response lower than this threshold are labeled red. (**A**) (±)-cis-3-methyl fentanyl and fentanyl both elicit an assay response. (**B**) MF2-mut does not respond to metabolites of fentanyl and its analogs such as norfentanyl that lack the phenethyl moiety. (**C**) MF2-mut does not bind to remifentanil and alfentanil, but does recognize sufentanil. (**D**) Dimethoxy-substituted fentanyl analogs containing bulky substituents at the aromatic ring of the phenethyl moiety are unable to bind MF2-mut, although the aptamer tolerates small substituents such as methyl groups. (**E**) MF2-mut tolerates various substituents at the ortho, meta, and para positions of the aniline moiety as well as (**F**) bulky groups at the propionyl moiety and even despropionyl analogs (e.g., 4-ANPP).

reacted strongly to interferents such as methamphetamine, levamisole, and quinine with a response similar to fentanyl.[27] Our assay also offers slightly better performance than existing lateral-flow immunoassays. Hayes and Lieberman assessed the responsiveness of two commercial lateral-flow immunoassays for fentanyl analogs[5] developed by BTNX and DanceSafe and found they could respectively detect 134 (Figure 3H) and 121 (SI, Figure S49) out of the 169 fentanyl analogs tested here. However, both of these assays have been reported to cross-react to methamphetamine, diphenhydramine, and lidocaine.[6,7]

Notably, our assay could recognize 11 fentanyl analogs that the BTNX assay was unable to, namely 4-ANPP (#10), benzyl carfentanil (#38), para-chloro cyclopentyl fentanyl (#106), (±)-cis-isofentanyl (#125), para-fluoro-4-ANBP (#131), despropionyl para-fluoro fentanyl (#132), despropionyl meta-methyl fentanyl (#133), despropionyl 2′-fluoro ortho fluorofentanyl (#135), N-(2C−D) fentanyl (#151), N-(DOC) fentanyl (#164), and N-(DOM) fentanyl (#167). To verify the results of our assay, we used ITC to determine the binding affinity of MF2-mut to these 11 analogs. We found that the aptamer could bind all such analogs with submicromolar to micromolar affinity (SI, Figures S50−S51 and Table S4). We further verified our assay results by determining the binding affinity of MF2-mut to fentanyl and 8 analogs that both our assay and the BTNX assay could detect. ITC revealed MF2-mut binds these 8 analogs with K_Ds of 74−1200 nM (SI, Figures S52−S53 and Table S4). Overall, the relatively broad cross-reactivity of our dye-displacement assay, coupled with its excellent specificity against other drugs of abuse, adulterants, and cutting agents, makes it a potentially better choice for screening fentanyl analogs in seized substances.

Relationship between Aptamer Binding and Target Moieties

We next examined our assay's cross-reactivity data to determine which structural elements of the various fentanyl analogs were conducive or detrimental to aptamer recognition/binding. The assay responded to (±)-cis-3-methyl fentanyl (#28) and fentanyl (#13) (Figure 4A) but not to fentanyl analog metabolites such as cis-3-methyl norfentanyl (#123), norfentanyl (#14), acetyl norfentanyl (#2), or butyryl norfentanyl (#16) (Figure 4B); using ITC, we confirmed MF2-mut lacks affinity for norfentanyl and acetyl norfentanyl (SI, Figure S54A−B). These all lack the phenethyl moiety common to most fentanyl analogs, implying that this group is important for binding.

The assay also did not respond to any analogs in which the phenethyl group is replaced with another moiety, such as alfentanil (#58) and remifentanil (#85) (Figure 4C). These two analogs also differ from fentanyl at position 3 of the piperidinyl ring; however, our assay was responsive to sufentanil (#98), which also harbors a modification at this same position but features an aromatic thiophenethyl in place of phenethyl (Figure 4C), as well as benzyl carfentanil (#38), which features a methyl ester group at this position. This indicates that certain modifications at position 3 can be

https://doi.org/10.1021/acs.analchem.6c03173
Anal. Chem. XXXX, XXX, XXX−XXX

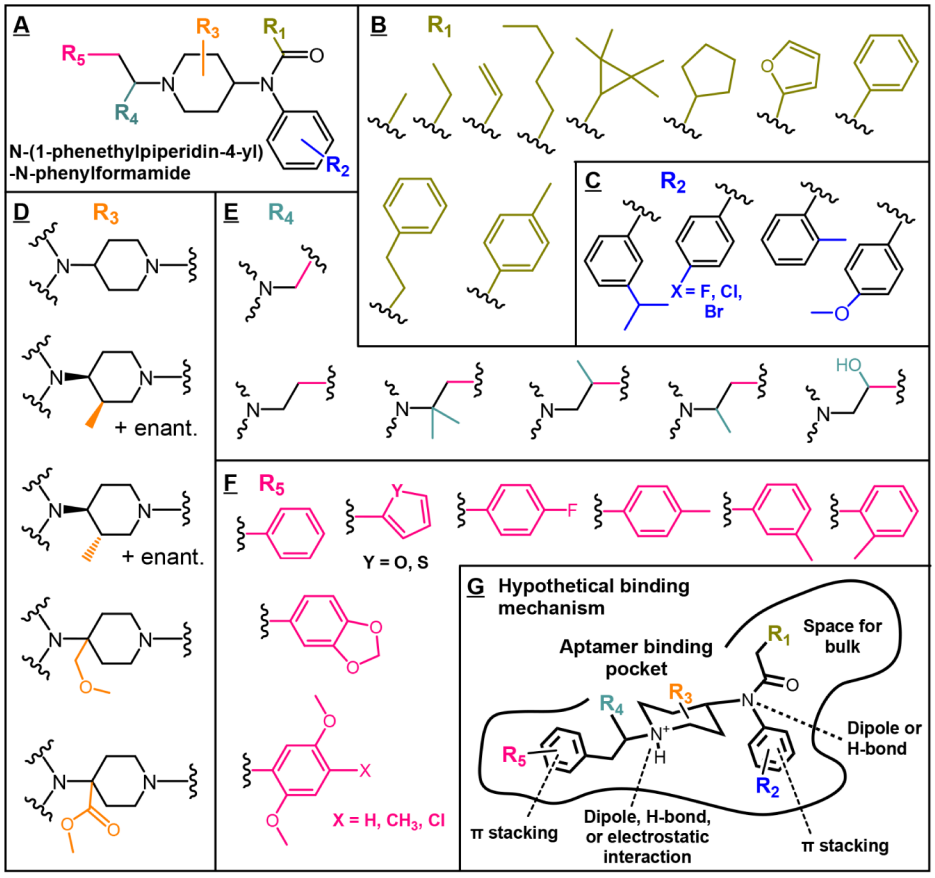

Figure 5. Structure−activity relationships associated with the recognition of fentanyl analogs by MF2-mut based on dye-displacement assay data. (**A**) The core structural framework of N-(1-phenethylpiperidin-4-yl)-*N*-phenylformamide. (**B**−**F**) Substituents tolerated by MF2-mut at (**B**) R_1, (**C**) R_2, (**D**) R_3, (**E**) R_4, and (**F**) R_5. (**G**) Proposed interaction mechanism between MF2-mut and fentanyl analogs based on experimental data in this work.

tolerated by the aptamer. The assay was also unresponsive to several analogs containing multiple substituents at the phenethyl moiety, such as N-(2C−B) fentanyl (#147) and N-(2C-G) fentanyl (#152) (SI, Figure S54C−D), N-(2C−I) fentanyl (#153), N-(2C-E) fentanyl (#146), N-(2C−P) fentanyl (#149), all of which feature substitutions on the aromatic ring at the both ortho and meta positions with 2-O-methyl and at the para position with halogens or alkyl chains (Figure 4D). However, the assay could respond to analogs in which the para position contained methyl (N-(2C−D) fentanyl #151) or chloro (N-(2C−C) fentanyl #148), implying that that substituent size at this position is particularly important. The assay was able to respond to analogs with modifications on the anilido ring (e.g., para-fluoro cyclopentyl fentanyl #92, para-chloro furanyl fentanyl #100, and para-bromo fentanyl #138, para-methoxy furanyl fentanyl #104, and para-chlorofentanyl #32) (Figure 4E). These results indicate that the aptamer is insensitive to substituents at this region. Finally, the fact that our assay is able respond analogs with bulky substituents at the propionyl group, such as phenyl fentanyl (#45), para-toluoyl fentanyl (#139) (Figure 4F), 2,2,3,3-tetramethyl cyclopropyl fentanyl (#109), and benzodioxole fentanyl (#60) indicates that such bulk does not impede aptamer binding, implying the presence of an exposed cavity in the binding pocket. Interestingly, the assay can also respond to 4-ANPP (#10), which entails the removal of the propionyl group from fentanyl, as well as analogs such as para-fluoro 4-ANBP (#131), implying that the carbonyl oxygen is not involved in molecular recognition (Figure 4F).

Despite being intolerant to a few fentanyl analogs, MF2-mut seems to tolerate most other changes to the core framework shared by these analogs. To describe this cross-reactivity, we assigned five different R groups to a core framework based on N-(1-phenethylpiperidin-4-yl)-*N*-phenylformamide (Figure 5A). At the amido position (R_1), the aptamer tolerates several different substituents as small as acetamide (e.g., para-fluoro acetyl fentanyl #64) and as large as valerylamide (valeryl fentanyl #70), as well as annular (e.g., cyclopentyl fentanyl #44 and cyclopropyl fentanyl #15) and aromatic groups (e.g., para-fluoro furanyl fentanyl #90 and phenyl fentanyl #45) and unsaturated moieties (e.g., acrylfentanyl #113) (Figure 5B). Furthermore, a wide range of substituents are tolerated at various positions (ortho, meta, para) on the anilido ring (R_2), such as halogens, methyl, O-methyl, and isopropyl groups (Figure 5C). However, the absence of larger or bulkier analogs in our study precludes us from completely ruling out limitations in substituent size at this position. Only a few of the analogs tested varied at R_3, on the piperidinyl ring, making it difficult to judge aptamer binding preferences here. The aptamer tolerates a methyl group at position 3 on the ring (R_3) in the form of both cis- and trans-3-methyl fentanyl as well as sufentanil, which features a methyl methoxy substituent (Figure 5D). However, we note that because the binding stoichiometry reported by ITC for MF2-mut is ∼0.5, it is possible that the aptamer only recognizes one of two

https://doi.org/10.1021/acs.analchem.6c03173
Anal. Chem. XXXX, XXX, XXX−XXX

enantiomers of both (±)-cis-3-methyl fentanyl and (±)-trans-3-methyl fentanyl. At R_4—the two-carbon bridge that links the phenyl and piperidinyl group—both methyl (e.g., a-methyl and b-methyl fentanyl) and hydroxyl (*e.g.,* beta-hydroxy thiofentanyl) groups are tolerated. Interestingly, the aptamer still recognizes analogs in which the two-carbon bridge is shortened to one carbon (e.g., benzyl fentanyl, thienyl fentanyl, (±)-cis-isofentanyl, or N-benzyl phenyl norfentanyl), indicating the flexibility of the aptamer for this epitope (Figure 5E). Finally, for R_5, replacement of the benzene ring with an aromatic isostere such as thiophene or furan is tolerated, but replacement with a nonaromatic moiety (e.g., an ester group in remifentanil) abolishes binding (Figure 5F). In addition, some substituents at the aromatic ring itself are unacceptable. For instance, methyl (*e.g.,* 2′-, 3′-, or 4′-methyl fentanyl), fluoro (*e.g.,* 4′-fluoro or para-fluoro trans-3-methyl fentanyl), and methylenedioxy (*e.g.,* N-MDA fentanyl) groups are acceptable. However, dimethoxy analogs containing bulky groups at the para position are not tolerated. Based the response of the fentanyl analogs to the dye displacement assay, we hypothesize that MF2-mut likely interacts with the 4-anilino-N-phenethylpiperidine core structure shared by all the analogs (via pi stacking with both aromatic rings and H-bonding, Debye, or Keesom interactions with the nitrogen-containing moieties) with good tolerance for bulk at R_1 and R_2, but less tolerance at R_5 (Figure 5G). This hypothetical model also explains our aptamer's specificity against most interferents, which contain only a subset of the functional groups featured in 4-anilino-N-phenethylpiperidine. Further experiments with high-resolution structure determination techniques such as nuclear magnetic resonance spectroscopy or X-ray crystallography are required to confirm our hypothetical model.

CONCLUSION

The binding properties of receptors directly define sensor response to analytes and interferents. In certain applications, high specificity toward a single analyte is of paramount interest, while in other cases, broad cross-reactivity to a variety of analytes is necessary. When the goal is to specifically detect an entire class of analytes (i.e., fentanyl analogs) while still rejecting structurally related interferents, a careful balance between specificity and cross-reactivity is needed. Our work here demonstrates the feasibility of generating a receptor—and a corresponding sensor—that exhibits the appropriate blend of specificity and cross-reactivity for such a task. In testing our aptamer-based dye-displacement assay against 169 fentanyl analogs, we found that the assay could respond to 139 analogs with a cross-reactivity of >20% relative to (±)-cis-3-methyl fentanyl. More importantly, the assay demonstrated minimal response to interferents, including those that commonly interfere with fentanyl immunoassays such as diphenhydramine. Nevertheless, the assay did yield a non-negligible response to methamphetamine at relatively high concentrations (>200 μM). In practical contexts, false positives by methamphetamine can be avoided by designing the assay in a manner such that even when it is challenged with pure methamphetamine, the concentration of this interferent does not exceed a certain threshold concentration (e.g., 100 μM). For example, a 1 mg methamphetamine sample dissolved in 10 mL of solvent (e.g., DMSO) would yield a final concentration of 670 μM. Diluting this solution by another 10-fold in selection buffer would bring the methamphetamine concentration down to 67 μM, a quantity below a threshold of 15% cross-reactivity. We note that this protocol decreases the likelihood of methamphetamine-induced false positives at the cost of reduced sensitivity to fentanyl/analogs. For instance, since the visual detection limit of the assay is 10 μM for fentanyl, the lowest proportion of fentanyl that could be detected in a 1 mg sample equates to ∼30%, and with the instrumental detection limit of 0.5 μM (using a plate reader), this would equate to a sample containing ∼2% fentanyl. Improvements in aptamer specificity through maturation techniques such as motif-SELEX[28] could perhaps reduce cross-reactivity to methamphetamine even further, thereby alleviating this trade-off in assay sensitivity and specificity.

We also note that, while the immunoassays conducted by the Lieberman group[6,7] employed deionized water, our aptamer-based assay was conducted in selection buffer (10 mM Tris pH 7.4, 20 mM NaCl, 0.5 mM $MgCl_2$), because such environment provides optimal conditions for the aptamer to function. This buffer may or may not be suitable for the immunoassay, however, deionized water would likely not support optimal aptamer function. Finally, in terms of fentanyl analog concentration, the Lieberman group tested concentrations of 20, 200, 2,000, and 20,000 ng/mL depending on responsiveness of the analog, which, using the molecular weight of fentanyl (336 g/mol) as an exemplar, translates to molar concentrations of 0.06, 0.6, 6, and 60 μM. In contrast, we tested the analogs at a concentration of 12.5−100 μM. While the comparison of our assay and the immunoassays are not exactly under the same conditions, they are both under realistic, application-relevant conditions. Nevertheless, because of such variations in testing conditions, it is important to exercise caution when comparing the performance of both assays.

Empirical evidence from the literature suggests that the specificity and cross-reactivity of receptors is dependent on their size and chemical complexity. For instance, small organic receptors such as cyclodextrins, which are fairly simple in structure, are typically very promiscuous, as they interact with analytes via nonspecific mechanisms such as the hydrophobic effect.[29−31] Thus, such receptors can achieve broad cross-reactivity against a group of analytes when used as recognition elements in sensors, but they also tend to exhibit poor specificity against interferents. For instance, Gao et al. reported a cucurbituril-based fluorescent sensor that could detect at least 58 different fentanyl analogs with high sensitivity. However, the sensor also generated the same magnitude of response to interferents such as methamphetamine and quinine,[27] most likely because the basis of interaction between cucurbituril and fentanyl or these interferents are similar, making them indistinguishable. Bioreceptors such as aptamers, which are selected from vast combinatorial libraries of oligonucleotides with 10^{15}−10^{18} unique constituents, offer greater specificity due to their greater chemical diversity relative to small organic receptors, and are generally more likely to assume flexible structures that can complement the shape of their target(s). Antibodies are also well-suited for molecular sensing, but they have one critical disadvantage relative to aptamers—since antibodies are generated *in vivo*, there is little to no control over the binding properties of the resulting receptors. As such, antibodies sometimes display unwanted cross-reactivity to interferents, such as methamphetamine and diphenhydramine in the case of fentanyl lateral-flow immunoassay test strips. In contrast, since SELEX is performed entirely *in vitro*, the screening process can be manipulated to

https://doi.org/10.1021/acs.analchem.6c03173
Anal. Chem. XXXX, XXX, XXX−XXX

reject aptamer candidates with undesirable cross-reactivity to interferents while also promoting the enrichment of aptamers that exhibit cross-reactive binding to desired analytes. In this work, we have demonstrated the extent to which molecular sensing can be balanced in terms of analyte selectivity, generating aptamer-based fentanyl analog sensors that achieve broad cross-reactivity and superior specificity relative to existing antibody-based assays. These results indicate that aptamers may generally offer a superior alternative to antibodies as a recognition element for the specific detection of classes of structurally similar analytes in interferent-rich samples.

■ ASSOCIATED CONTENT

Supporting Information

The Supporting Information is available free of charge at https://pubs.acs.org/doi/10.1021/acs.analchem.6c03173.

X-732−91C synthesis, NMR characterization, and MS characterization procedures; exonuclease-based fluorescence assay procedure; DNA sequences employed in this work; selection conditions for library-immobilized SELEX; HTS statistics from selection; summary of ITC experimental conditions and results; gel elution assay data; ITC data used to determine aptamer target-binding affinity; exonuclease-based fluorescence assay specificity data for MF1, MF2, MF3, MF4, and MF5; NUPACK-predicted secondary structures of MF2 and MF2-mut; X-732−91C ^{1}H- and ^{13}C NMR spectra; X-732−91C mass spectra; absorbance spectra for X-732−91C and calibration curves to determine the molar absorptivity in DMSO and buffer; MF2-mut and X-732−91C dye-displacement assay optimization data; photograph of MF2-mut and X-732−91C dye-displacement assay for detection of (±)-*cis*-3-methyl fentanyl; control absorbance spectra for MF2-mut and X-732−91C dye-displacement assay against (±)-cis-3-methyl fentanyl; chemical structures of the interferent molecules employed in exonuclease-based fluorescence assay and dye-displacement specificity experiments; absorbance spectra for MF2-mut and X-732−91C dye-displacement assay specificity experiments; absorbance spectra, calibration curve, and photograph of MF2-mut and X-732−91C dye-displacement assay against fentanyl, (+)-methamphetamine, cocaine, and diphenhydramine; absorbance spectra for MF2-mut and X-732−91C dye-displacement assay detection of fentanyl in binary mixtures; chemical structures of the fentanyl analogs studied in this work; chemical structures of the U-47700-derived synthetic opioids studied in this work; absorbance spectra for MF2-mut and X-732−91C dye-displacement assay experiments with fentanyl analogs; absorbance spectra for MF2-mut and X-732−91C dye-displacement assay experiments with U-47700-derived synthetic opioids; summary of dye-displacement sensor response to U-47700-derived synthetic opioids; reactivity heatmap of DanceSafe lateral-flow immunoassay to the fentanyl analogs studied in this work; ITC data for binding of select fentanyl analogs to MF2-mut (PDF)

■ AUTHOR INFORMATION

Corresponding Author

Yi Xiao − *Department of Chemistry, North Carolina State University, Raleigh, North Carolina 27607, United States;* orcid.org/0000-0001-7278-9811; Email: yxiao34@ncsu.edu

Authors

Linlin Wang − *Department of Chemistry, North Carolina State University, Raleigh, North Carolina 27607, United States;* orcid.org/0000-0003-0727-3397

Gabriel Castro − *Department of Chemistry, North Carolina State University, Raleigh, North Carolina 27607, United States*

Obtin Alkhamis − *Department of Chemistry, North Carolina State University, Raleigh, North Carolina 27607, United States*

Madhu Sudhana Reddy Gangireddy − *Department of Chemistry and Biochemistry, Florida International University, Miami, Florida 33199, United States*

Konstantin V. Bukhryakov − *Department of Chemistry and Biochemistry, Florida International University, Miami, Florida 33199, United States;* orcid.org/0000-0002-8425-9671

Nelson R. Vinueza − *Department of Chemistry, North Carolina State University, Raleigh, North Carolina 27607, United States; Department of Textile Engineering, Chemistry, Science, Wilson College of Textiles, North Carolina State University, Raleigh, North Carolina 27695, United States;* orcid.org/0000-0002-2608-5431

Complete contact information is available at: https://pubs.acs.org/10.1021/acs.analchem.6c03173

Author Contributions

‖L.W. and G.C. contributed equally to this work.

Notes

The authors declare no competing financial interest.

■ ACKNOWLEDGMENTS

This work was supported by the National Institute of Justice, Grant Office of Justice Programs, U.S. Department of Justice, Award 2022-GG-04440-RESS, and the National Science Foundation [ECCS-2532545].

■ REFERENCES

(1) Volkow, N. D.; Blanco, C. The Changing Opioid Crisis: Development, Challenges and Opportunities. *Mol. Psychiatry* **2021**, *26*, 218−233.

(2) National Institute on Drug Abuse *Drug Overdose Deaths: Facts and Figures*; https://nida.nih.gov/research-topics/trends-statistics/overdose-death-rates, (accessed 07 July 2026). 2024.

(3) Burns, S. M.; Cunningham, C. W.; Mercer, S. L. DARK Classics in Chemical Neuroscience: Fentanyl. *ACS Chem. Neurosci.* **2018**, *9* (10), 2428−2437.

(4) Weicker, N. P.; Owczarzak, J.; Urquhart, G.; Park, J. N.; Rouhani, S.; Ling, R.; Morris, M.; Sherman, S. G. Agency in the Fentanyl Era: Exploring the Utility of Fentanyl Test Strips in an Opaque Drug Market. *Int. J. Drug Policy* **2020**, *84*, 102900.

(5) Hayes, K. L.; Lieberman, M. Assessment of Two Brands of Fentanyl Test Strips with 251 Synthetic Opioids Reveals "Blind Spots" in Detection Capabilities. *Harm Reduct. J.* **2023**, *20* (1), 175.

(6) Halifax, J. C.; Lim, L.; Ciccarone, D.; Lynch, K. L. Testing the Test Strips: Laboratory Performance of Fentanyl Test Strips. *Harm Reduct. J.* **2024**, *21* (1), 14.
(7) Lockwood, T. L. E.; Vervoordt, A.; Lieberman, M. High Concentrations of Illicit Stimulants and Cutting Agents Cause False Positives on Fentanyl Test Strips. *Harm Reduct. J.* **2021**, *18* (1), 30.
(8) Tuerk, C.; Gold, L. Systematic Evolution of Ligands by Exponential Enrichment: RNA Ligands to Bacteriophage T4 DNA Polymerase. *Science* **1990**, *249* (4968), 505−510.
(9) Ellington, A. D.; Szostak, J. W. In Vitro Selection of RNA Molecules That Bind Specific Ligands. *Nature* **1990**, *346* (6287), 818−822.
(10) Jenison, R. D.; Gill, S. C.; Pardi, A.; Polisky, B. High-Resolution Molecular Discrimination by RNA. *Science* **1994**, *263* (5152), 1425−1429.
(11) White, R.; Rusconi, C.; Scardino, E.; Wolberg, A.; Lawson, J.; Hoffman, M.; Sullenger, B. Generation of Species Cross-Reactive Aptamers Using "Toggle" SELEX. *Mol. Ther.* **2001**, *4* (6), 567−573.
(12) Yang, W.; Yu, H.; Alkhamis, O.; Liu, Y.; Canoura, J.; Fu, F.; Xiao, Y. In Vitro Isolation of Class-Specific Oligonucleotide-Based Small-Molecule Receptors. *Nucleic Acids Res.* **2019**, *47* (12), No. e71.
(13) Yang, K. A.; Pei, R.; Stojanovic, M. N. In Vitro Selection and Amplification Protocols for Isolation of Aptameric Sensors for Small Molecules. *Methods* **2016**, *106*, 58−65.
(14) Martin, M. Cutadapt Removes Adapter Sequences from High-Throughput Sequencing Reads. *EMBnet J.* **2011**, *17* (1), 10−12.
(15) Alam, K. K.; Chang, J. L.; Burke, D. H. FASTAptamer: A Bioinformatic Toolkit for High-Throughput Sequence Analysis of Combinatorial Selections. *Mol. Ther Nucleic Acids* **2015**, *4* (3), No. e230.
(16) Nutiu, R.; Li, Y. In Vitro Selection of Structure-Switching Signaling Aptamers. *Angew. Chem., Int. Ed.* **2005**, *44* (7), 1061−1065.
(17) Canoura, J.; Yu, H.; Alkhamis, O.; Roncancio, D.; Farhana, R.; Xiao, Y. Accelerating Post-SELEX Aptamer Engineering Using Exonuclease Digestion. *J. Am. Chem. Soc.* **2021**, *143* (2), 805−816.
(18) Alkhamis, O.; Canoura, J.; Ly, P. T.; Xiao, Y. Using Exonucleases for Aptamer Characterization, Engineering, and Sensing. *Acc. Chem. Res.* **2023**, *56* (13), 1731−1743.
(19) Zadeh, J. N.; Steenberg, C. D.; Bois, J. S.; Wolfe, B. R.; Pierce, M. B.; Khan, A. R.; Dirks, R. M.; Pierce, N. A. NUPACK: Analysis and Design of Nucleic Acid Systems. *J. Comput. Chem.* **2011**, *32* (1), 170−173.
(20) Stojanovic, M. N.; Landry, D. W. Aptamer-Based Colorimetric Probe for Cocaine. *J. Am. Chem. Soc.* **2002**, *124* (33), 9678−9679.
(21) Alkhamis, O.; Canoura, J.; Bukhryakov, K. V.; Tarifa, A.; DeCaprio, A. P.; Xiao, Y. DNA Aptamer−Cyanine Complexes as Generic Colorimetric Small-Molecule Sensors. *Angew. Chem., Int. Ed.* **2022**, *61* (3), No. e202112305.
(22) Kuenemann, M. A.; Szymczyk, M.; Chen, Y.; Sultana, N.; Hinks, D.; Freeman, H. S.; Williams, A. J.; Fourches, D.; Vinueza, N. R. Weaver's Historic Accessible Collection of Synthetic Dyes: A Cheminformatics Analysis. *Chem. Sci.* **2017**, *8* (6), 4334−4339.
(23) Tomilov, Y. V.; Platonov, D. N.; Frumkin, A. E.; Lipilin, D. L.; Salikov, R. F. Synthesis of Condensed Heterocycles via Cyclopropylimine Rearrangement of Cyclopropylazoles. *Tetrahedron Lett.* **2010**, *51* (39), 5120−5123.
(24) Babichev, F. S.; Shchetsinskaya, E.; Mono, E. Tri- and Pentamethinecyanines from 2,3-(Polymethylene)Benzothiazolium Salts. *Zh. Obshch. Khim.* **1964**, *34*, 2445−2455.
(25) Fiorentin, T. R.; Krotulski, A. J.; Martin, D. M.; Browne, T.; Triplett, J.; Conti, T.; Logan, B. K. Detection of Cutting Agents in Drug-Positive Seized Exhibits within the United States. *J. Forensic Sci.* **2019**, *64* (3), 888−896.
(26) U.S. Drug Enforcement Administration. *National Drug Threat Assessment*; U.S. Department of Justice, U.S. Drug Enforcement Administration, 2025.
(27) Gao, Y.; Shirinichi, F.; Hansrisuk, A.; Zhu, R.; Xian, S.; Lieberman, M.; Webber, M. J.; Wang, Y. A Supramolecular−Quantum Dot System for Broad-Spectrum Detection of Fentanyl Analogs. *Small* **2025**, *21* (16), No. e2407702.
(28) Yu, H.; Canoura, J.; Byrd, C.; Alkhamis, O.; Bacon, A.; Yan, A.; Sullenger, B. A.; Xiao, Y. Improving Aptamer Affinity and Determining Sequence-Activity Relationships via Motif-SELEX. *J. Am. Chem. Soc.* **2025**, *147*, 9472−9486.
(29) Szejtli, J. Introduction and General Overview of Cyclodextrin Chemistry. *Chem. Rev.* **1998**, *98* (5), 1743−1754.
(30) Fürer, A.; Marti, T.; Diederich, F.; Künzer, H.; Brehm, M. Structure-Function Relationships in the Complexation of Steroids by a Synthetic Receptor. *Helv. Chim. Acta* **1999**, *82* (11), 1843−1859.
(31) Barrow, S. J.; Kasera, S.; Rowland, M. J.; Del Barrio, J.; Scherman, O. A. Cucurbituril-Based Molecular Recognition. *Chem. Rev.* **2015**, *115* (22), 12320−12406.

https://doi.org/10.1021/acs.analchem.6c03173
Anal. Chem. XXXX, XXX, XXX−XXX

Supporting Information for:

A Selective, Class-Specific Aptamer for Fentanyl Analog Screening

Linlin Wang,[1†] Gabriel Castro,[1†] Obtin Alkhamis,[1] Madhu Sudhana Reddy Gangireddy[2], Konstantin V. Bukhryakov,[2] Nelson R. Vinueza[1,3] and Yi Xiao[1]*

1. Department of Chemistry, North Carolina State University, 2620 Yarbrough Drive, Raleigh, NC, USA, 27607. 2. Department of Chemistry and Biochemistry, Florida International University, 11200 SW 8th Street, Miami, FL, USA, 33199. 3. Department of Textile Engineering, Chemistry, Science, Wilson College of Textiles, North Carolina State University, Raleigh, NC, 27695, USA.

*Corresponding author: yxiao34@ncsu.edu

† These authors contributed equally to this work.

Table of Contents

Synthesis of X-732-91C. The synthesis of **X-732-91C** was adapted from a previously published procedure.[1]

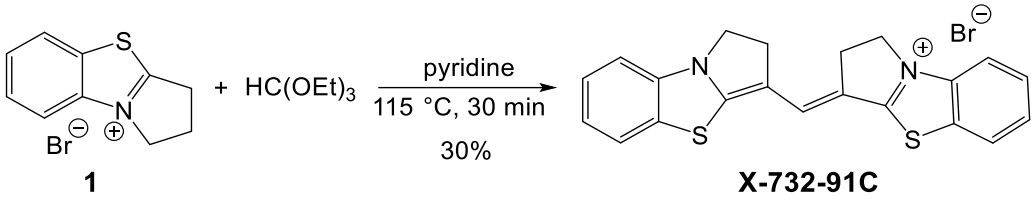

1 **X-732-91C**

Compound **1** was synthesized as described previously.[2] Triethyl orthoformate (0.5 ml, 444 mg, 3.00 mmol, 1.92 equiv.) was added to the suspension of **1** (400 mg, 1.56 mmol, 1.00 equiv.) in 4.0 ml of pyridine. The reaction mixture was refluxed under nitrogen for 30 min and then cooled to room temperature. The product was filtered off, washed with water, ethanol, and diethyl ether, and dried under vacuum to provide the product (105 mg, 30%).

^{1}H NMR (400 MHz; DMSO-d_6): δ 7.97 (d, *J* = 7.8 Hz, 2H), 7.69 (s, 1H), 7.52-7.44 (m, 4H), 7.32 (t, *J* = 7.5 Hz, 2H), 4.42 (t, *J* = 8.3 Hz, 4H), 3.63 (t, *J* = 8.1 Hz, 4H).

^{13}C NMR (101 MHz; DMSO-d_6): δ 166.3, 137.6, 132.9, 130.9, 128.4, 124.63, 124.53, 112.6, 108.9, 47.5, 30.7

Determining the molecular weight of X-732-91C dye using mass spectrometry. High-resolution mass spectrometry was performed using a Thermo Fisher Scientific Ultimate 3000 system coupled with an Exactive Plus Orbitrap mass spectrometer. A stock solution of 500 µM dye in methanol was diluted 100-fold in methanol, and a 2 µL aliquot of the diluted sample was injected at a flow-rate of 0.2 mL/min. Chromatographic separation was achieved on a Hypersil Gold C18 column (50 × 2.1 mm, 1.9 µm) using gradient elution with water containing 0.1% formic acid (mobile phase A) and methanol (mobile phase B), following a program of 20% B (0–0.5 min), increasing to 90% B (0.5–3 min), maintained at 90% B (3–8 min), and returning to 20% B (8.1–10 min). Mass spectrometry detection was performed in positive ion mode with a scan range of m/z 250–600 and a resolution of 140,000 FWHM at m/z 200. The automatic gain control target was set at 1e6. Operational parameters included a sheath gas flow-rate of 30, an auxiliary gas flow-rate of 10, and a sweep gas flow-rate of 2. The capillary temperature was held at 320 °C, the S-lens RF level was adjusted to 55, and the auxiliary gas heater was maintained at 150 °C.

Exonuclease-based fluorescence assay. The exonuclease assay was performed as previously described.[3] Each aptamer (final concentration: 0.5 µM) was diluted in 10 mM Tris buffer (pH 7.4), heated to 95 °C for 10 min, and immediately cooled on ice for 1 min. 0.5 mM $MgCl_2$, 20 mM NaCl and 0.1 mg/mL BSA were then added. 5 µL of this aptamer solution was mixed with 20 µL of selection buffer containing (±)-cis-3-methyl fentanyl (final concentration: 100 µM) or potential interferents ((+)-methamphetamine, procaine, lidocaine, acetaminophen, cis-tramadol, methadone, codeine, morphine, benzocaine, diphenhydramine, cocaine, heroin, (+)-pseudoephedrine, metamizole, lactose, mannitol, or caffeine) at a final concentration of 250 µM. Other interferents were included at lower concentrations, including chlorpromazine and quinine (100 µM) and papaverine, noscapine, and lorazepam (50 µM), with the latter three dissolved in buffer containing 1% methanol. The mixture was incubated at 25 °C for 30 min before initiating the digestion

reaction by adding 25 μL of exonuclease solution containing T5 Exo and Exo I (final concentrations: 0.2 U/μL and 0.015 U/μL, respectively) in selection buffer supplemented with 0.1 mg/mL BSA. 5 μL aliquots were collected at various timepoints and immediately quenched in 30 μL of quenching solution (10 mM Tris, 1.16× SYBR Gold, 25 mM EDTA, and 14.6% (v/v) formamide) in a 384-well black microplate. SYBR Gold fluorescence was measured using a Tecan Spark plate reader (excitation wavelength: 495 nm, emission wavelength: 537 nm, bandwidth: 5 nm). Fluorescence intensity was plotted over time to generate digestion time-course curves for each sample. Enzymatic inhibition was quantified using the resistance value, calculated as $(AUC_t/AUC_0) - 1$, where AUC_t and AUC_0 represent the areas under the fluorescence curve with and without the target, respectively. The integration time for each aptamer was customized and defined as the point where fluorescence dropped to 10% of its initial value. Each fluorescence measurement was recorded 10 times, and the average values were used for analysis.

References

(1) Babichev, F. S.; Shchetsinskaya, E. Mono-, Tri- and Pentamethinecyanines from 2,3-(Polymethylene)Benzothiazolium Salts. *Zh. Obshch. Khim.* **1964**, *34*, 2441–2448.

(2) Tomilov Y. V.; Platonov D. N.; Frumkin A. E.; Lipilin D. L.; Salikov R. F. Synthesis of condensed heterocycles via cyclopropylimine rearrangement of cyclopropylazoles. *Tet. Lett.*, **2010**, 51, 5120–5123. DOI: 10.1016/j.tetlet.2010.07.096

(3) Canoura, J.; Yu, H.; Alkhamis, O.; Roncancio, D.; Farhana, R.; Xiao, Y. Accelerating Post-SELEX Aptamer Engineering Using Exonuclease Digestion. *J. Am. Chem. Soc.* **2021**, *143*, 805–816. DOI: 10.1021/jacs.0c09559

(4) Hayes, K. L.; Lieberman, M. Assessment of Two Brands of Fentanyl Test Strips with 251 Synthetic Opioids Reveals “Blind Spots” in Detection Capabilities. *Harm Reduct. J.* **2023**, *20*, 175. DOI: 10.1186/s12954-023-00911-w

Table S1. Sequences of oligonucleotides used in this work.

Seq. ID	Sequence (5' to 3')
cDNA 15	TTTTTGTCGTAAGTTCTGCCATTTT/3BioTEG/
Library	CGAGCATAGGCAGAACTTACGAC (N30) GTCGTAAGAGCGAGTCATTC
FP	CGAGCATAGGCAGAACTTAC
RP-bio	/5Biosg/GAATGACTCGCTCTTACGAC
FP-HTS	ACACTCTTTCCCTACACGACGCTCTTCCGATCT (N45) CGAGCATAGGCAGAACTTAC
RP-HTS	GACTGGAGTTCAGACGTGTGCTCTTCCGATCT (N43) GAATGACTCGCTCTTACGAC
MF1	CTTACGACCTAGCAAGGGGGTTTCGGTGGGCAGGTGTGGTCGTAAG
MF2	CTTACGACGGGAGGTGTTTGCACTAAGTCCGGTTTTCCGTCGTAAG
MF2-mut	CTTACGACGGGAGGTGTTTGCACTAAGTCCGGTTTCCCGTCGTAAG
MF3	CTTACGACTGGCGCACAGGTTCGGGTTTCCTACAGAAGTCGTAAG
MF4	CTTACGACTCGAGGTGTCCTGCTAGGTGGTTCGGTTGAGTCGTAAG
MF5	CTTACGACAGGGTGGCAAAGGGTCGGGTGTGGGAAAGCTGTCGTAAG

/3BioTEG/ and /5Biosg/ = 3′ and 5′ biotin modification, respectively. Mutated nucleotide is labeled red.

Table S2. SELEX conditions for selecting fentanyl analog aptamers.

Round	Pool size (pmol)	# Washes Before	Counter-targets	# Washes After	(±)-cis-3mF Conc. (μM)
1	1,000	10×	NA	NA	100
2	400	20×	50 μM NOS (250 μL×3), 50 μM PAP (250 μL×3),50 μM LOR (250 μL×3),100 μM CPZ (250 μL×3),100 μM METH (250 μL×3),100 μM PRO (250 μL×3),100 μM LID (250 μL×3),100 μM ACM (250 μL×3),100 μM TRD (250 μL×3),100 μM MTD (250 μL×3),100 μM COD (250 μL×3),100 μM MOR (250 μL×3),100 μM G1 (250 μL×3), 100 μM G2 (250 μL×3), 100 μM G3 (250 μL×3), 100 μM G4 (250 μL×3)	20×	100
3	300	30×	The same as previous round	30×	100
4	300	30×	50 μM NOS (250 μL×3),50 μM PAP (250 μL×3), 50 μM LOR (250 μL×3), 100 μM CPZ (250 μL×3),250 μM METH (250 μL×3),250 μM PRO (250 μL×3), 250 μM LID (250 μL×3), 250 μM ACM (250 μL×3) , 250 μM TRD (250 μL×3), 250 μM MTD (250 μL×3), 250 μM COD (250 μL×3), 250 μM MOR (250 μL×3), G1 (100 μM quinine, 250 μM other, 250 μL×3), 250 μM G2 (250 μL×3) , 250 μM G3 (250 μL×3), 250 μM G4 (250 μL×3)	30×	50
5	300	30×	The same as previous round	30×	50
6	300	30×	The same as previous round	30×	50
7	300	30×	The same as previous round	30×	50
8	300	30×	50 μM NOS (250 μL×3),50 μM PAP (250 μL×3), 50 μM LOR (250 μL×3), 100 μM CPZ (250 μL×3),250 μM METH (250 μL×3),250 μM PRO (250 μL×3), 250 μM LID (250 μL×3), 250 μM ACM (250 μL×3), 250 μM TRD (250 μL×3), 250 μM MTD (250 μL×3), 250 μM COD (250 μL×3), 250 μM MOR (250 μL×3), 100 μM Quinine (250 μL×3),250 μM BNZ (250 μL×3),250 μM DPH (250 μL×3), 250 μM COC (250 μL×3), 250 μM HER (250 μL×3), 250 μM PSU (250 μL×3), 250 μM MET (250 μL×3), 250 μM LAC (250 μL×3), 250 μM MAN(250 μL×3), 250 μM CAF(250 μL×3)	30×	5
9	300	30	The same as previous round	30	1
10	300	30	The same as previous round	30	0.2
11	300	30	The same as previous round	30	0.2
12	300	30	The same as previous round	30	0.2
13	300	30	The same as previous round	30	0.2

NOS (Noscapine), PAP (Papaverine), LOR (Lorazepam), CPZ (Chlorpromazine), METH ((+)Methamphetamine), PRO (Procaine), LID (Lidocaine), ACM (Acetaminophen), TRD (cis-Tramadol), MTD (Methadone), COD (Codeine), MOR (Morphine), QUI (Quinine), BNZ (Benzocaine), DPH (Diphenhydramine), COC (Cocaine), HER (Heroin), PSU (Pseudoephedrine), MET (Metamizole), LAC (Lactose), MAN(Mannitol), CAF(Caffeine), G1 (QUI, BNZ, DPH), G2 (COC, HER), G3 (PSU, MET), G4 (LAC, MAN, CAF)

Table S3. Statistics for high-throughput sequencing of enriched SELEX pools.

Pool	Total Reads	Reads with Adapters	Total Sequences	Unique Sequences	Unique Sequences
R7	890,304	86.5%	767,622	287,258	37.4%
R13	579,046	96.7%	538,626	146,621	27.2%

Table S4. Aptamer affinity to fentanyl analogs determined by isothermal titration calorimetry.

Aptamer	Target (Analog #)	[Aptamer] (μM)	[Target] (μM)	K_D (nM)	ΔH (kcal/mol)	ΔS (cal/mol/K)
MF1	(±)-cis-3-methyl fentanyl (#**28**)	20	250	1,200 ± 200	-26.6 ± 0.8	-62.8
MF2		20	200	309 ± 9	-20.9 ± 0.1	-40.9
MF3		20	250	1,100 ± 100	-16.0 ± 0.3	-26.7
MF4		20	150	341 ± 25	-20.8 ± 0.2	-40.8
MF5		20	150	158 ± 20	-26.9 ± 0.3	-59.9
MF2-mut		20	150	73 ± 13	-19.8 ± 0.2	-34.2
MF2-mut	Acetyl norfentanyl (#**2**)	300	20	No Binding	N/A	N/A
	4-ANPP (#**10**)	300	20	684 ± 73	-15.3 ± 0.2	-23.3
	fentanyl (#**13**)	300	20	115 ± 8	-12.7 ± 0.1	-11.1
	norfentanyl (#**14**)	300	20	No Binding	N/A	N/A
	cyclopropyl fentanyl (#**15**)	300	20	74 ± 6	-12.6 ± 0.1	-9.8
	benzyl carfentanil (#**38**)	300	20	6,950 ± 1910	-3.4 ± 0.2	12.0
	(±)-cis-3-methyl thiofentanyl (#**80**)	300	20	378 ± 27	-12.1 ± 0.1	-11.3
	para-fluoro cyclopentyl fentanyl (#**92**)	300	20	1,170 ± 200	-3.8 ± 0.1	14.5
	ortho-methyl phenyl fentanyl (#**93**)	300	20	636 ± 52	-9.1 ± 0.1	-2.2
	para-chloro furanyl fentanyl (#**100**)	300	20	781 ± 91	-5.4 ± 0.1	9.8
	para-chloro cyclopentyl fentanyl (#**106**)	300	20	985 ± 67	-5.9 ± 0.1	7.6
	(±)-cis-Isofentanyl (#**125**)	300	20	3,040 ± 227	-10.6 ± 0.2	-10.4
	para-fluoro 4-ANBP (#**131**)	300	20	1,370 ± 96	-9.1 ± 0.1	-3.7
	Despropionyl para-Fluorofentanyl (#**132**)	300	20	889 ± 61	-9.3 ± 0.1	-3.8
	Despropionyl meta-Methylfentanyl (#**133**)	300	20	3,470 ± 473	-14.1 ± 0.4	-22.4
	despropionyl 2'-fluoro ortho-fluorofentanyl (#**135**)	300	20	1,040 ± 70	-9.4 ± 0.1	-4.2
	para-bromo fentanyl (#**138**)	300	20	709 ± 70	-9.4 ± 0.1	-3.7
	para-toluoyl fentanyl (#**139**)	300	20	188 ± 16	-10.6 ± 0.1	-5.0
	N-(2C-B) Fentanyl (#**147**)	300	20	No Binding	N/A	N/A
	N-(2C-D) Fentanyl (#**151**)	300	20	24,500 ± 10,200	-5.6 ± 0.3	2.2
	N-(2C-G) fentanyl (#**152**)	300	20	No Binding	N/A	N/A
	N-(DOC) Fentanyl (#**164**)	300	20	23,200 ± 11600	-9.7 ± 1.1	-11.6
	N-(DOM) Fentanyl (#**167**)	300	20	26,900 ± 4340	-4.7 ± 0.5	5.2

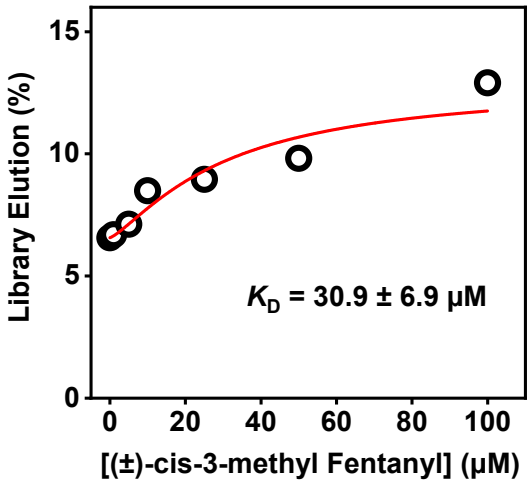

Figure S1. Binding affinity of the Round 13 SELEX pool to (±)-cis-3-methyl fentanyl, as determined using a gel elution assay.

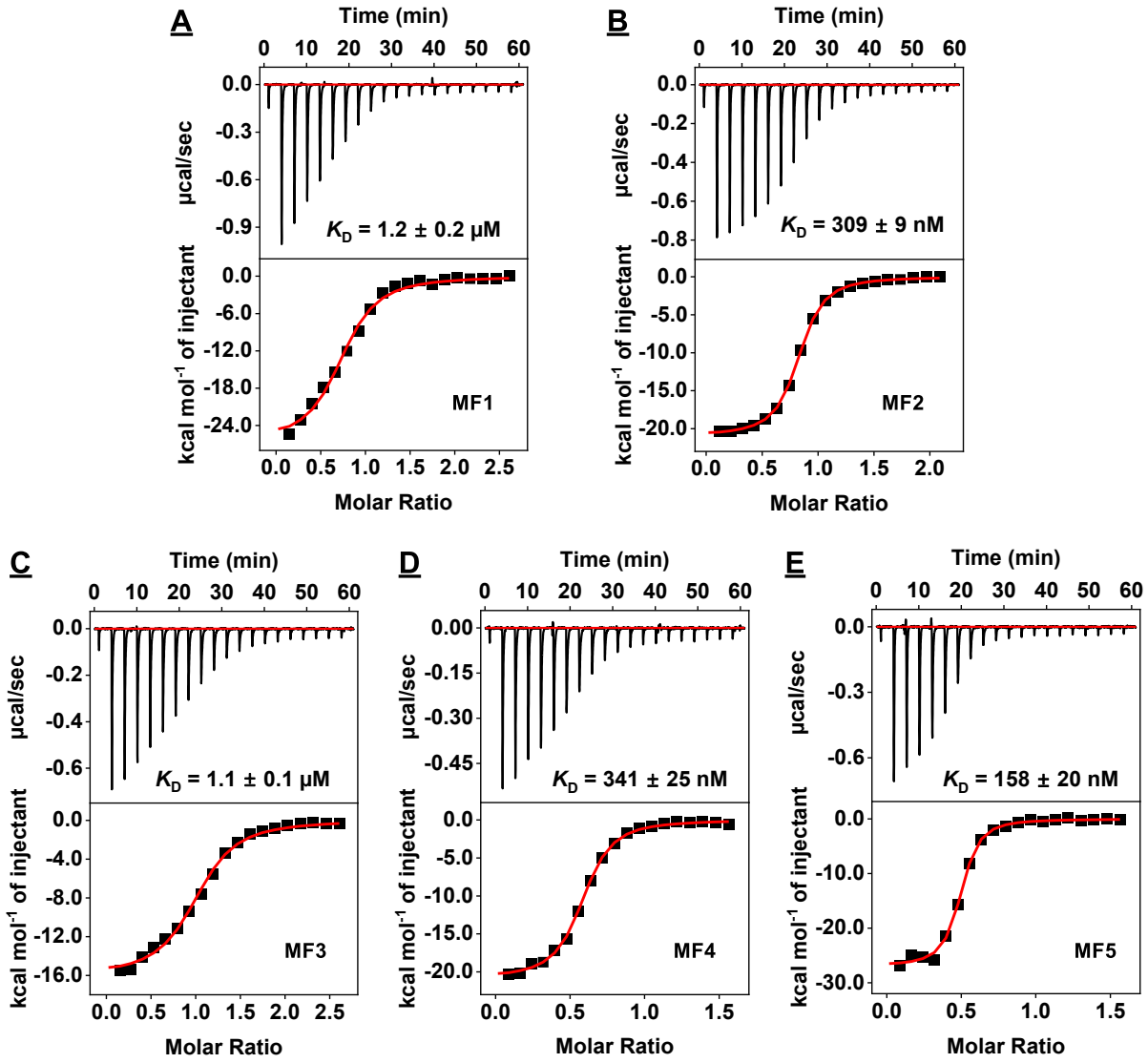

Figure S2. Binding affinity of aptamers to (±)-cis-3-methyl fentanyl using isothermal titration calorimetry (ITC). Top panels display the heat generated from each titration of (±)-cis-3-methyl fentanyl into (**A**) MF1, (**B**) MF2, (**C**) MF3, (**D**) MF4, and (**E**) MF5, respectively. Bottom panels show the integrated heat of each titration after correcting for the heat of dilution of the titrant.

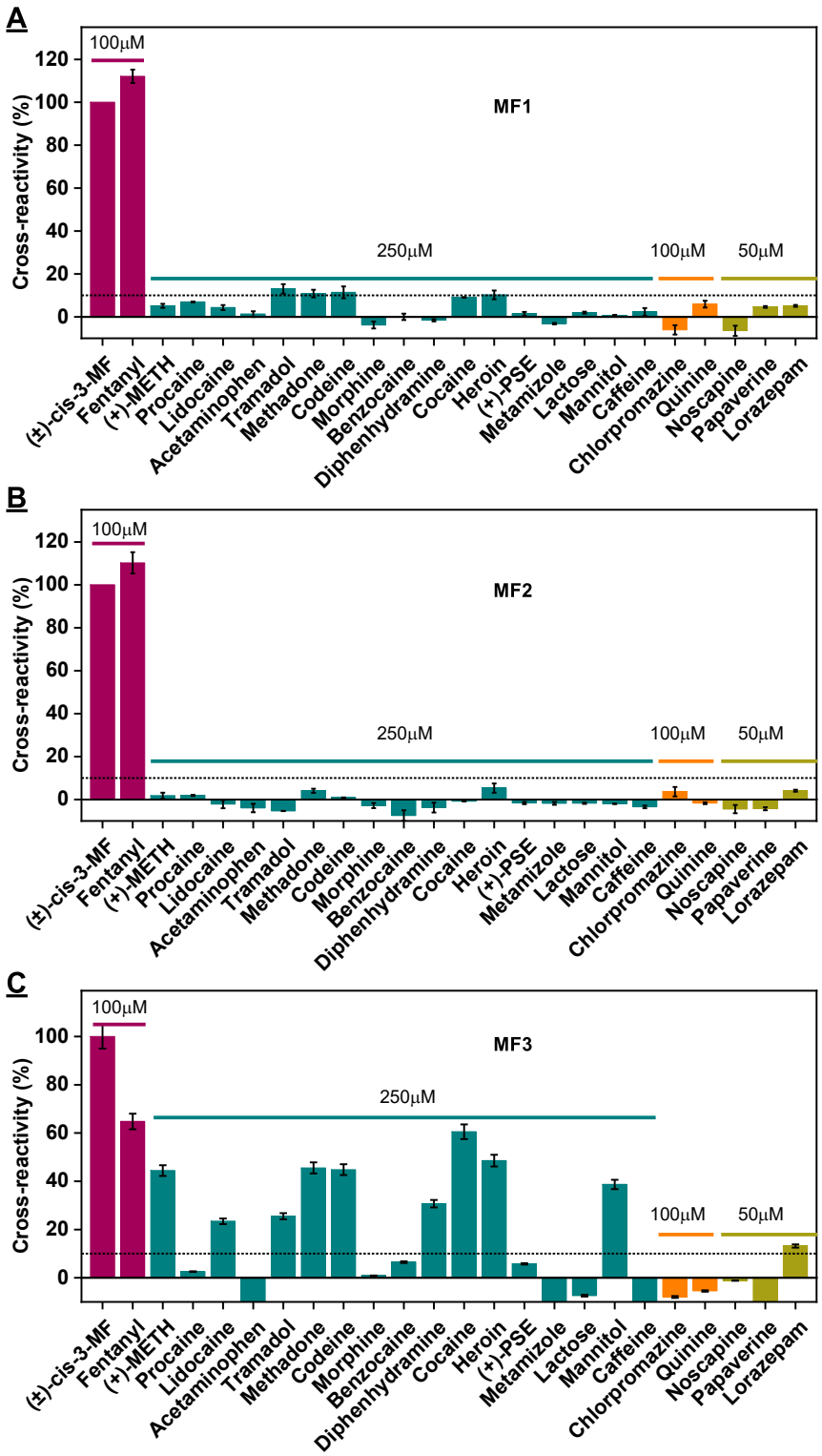

Figure S3. Determining the specificity of aptamers using an exonuclease-based fluorescence assay. Specificity data for (**A**) MF1, (**B**) MF2, and (**C**) MF3. Dashed line indicates a threshold of 10% cross-reactivity. Abbreviations: (±)-cis-3-MF: (±)-cis-3-methyl fentanyl, (+)-METH: (+)-methamphetamine, PSE: (+)-pseudoephedrine.

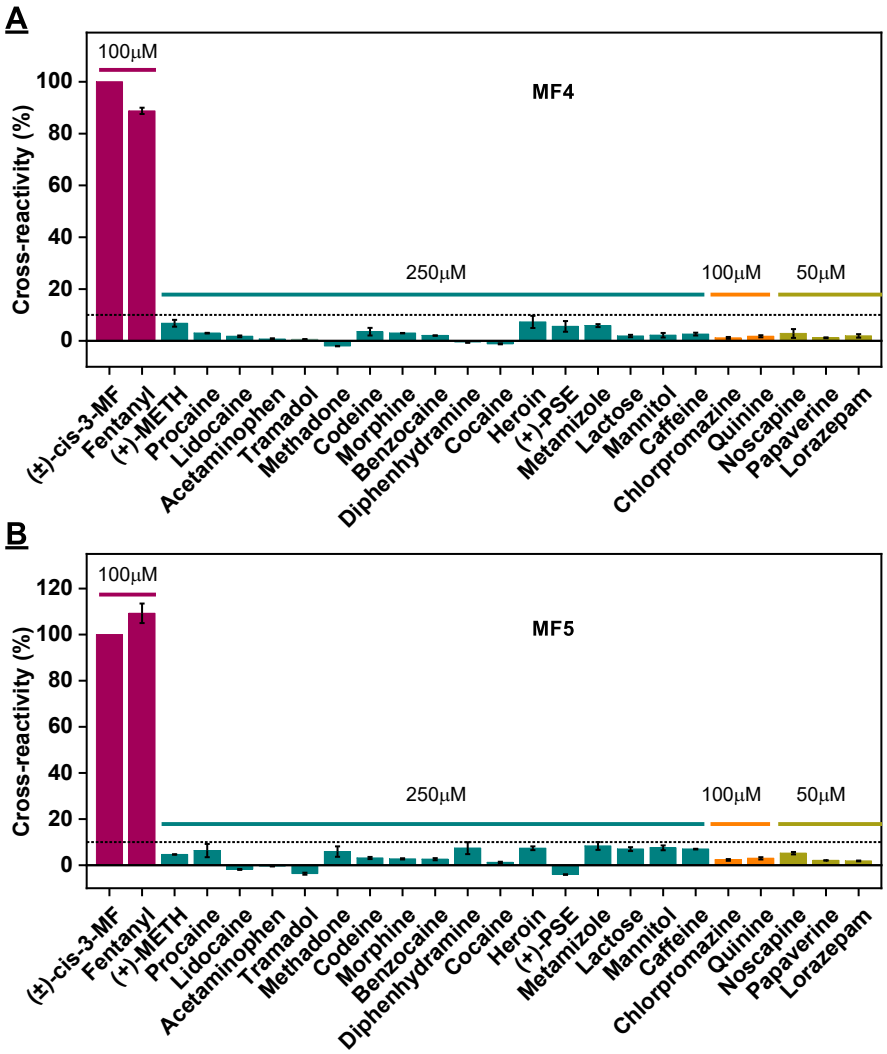

Figure S4. Determining the specificity of aptamers using an exonuclease-based fluorescence assay. Specificity data for (**A**) MF4 and (**B**) MF5. Dashed line indicates a threshold of 10% cross-reactivity Abbreviations: (±)-cis-3-MF: (±)-cis-3-methyl fentanyl, (+)-METH: (+)-methamphetamine, PSE: (+)-pseudoephedrine.

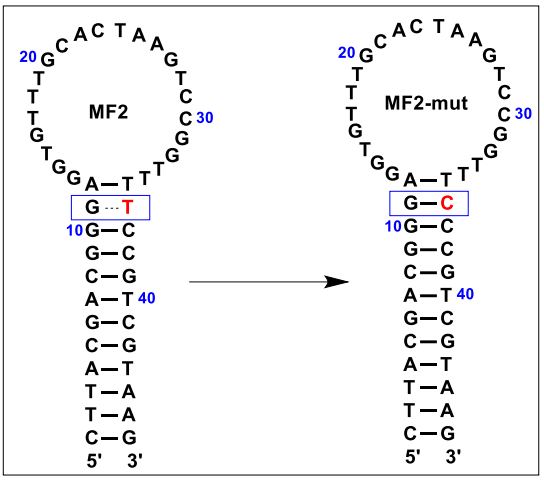

Figure S5. Secondary structure of MF2 and MF2-mut, as predicted by NUPACK.

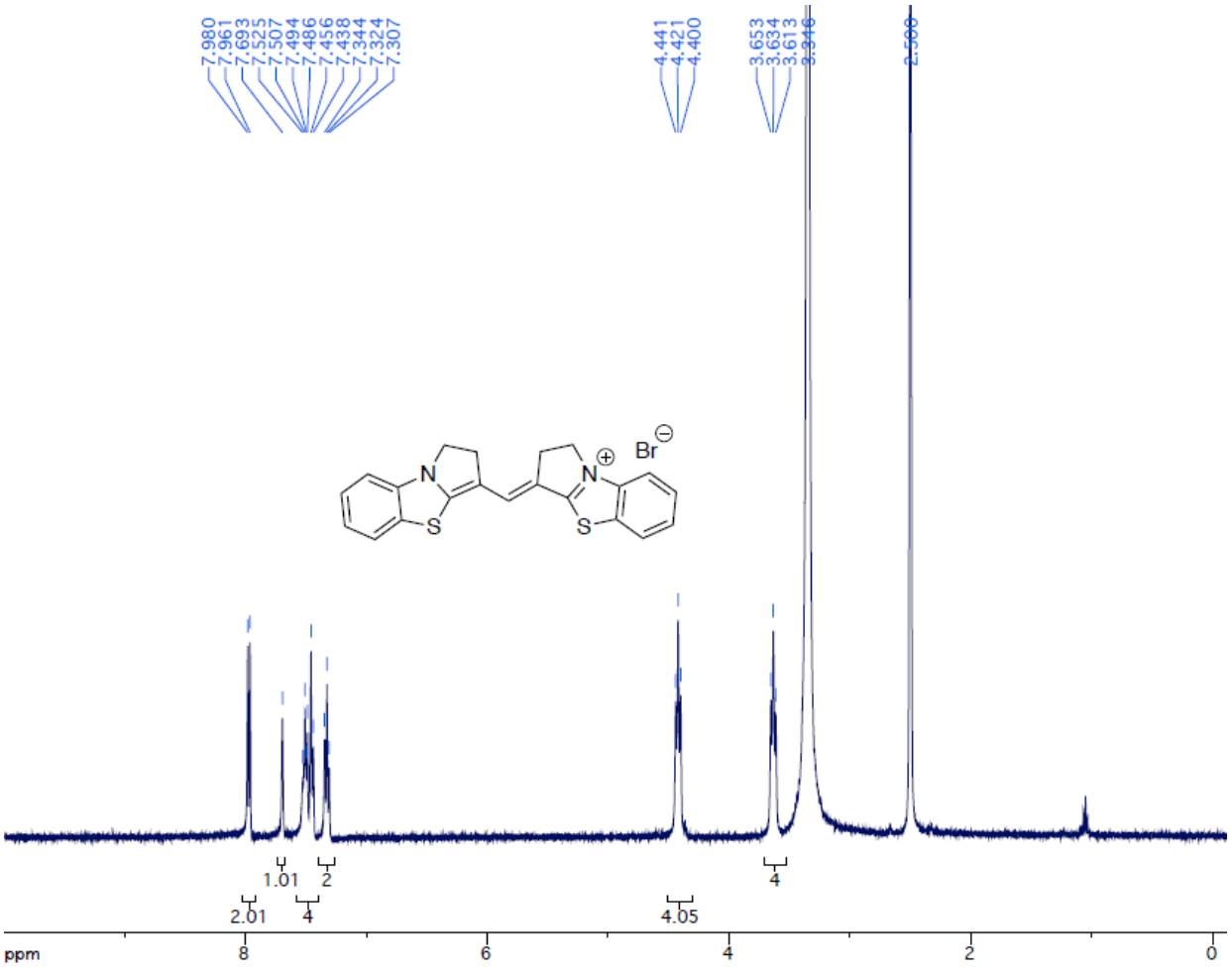

Figure S6. ^{1}H NMR spectrum of X-732-91C (DMSO-d_6, 400 MHz, 22°C).

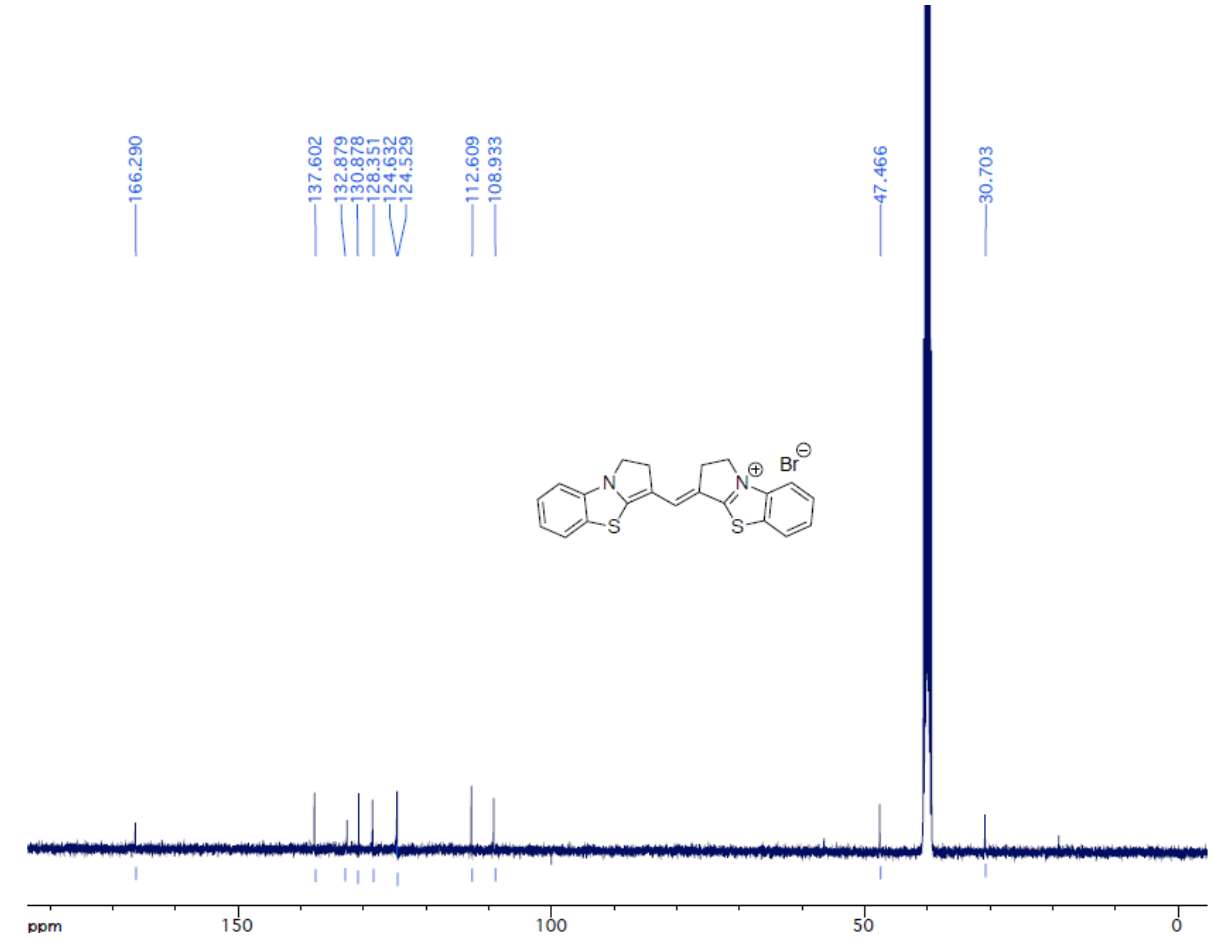

Figure S7. ^{13}C NMR spectrum of X-732-91C (DMSO-d_6, 101 MHz, 22°C).

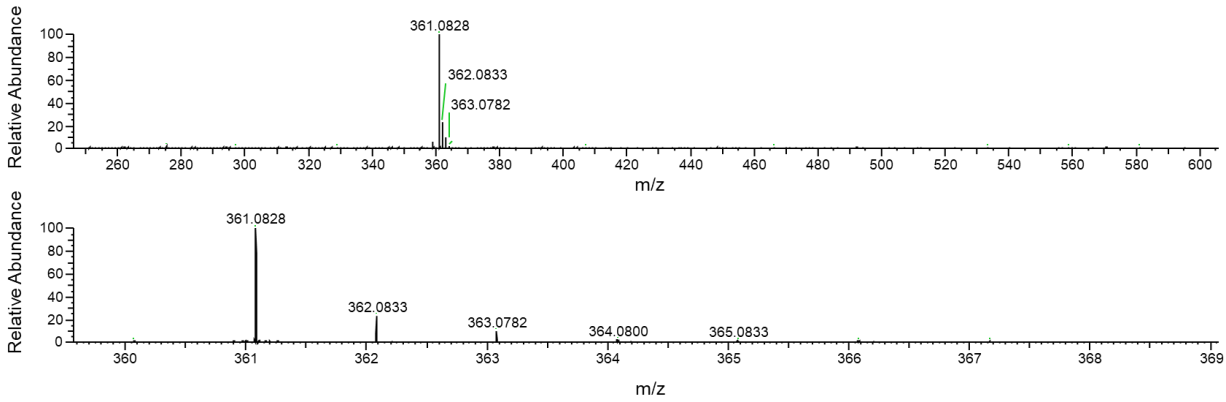

Figure S8. Mass spectra of X-732-91C runs in positive mode using a Thermo Fisher Scientific Ultimate 3000 system coupled with an Exactive Plus Orbitrap mass spectrometer. (**A**) The spectrum of X-732-91C. (**B**) A magnification of the spectrum in **A** from m/z 360–369. The cation of X-732-91C dye has an m/z of 361.0828 with an error of 0.083 ppm compared to its theoretical m/z of 361.08277, yielding a chemical formula of $C_{21}H_{17}N_2S_2^+$.

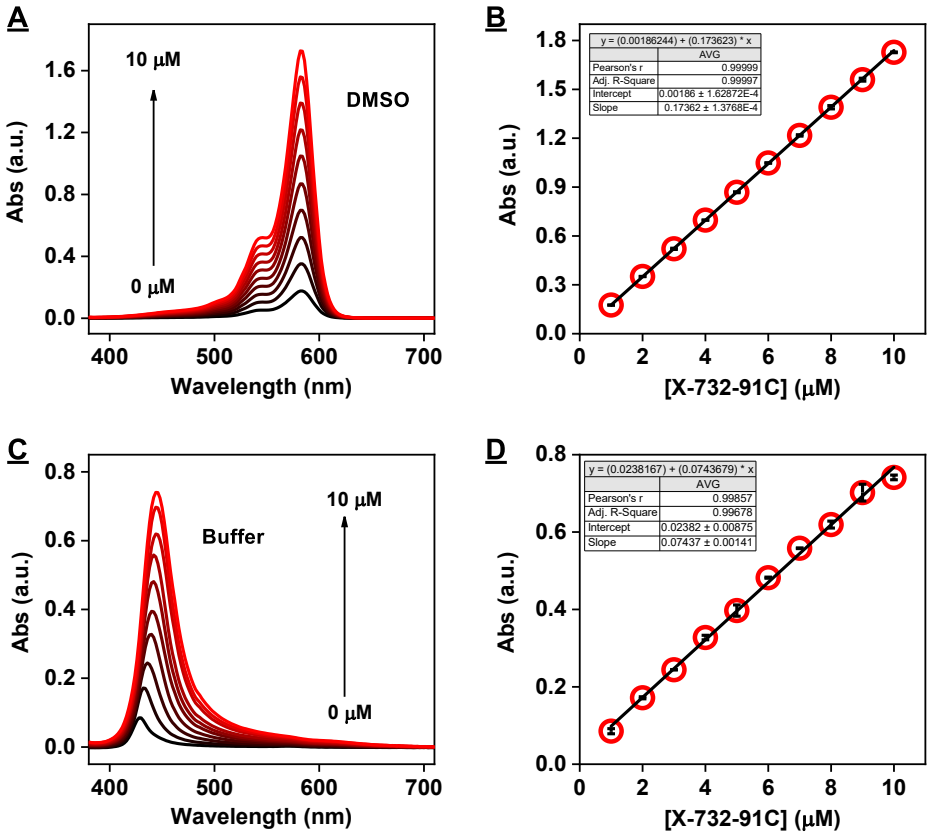

Figure S9. Determination of molar absorptivity of the dye X-732-91C. (**A**) Absorbance spectra of various concentrations of X-732-91C in pure DMSO. (**B**) Molar absorptivity was determined by plotting dye absorbance at 585 nm against dye concentration in the range of 1–10 µM. (**C**) Absorbance spectra of various concentrations of X-732-91C collected in 10 mM Tris buffer (pH 7.4) containing 20 mM NaCl, 0.5 mM $MgCl_2$, 2% DMSO, 0.01% SDS, and 0.001% Triton X-100. (**D**) Molar absorptivity was determined by plotting dye peak absorbance at 430 – 445 nm against concentration in the range of 1–10 µM. For panels **A** and **C**, black to red color gradient reflects increasing dye concentrations.

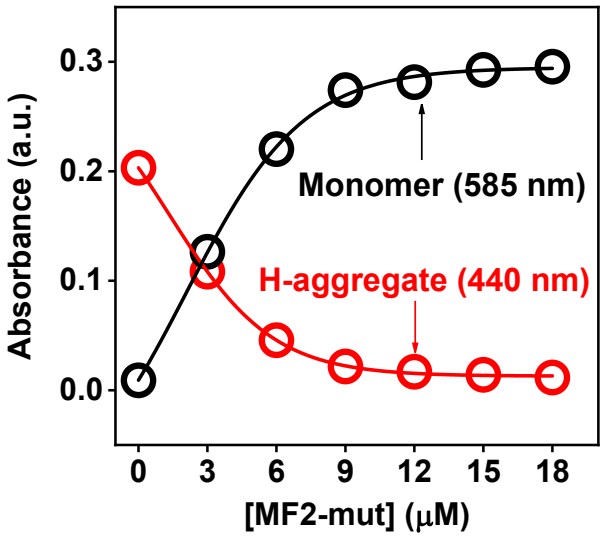

Figure S10. Optimization of aptamer concentration for the dye-displacement assay. Absorbance of X-732-91C at 440 nm and 585 nm plotted as a function of aptamer concentration.

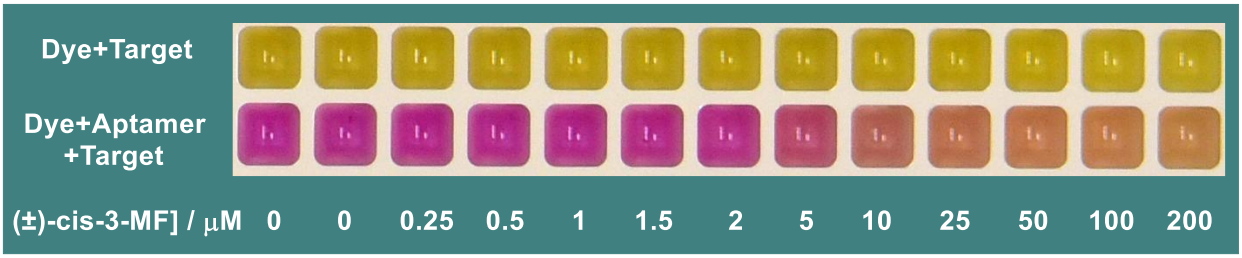

Figure S11. Photograph of (±)-cis-3-methyl fentanyl detection with the X-732-91C displacement assay taken 5 min after mixing the aptamer-dye complexes with target at various concentrations.

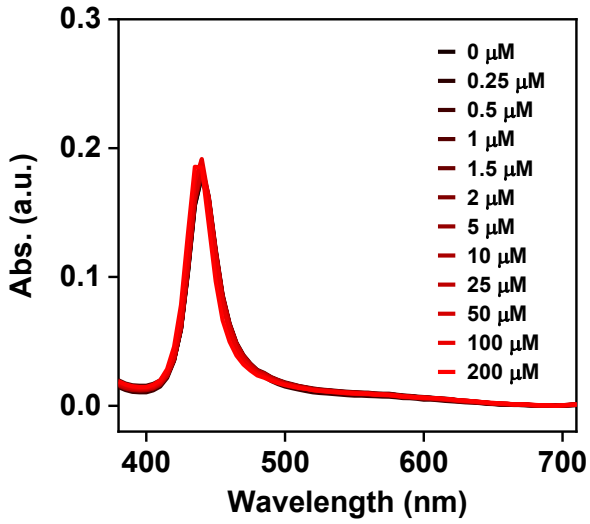

Figure S12. Control experiment for the dye-displacement assay. Plot shows the absorbance spectrum of 3 μM X-732-91C in the presence of various concentrations of (±)-cis-3-methyl fentanyl with no aptamer present.

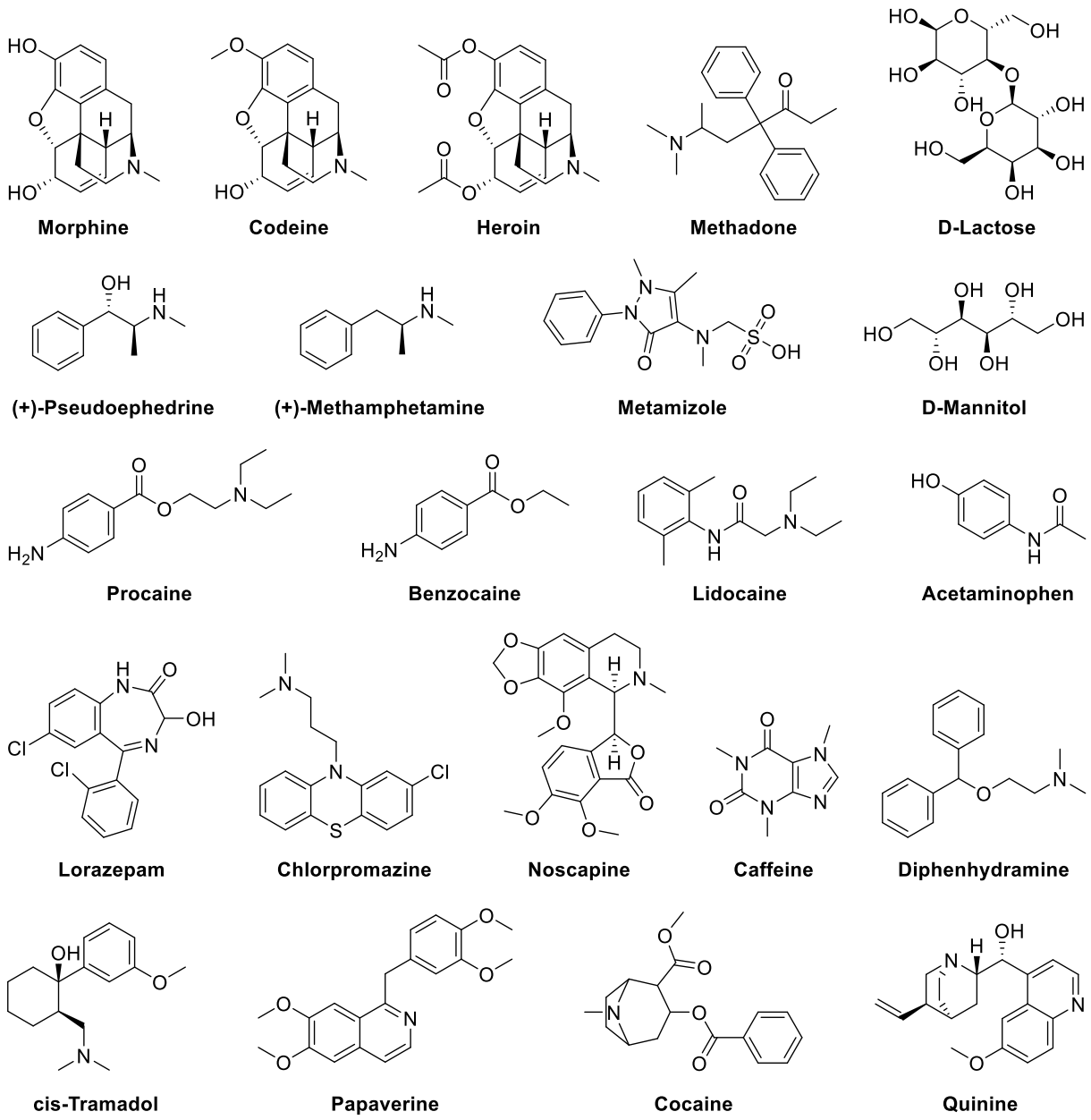

Figure S13. Structures of the interferent molecules employed in this work.

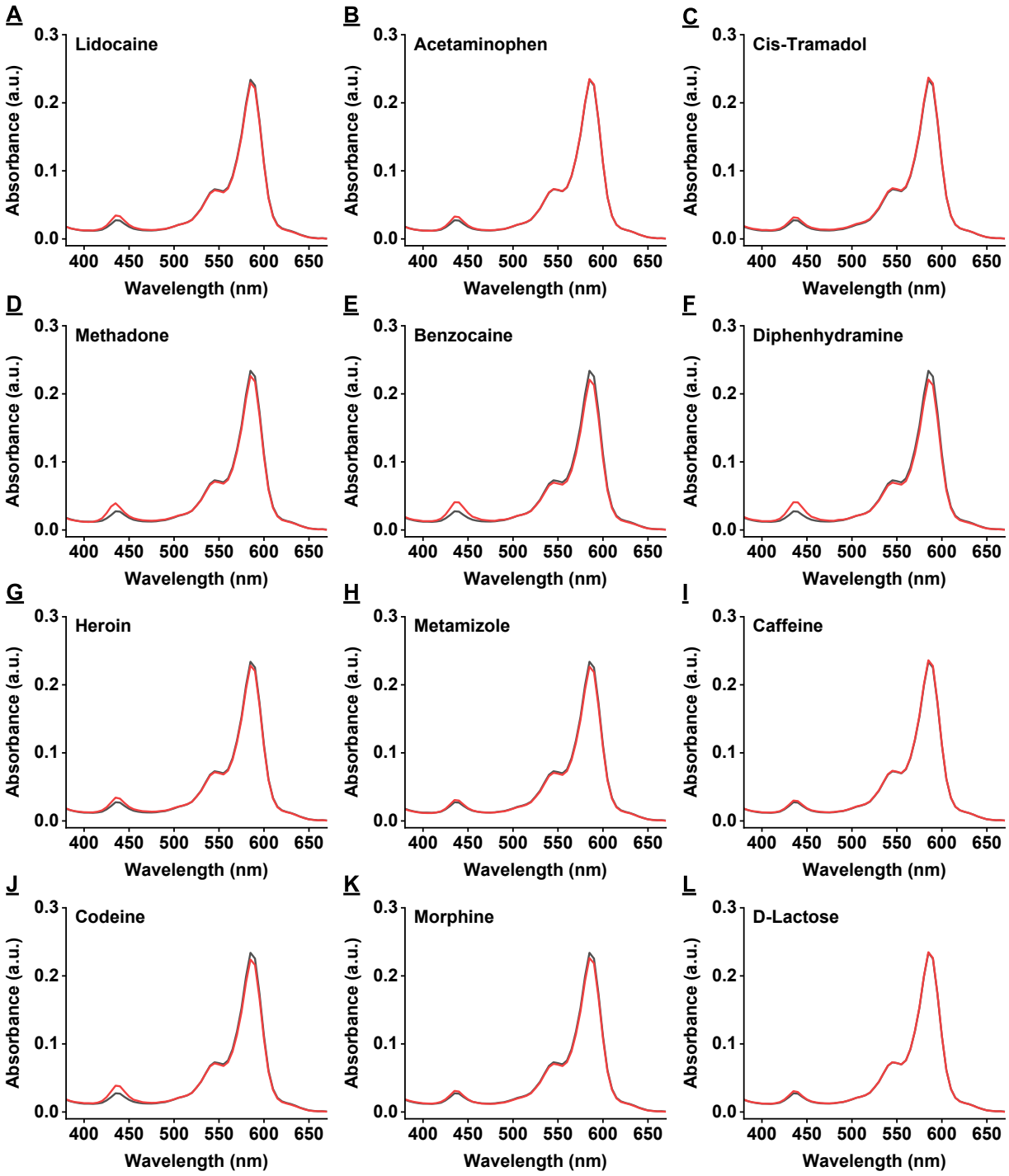

Figure S14. Absorbance spectra from the X-732-91C dye displacement assay with MF2-mut and interferents (**A**) lidocaine, (**B**) acetaminophen, (**C**) cis-tramadol, (**D**) methadone, (**E**) benzocaine, (**F**) diphenhydramine, (**G**) heroin, (**H**) metamizole, (**I**) caffeine, (**J**) codeine, (**K**) morphine, and (**L**) D-lactose. The red and black curves respectively indicate data for samples with and without ligand.

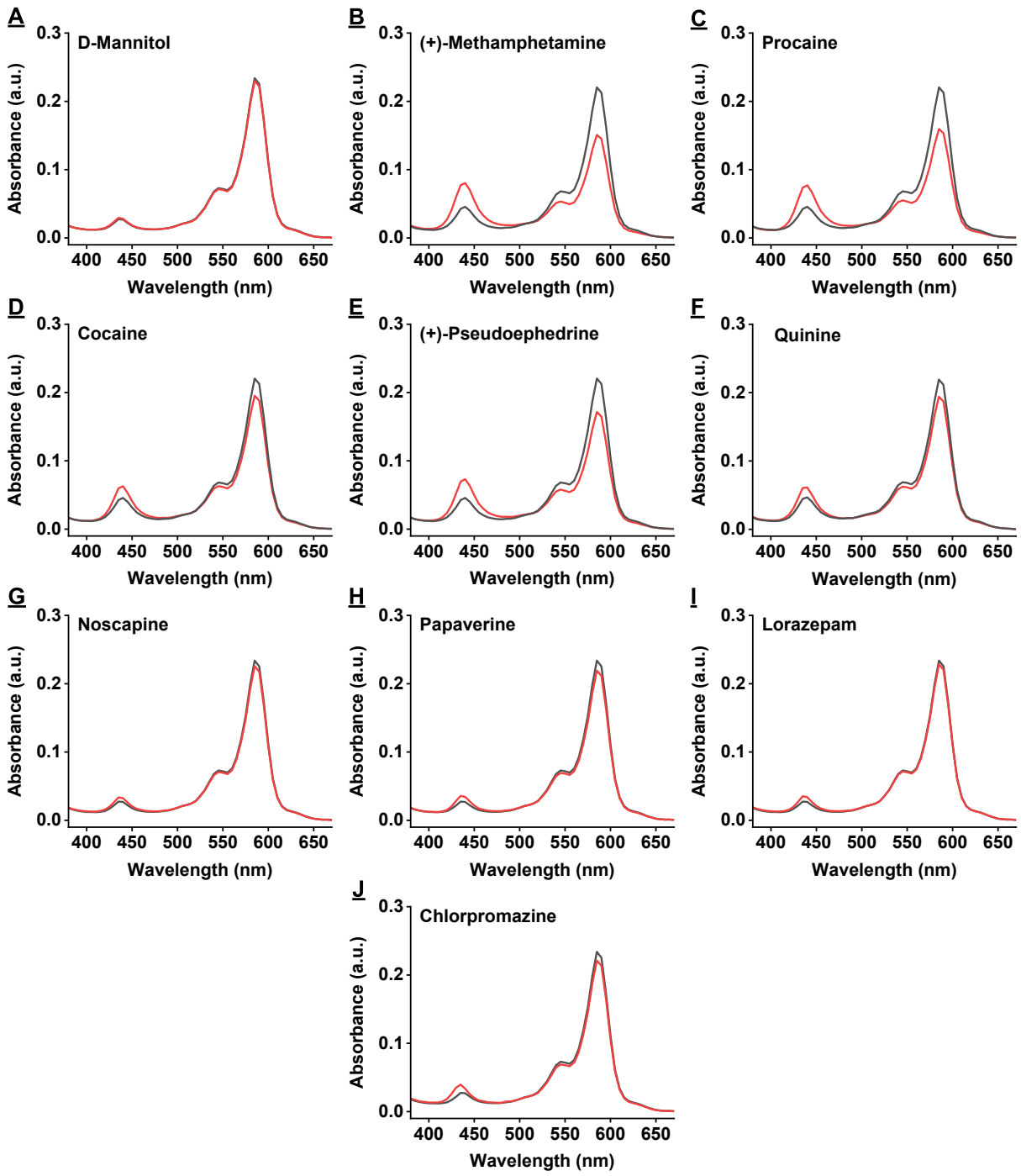

Figure S15. Absorbance spectra from the X-732-91C dye displacement assay with MF2-mut and interferents (**A**) D-mannitol, (**B**) (+)-methamphetamine, (**C**) procaine, (**D**) cocaine, (**E**) (+)-pseudoephedrine, (**F**) quinine, (**G**) noscapine, (**H**) papaverine, (**I**) lorazepam, and (**J**) chlorpromazine. The red and black curves respectively indicate data for samples with and without ligand.

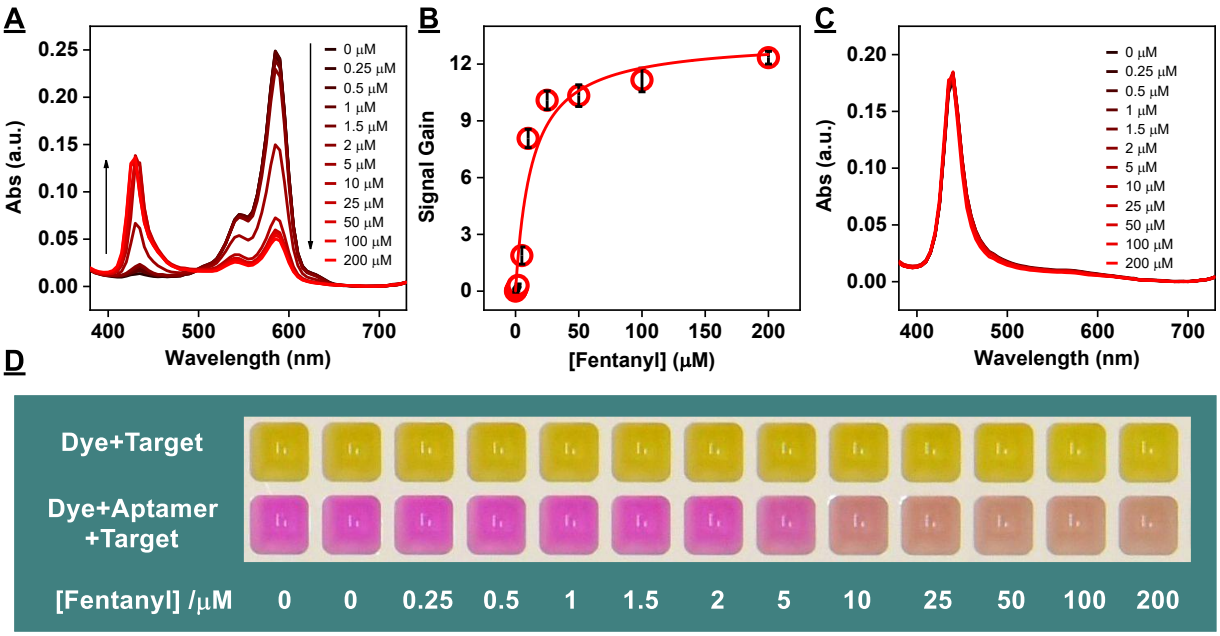

Figure S16. Detection of fentanyl using an aptamer-based dye displacement assay. (**A**) Absorbance spectra of solutions containing 3 μM X-732-91C and 9 μM MF2-mut challenged with 0, 0.25, 0.5, 1, 1.5, 2, 5, 10, 25, 50, 100, or 200 μM of fentanyl, where the black-to-red color gradient reflects increasing drug concentration. (**B**) Plot shows the corresponding calibration curve. (**C**) Absorbance spectra of 3 μM X-732-91C in the presence of 0, 0.25, 0.5, 1, 1.5, 2, 5, 10, 25, 50, 100, or 200 μM fentanyl with no aptamer present. Black-to-red color gradient represents increasing concentrations of fentanyl. (**D**) Photograph of fentanyl detection with the X-732-91C dye-displacement assay taken 5 min after mixing aptamer-dye complex with target. [MF2-mut] = 9.0 μM, [X-732-91C] = 3.0 μM.

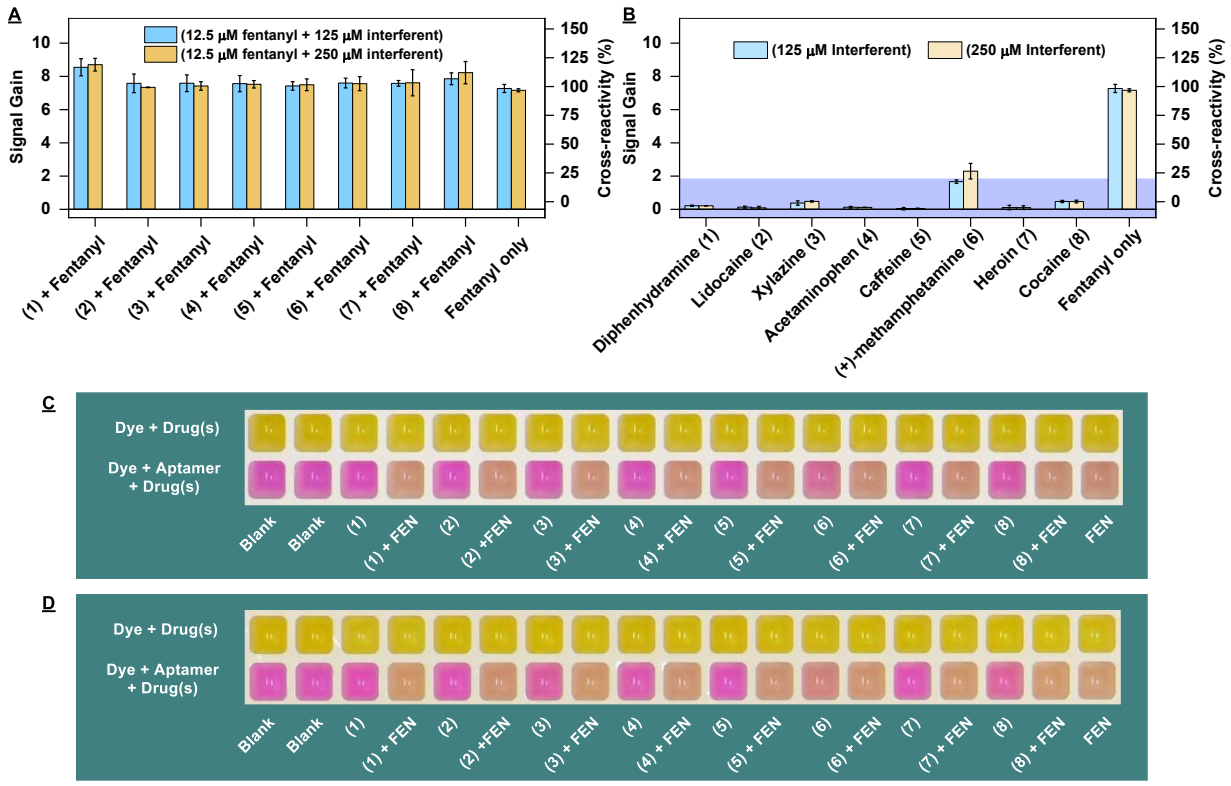

Figure S17. Detection of fentanyl in binary mixtures with our dye-displacement assay. (**A**) Assay response to binary mixtures containing 12.5 µM fentanyl with 125 µM or 250 µM interferent. (**B**) Assay response to 125 µM or 250 µM concentrations of various interferent molecules. 20% cross-reactivity is indicated by the blue region. (**C–D**) Photographs of assay challenged with buffer, 12.5 µM fentanyl, interferent alone, or a mixture of 12.5 µM fentanyl with interferent. Interferent concentration is 125 µM in **C** and 250 µM in **D**. Interferents are numbered as shown in **A**. For both **C** and **D**, the bottom row of samples contains aptamer-dye solution and the top row contains dye alone.

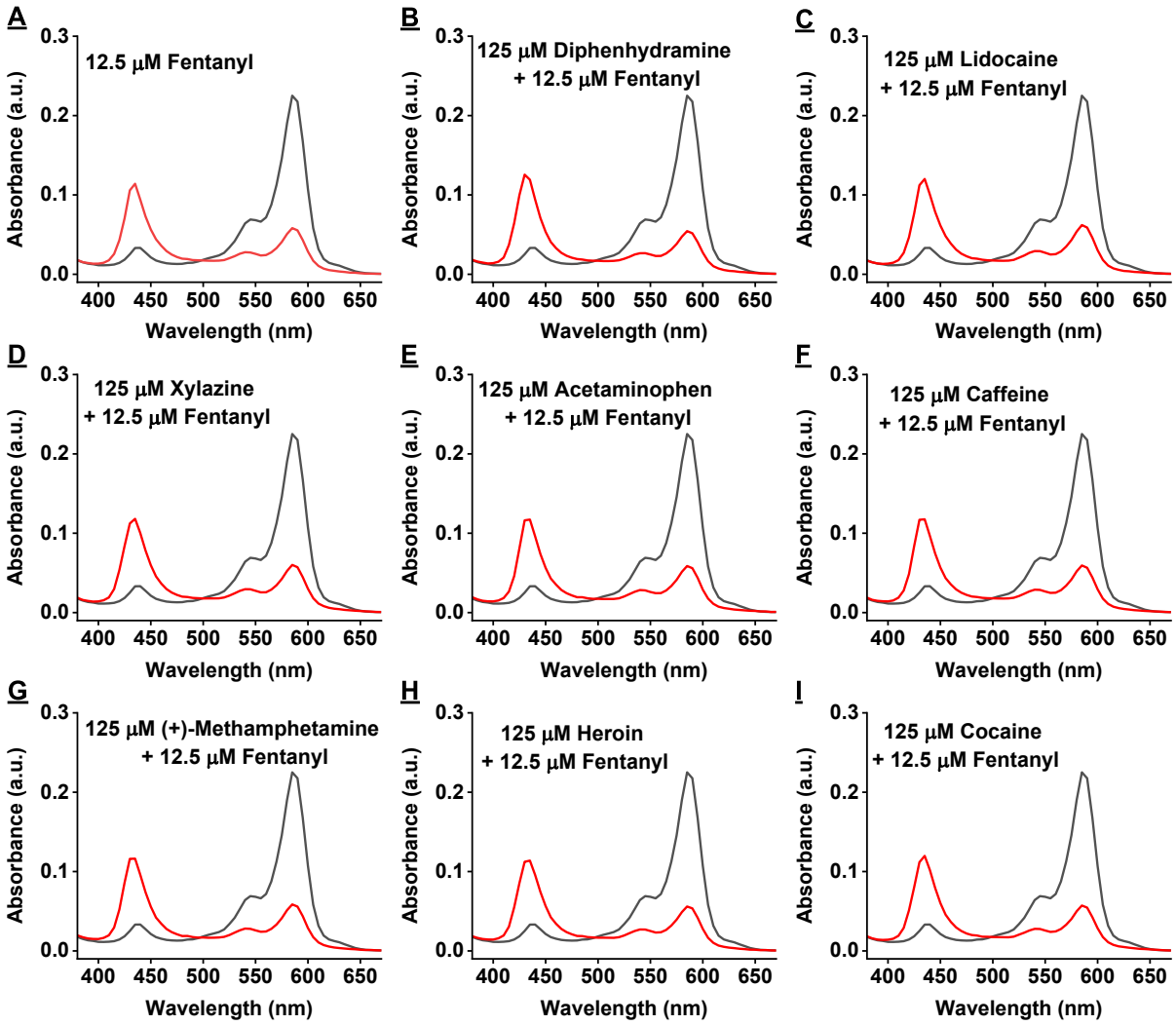

Figure S18. Detection of fentanyl in 10% binary mixtures with a dye-displacement assay based on X-732-91C and MF2-mut. Absorbance spectra of samples challenged with (**A**) fentanyl and binary mixtures of fentanyl with (**B**) diphenhydramine, (**C**) lidocaine, (**D**) xylazine, (**E**) acetaminophen, (**F**) caffeine, (**G**) (+)-methamphetamine, (**H**) heroin, (**I**) or cocaine. The red and black curves respectively indicate data for samples with and without target/interferent.

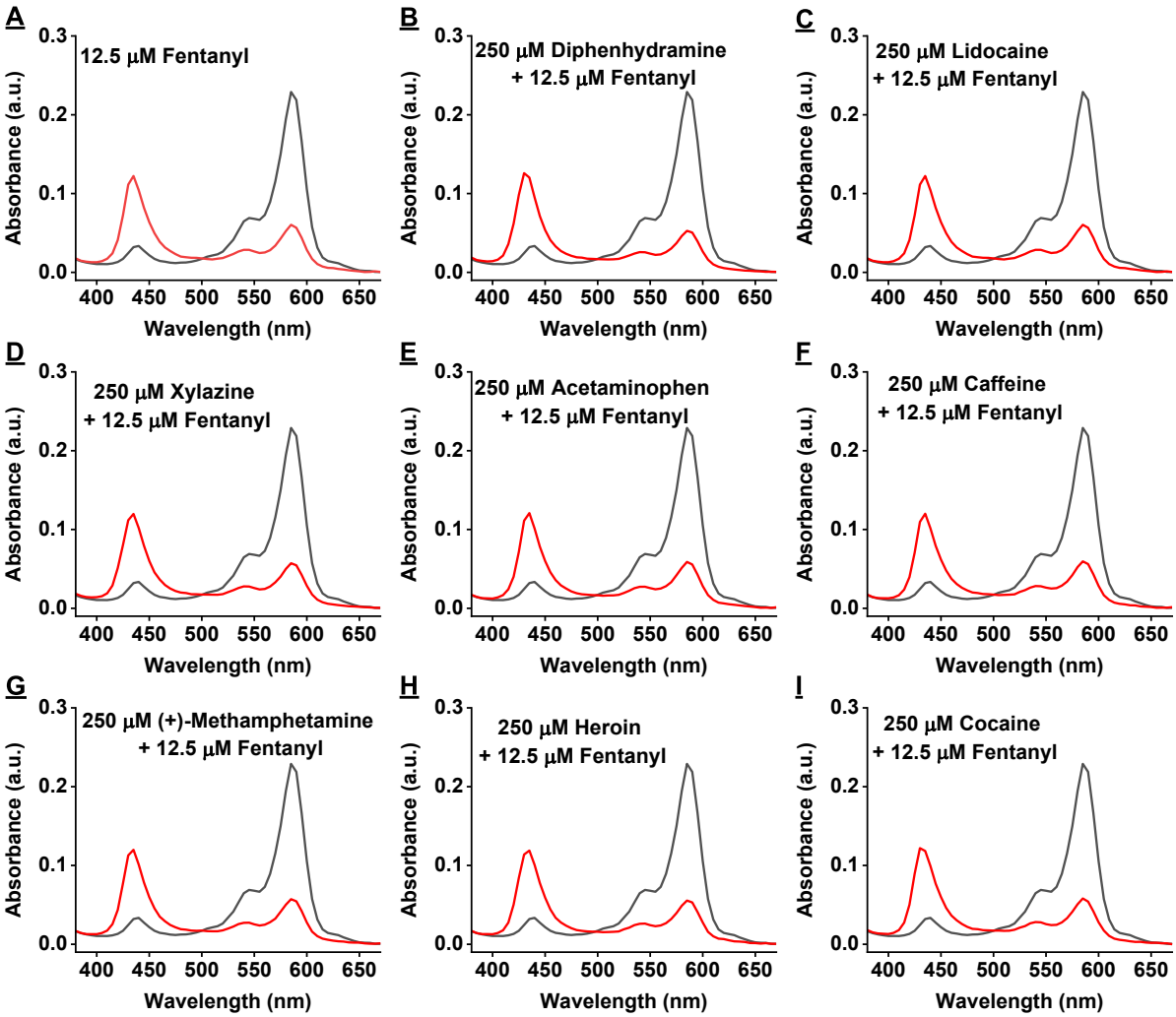

Figure S19. Detection of fentanyl in 5% binary mixtures with a dye-displacement assay based on X-732-91C and MF2-mut. Absorbance spectra of samples challenged with (**A**) fentanyl and binary mixtures of fentanyl with (**B**) diphenhydramine, (**C**) lidocaine, (**D**) xylazine, (**E**) acetaminophen, (**F**) caffeine, (**G**) (+)-methamphetamine, (**H**) heroin, or (**I**) cocaine. The red and black curves respectively indicate data for samples with and without target/interferent.

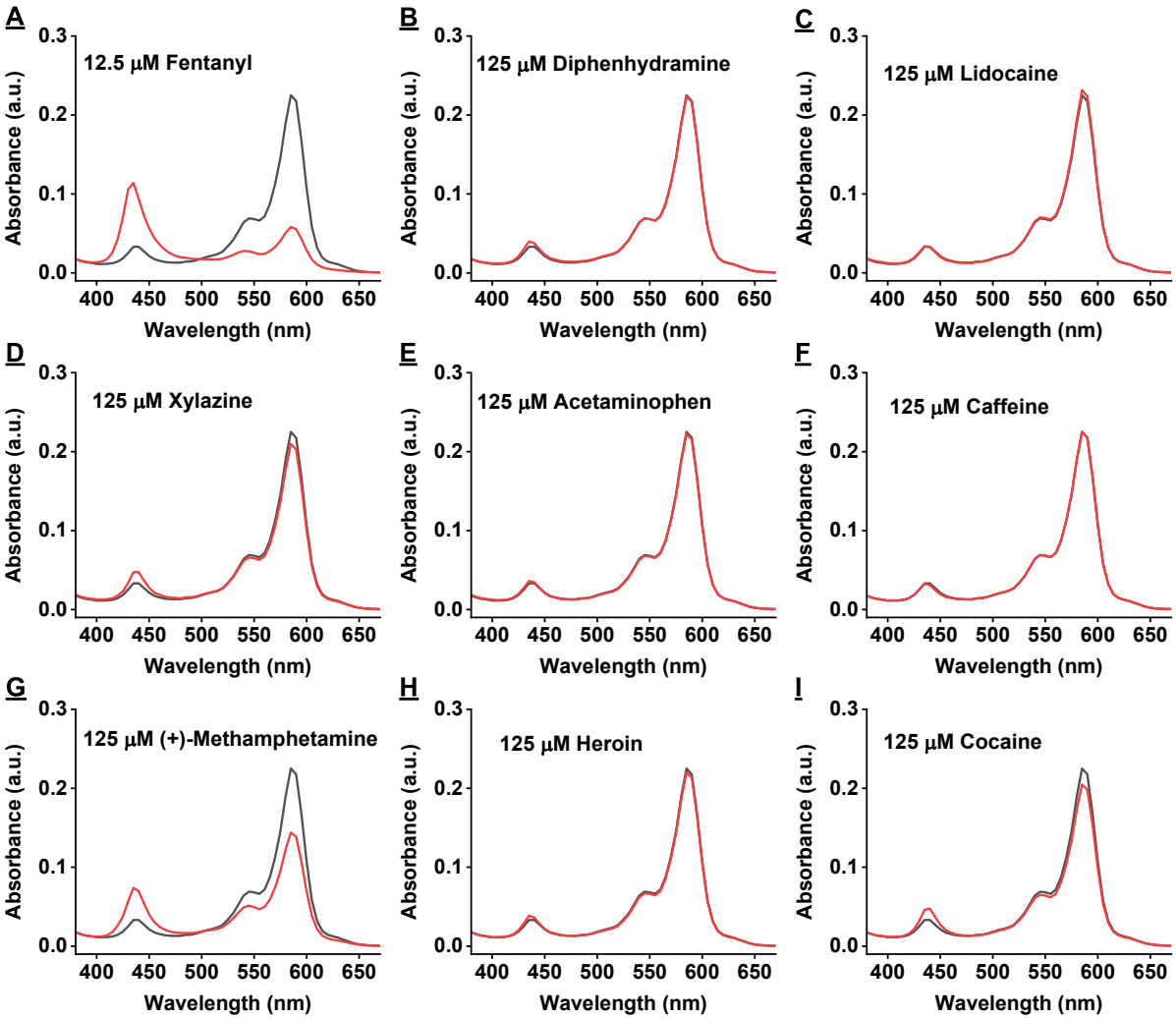

Figure S20. Specificity of dye-displacement assay based on X-732-91C and MF2-mut. Absorbance spectra of samples challenged with (**A**) 12.5 μM fentanyl, (**B**) 125 μM diphenhydramine, (**C**) 125 μM lidocaine, (**D**) 125 μM xylazine, (**E**) 125 μM acetaminophen, (**F**) 125 μM caffeine, (**G**) 125 μM (+)-methamphetamine, (**H**) 125 μM heroin, or (**I**) 125 μM cocaine. The red and black curves respectively indicate data for samples with and without target/interferent.

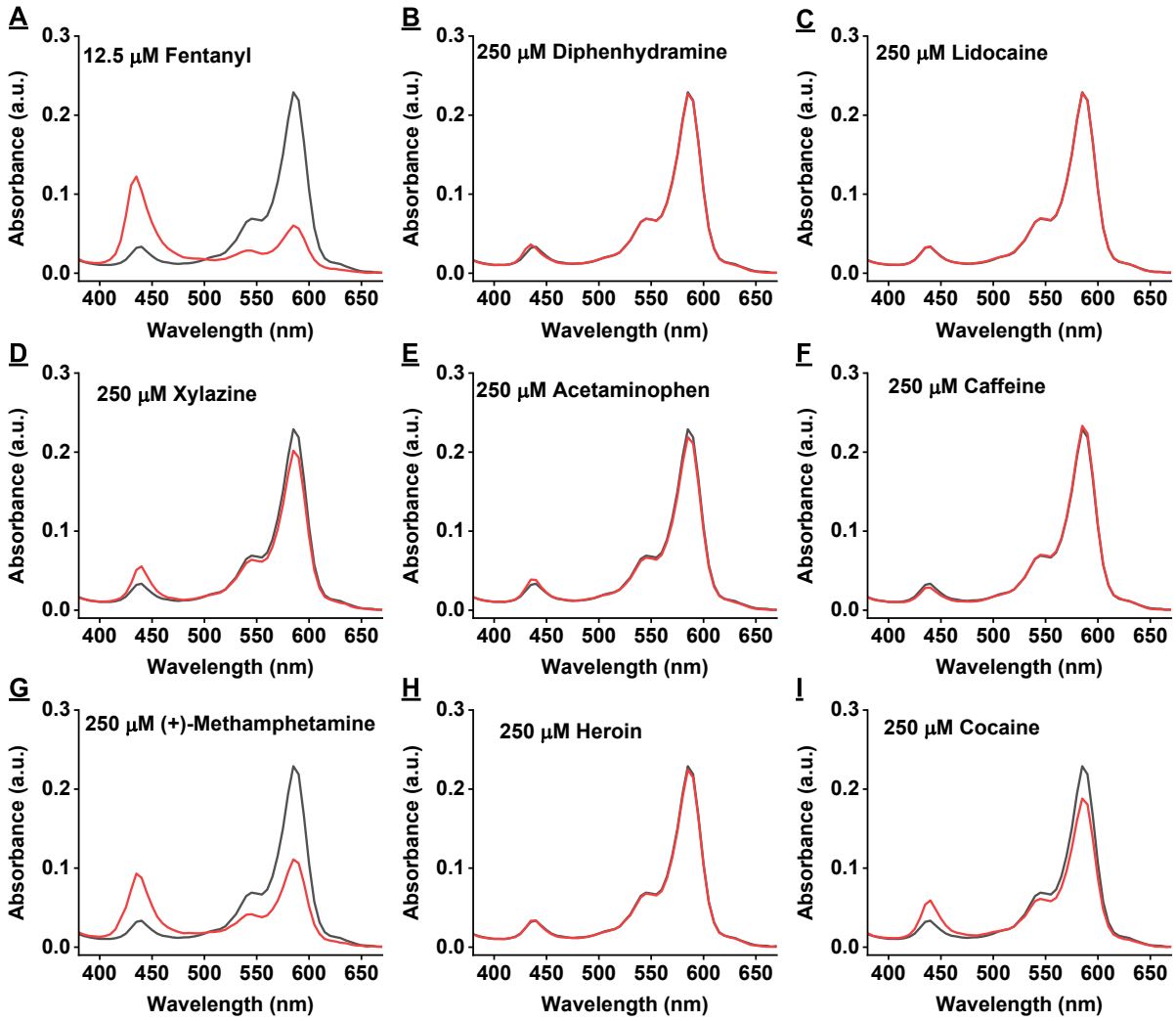

Figure S21. Specificity of dye-displacement assay based on X-732-91C and MF2-mut. Absorbance spectra of samples challenged with (**A**) 12.5 μM fentanyl, (**B**) 250 μM diphenhydramine, (**C**) 250 μM lidocaine, (**D**) 250 μM xylazine, (**E**) 250 μM acetaminophen, (**F**) 250 μM caffeine, (**G**) 250 μM (+)-methamphetamine, (**H**) 250 μM heroin, or (**I**) 250 μM cocaine. The red and black curves respectively indicate data for samples with and without target/interferent.

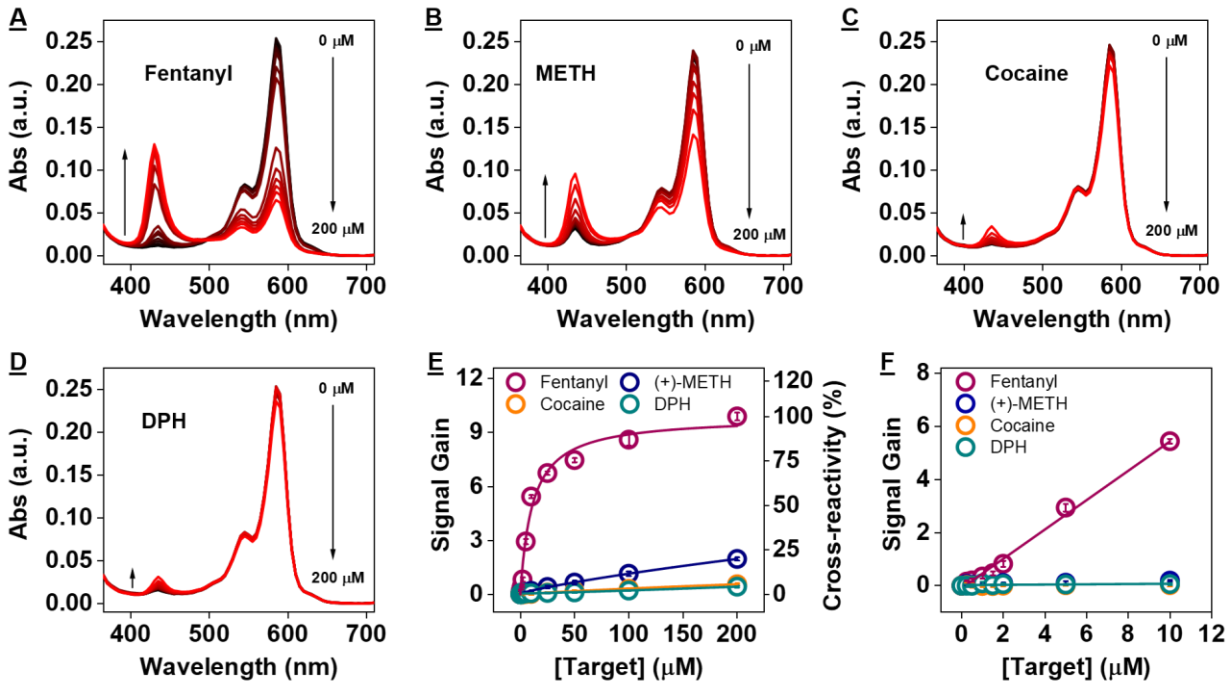

Figure S22. Specificity performance of a dye-displacement assay utilizing the aptamer MF2-mut and X-732-91C dye. Absorbance spectra of solutions containing 3 μM X-732-91C and 9 μM MF2-mut challenged with 0, 0.25, 0.5, 1.0, 1.5, 2.0, 5.0, 10, 25, 50, 100 or 200 μM of (**A**) fentanyl, (**B**) methamphetamine (METH), (**C**) cocaine and (**D**) diphenhydramine (DPH), where the black-to-red color gradient reflects increasing concentrations of target/interferent. (**E**) Calibration curve for analyte detection and (**F**) linear range at low concentrations of analytes.

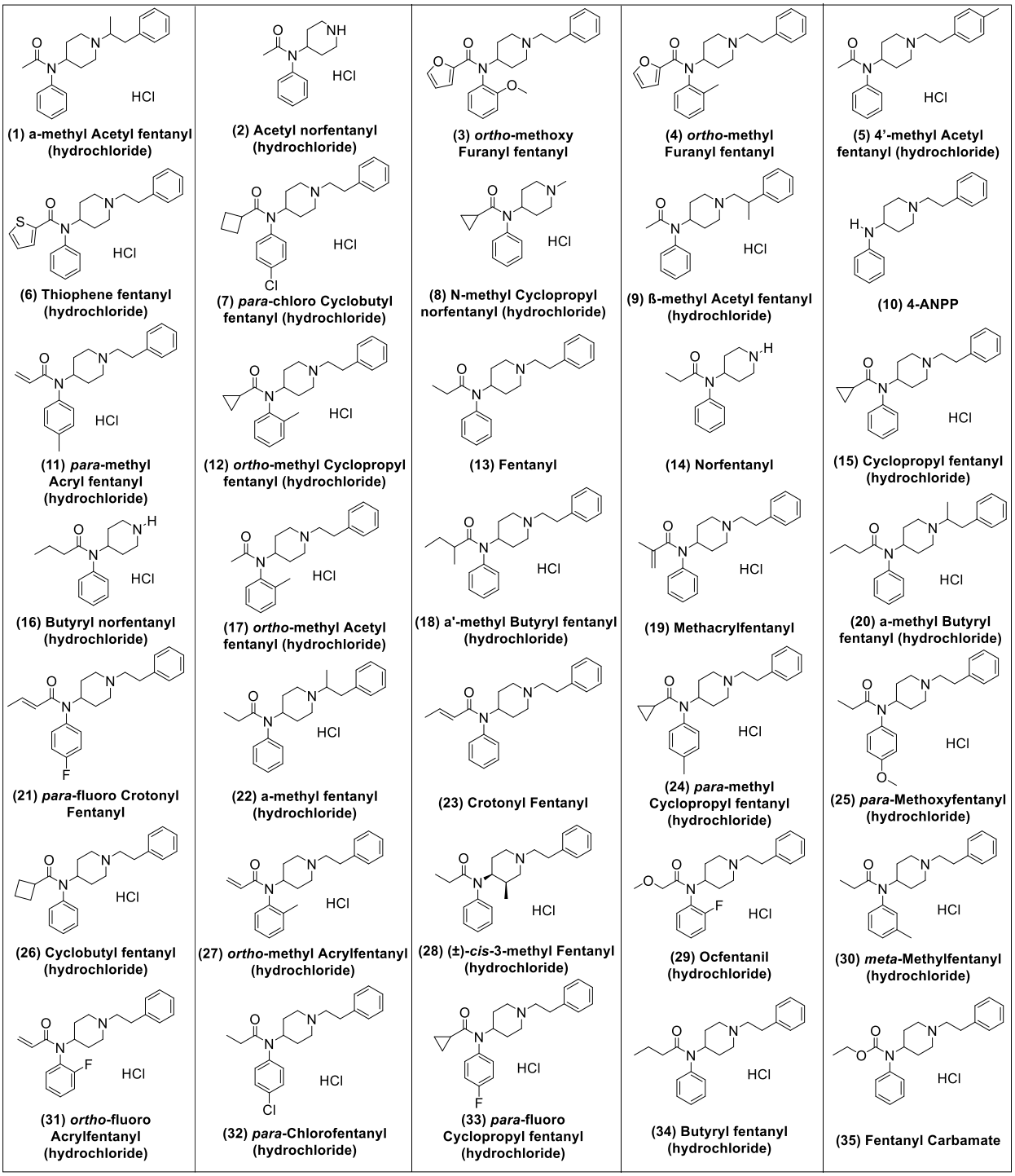

Figure S23. Chemical structures of fentanyl analogs (1-35) used in this work.

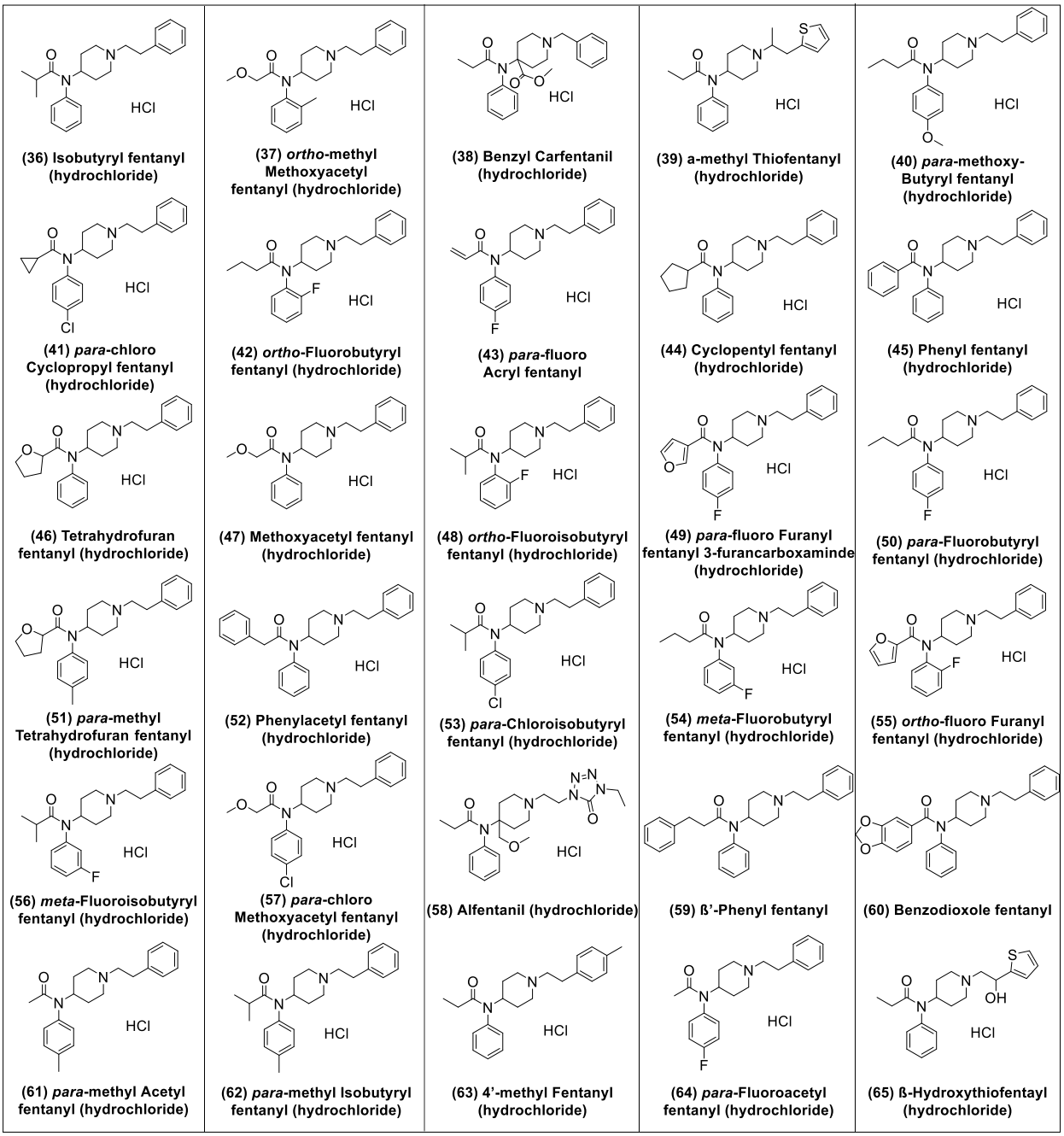

Figure S24. Chemical structures of fentanyl analogs (36-65) used in this work.

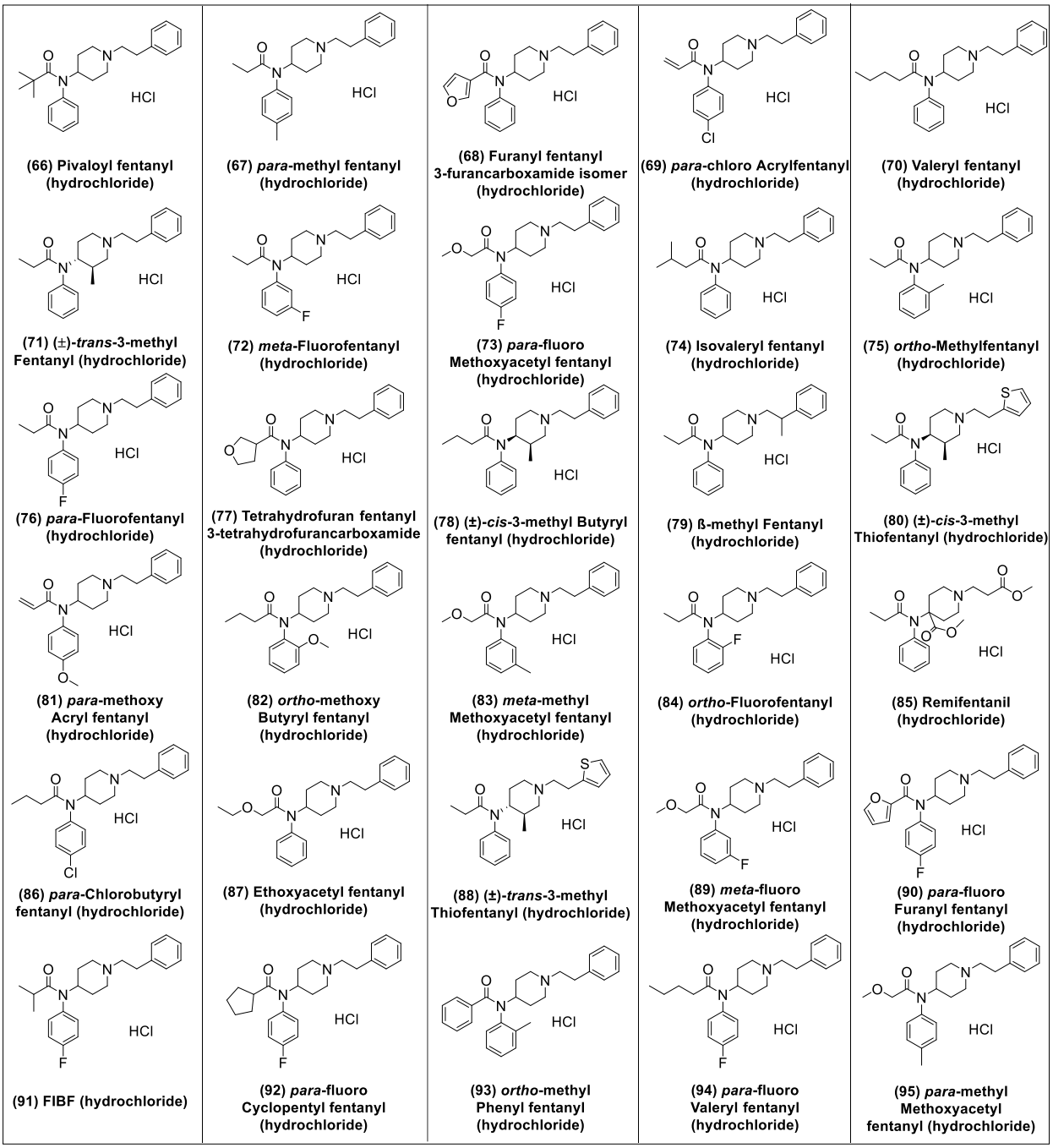

Figure S25. Chemical structures of fentanyl analogs (66-95) used in this work.

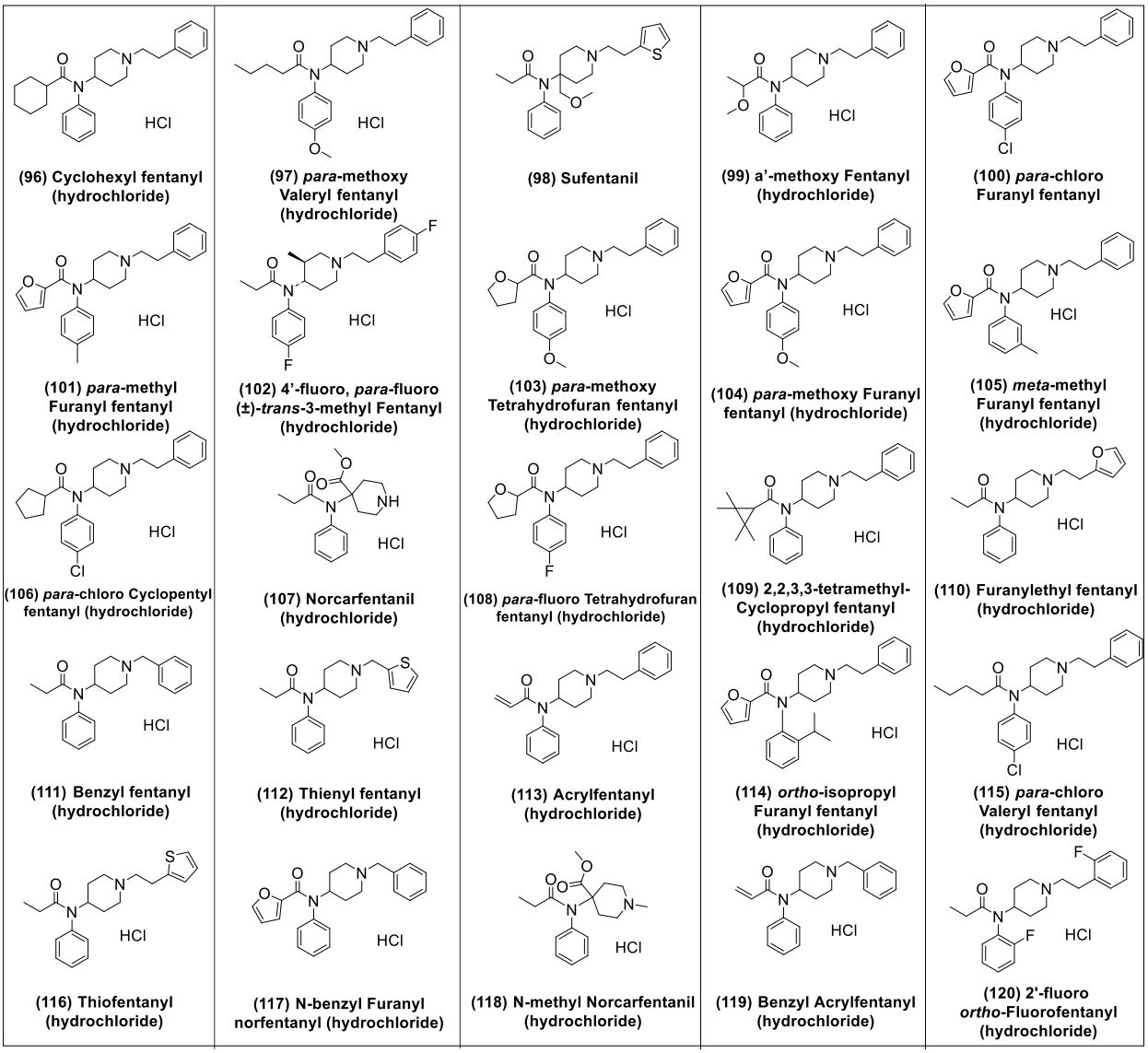

Figure S26. Chemical structures of fentanyl analogs (96-120) used in this work.

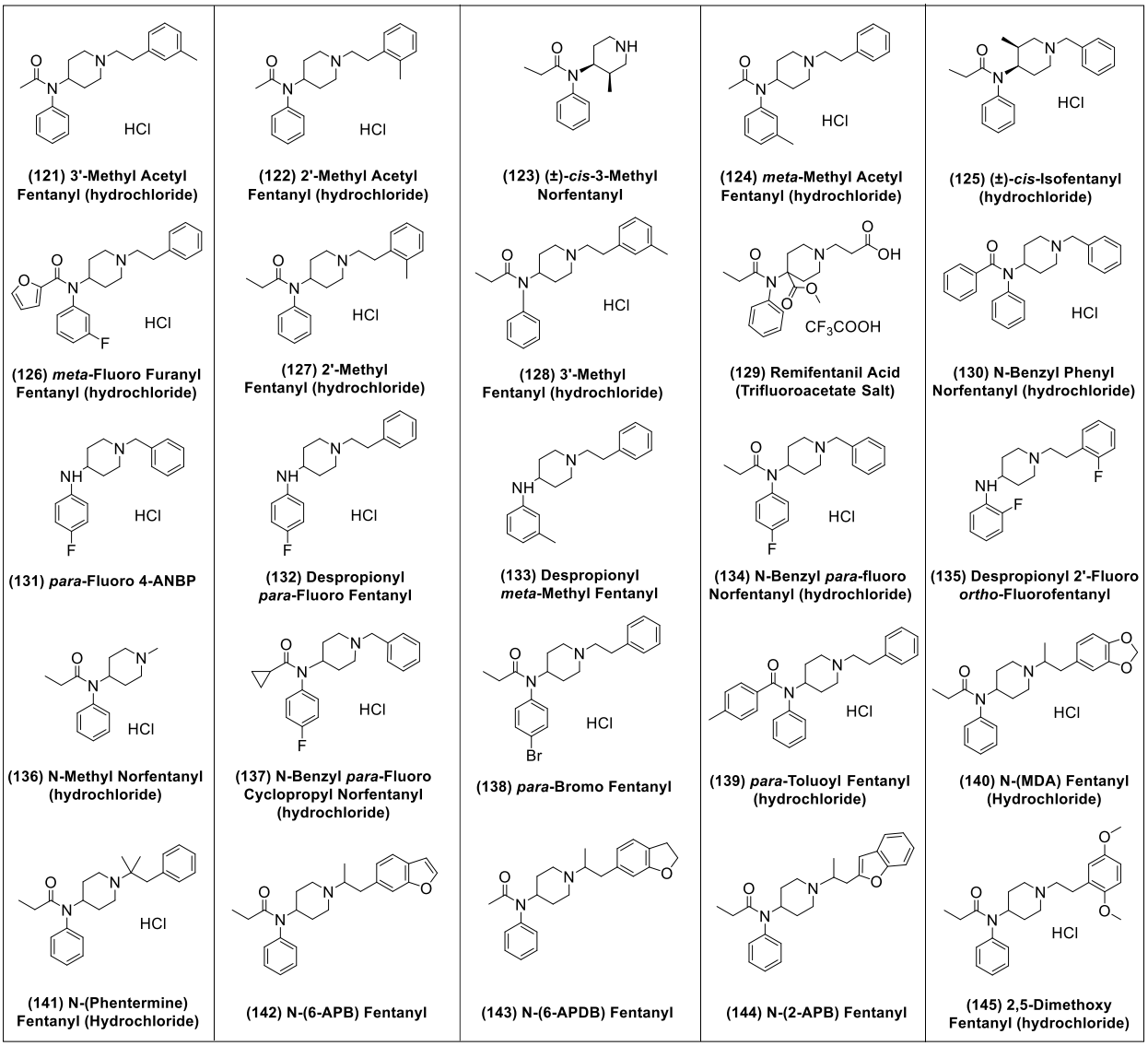

Figure S27. Chemical structures of fentanyl analogs (121-145) used in this work.

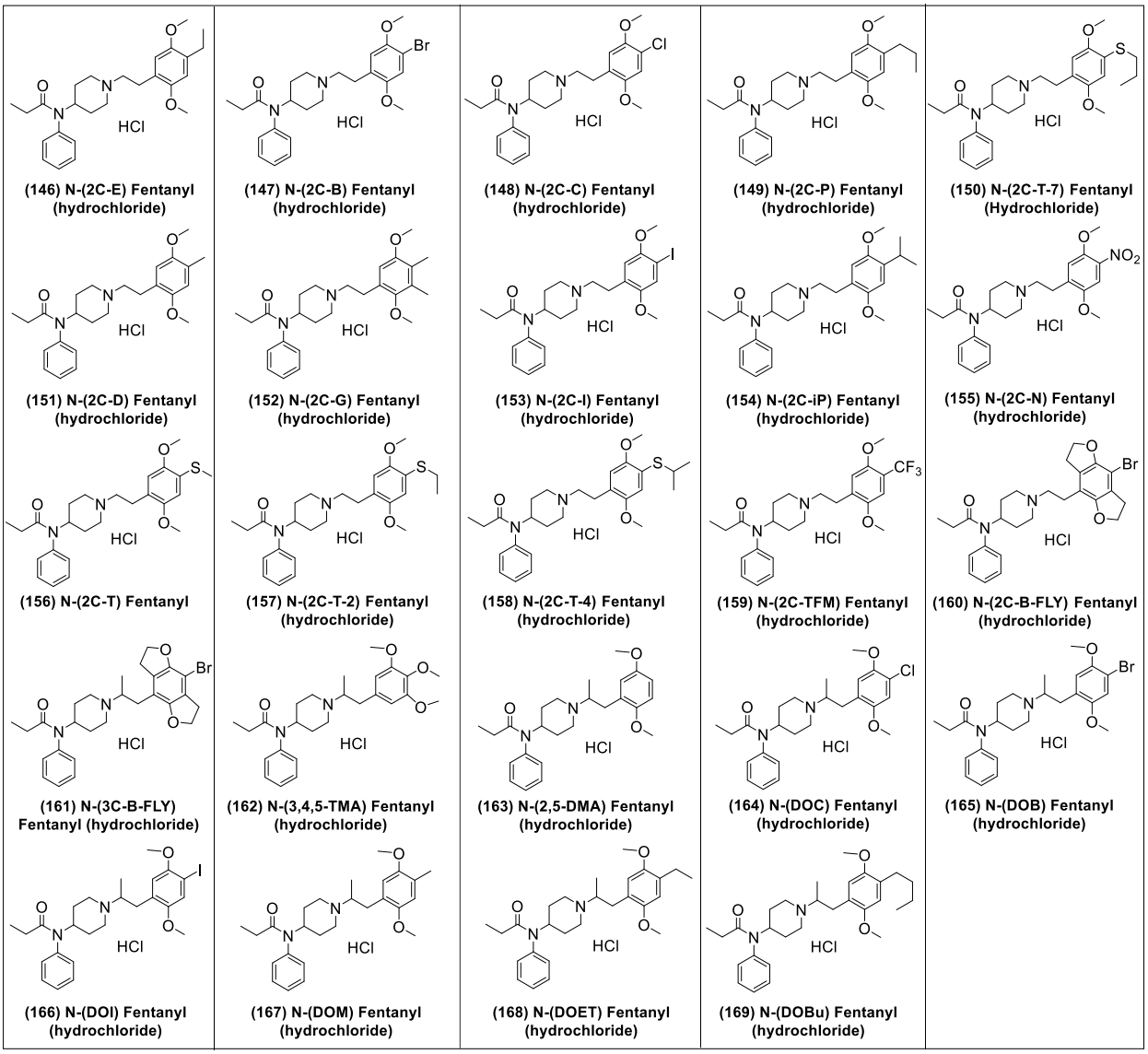

Figure S28. Chemical structures of fentanyl analogs (146-169) used in this work.

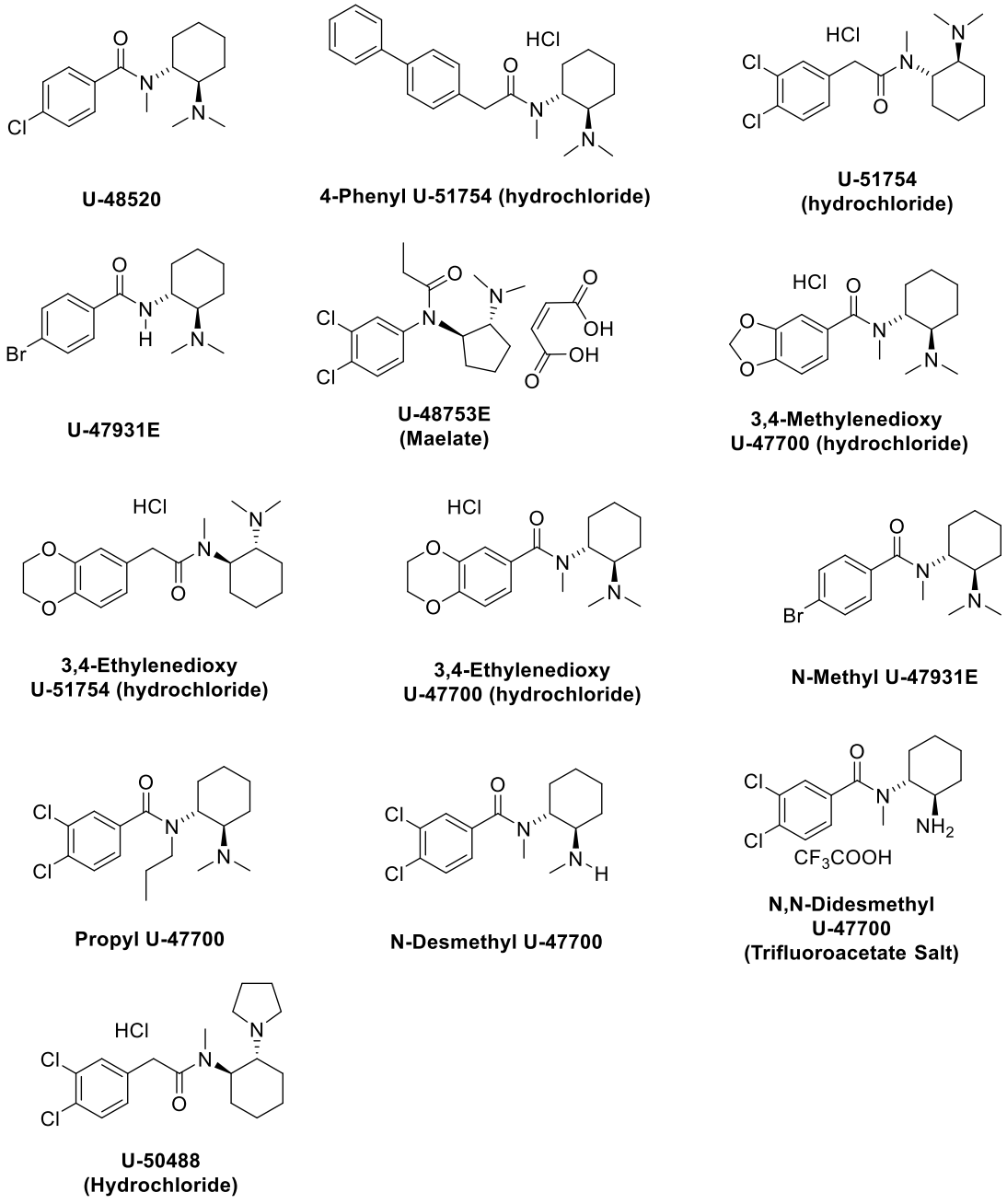

Figure S29. Chemical structures of 13 U-47700-derived synthetic opioids used in this work.

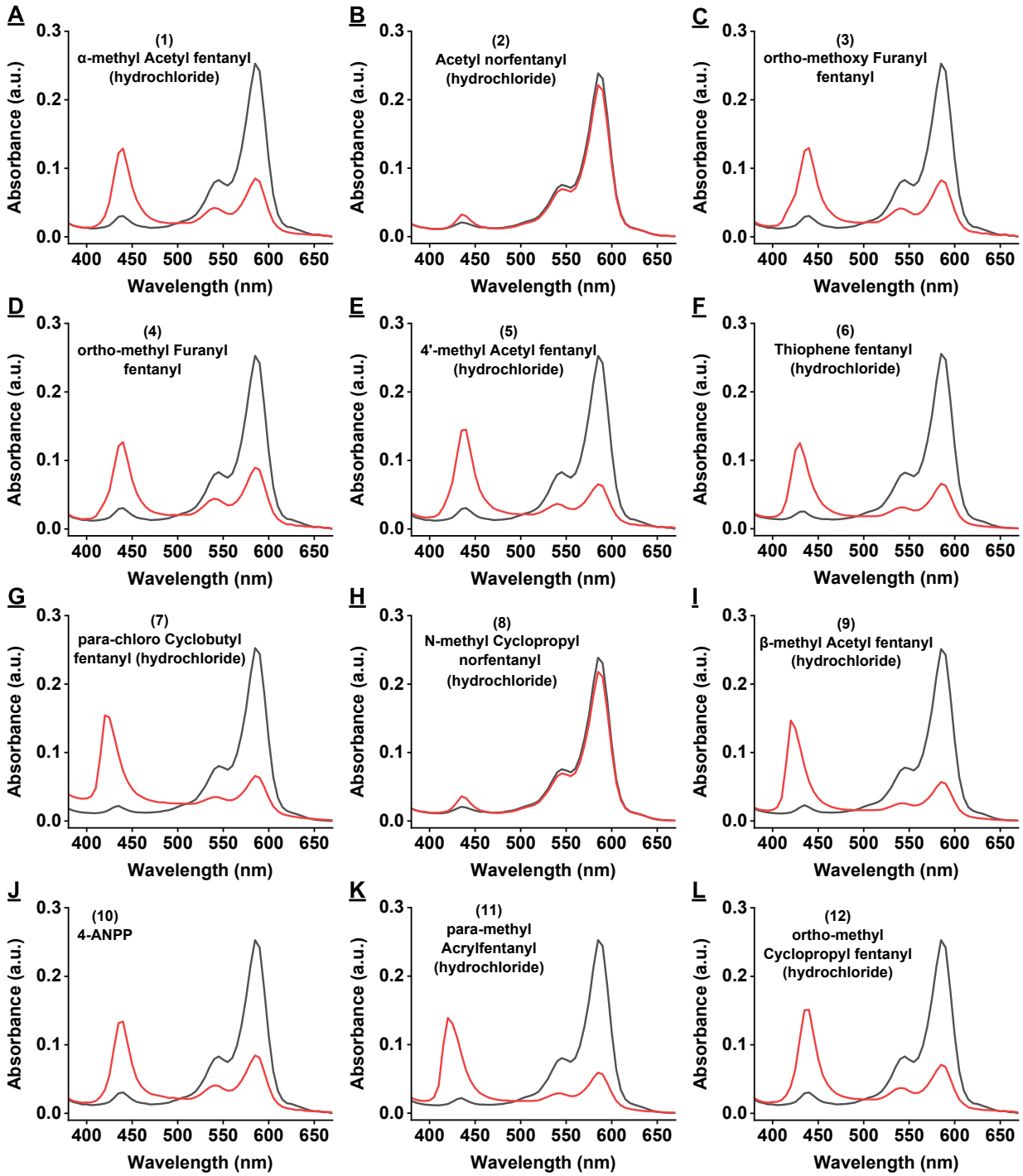

Figure S30. Absorbance spectra from the X-732-91C dye displacement assay with MF2-mut and fentanyl analogs (**A**) 1, (**B**) 2, (**C**) 3, (**D**) 4, (**E**) 5, (**F**) 6, (**G**) 7, (**H**) 8, (**I**) 9, (**J**) 10, (**K**) 11, and (**L**) 12. The red and black curves respectively indicate data for samples with and without ligand.

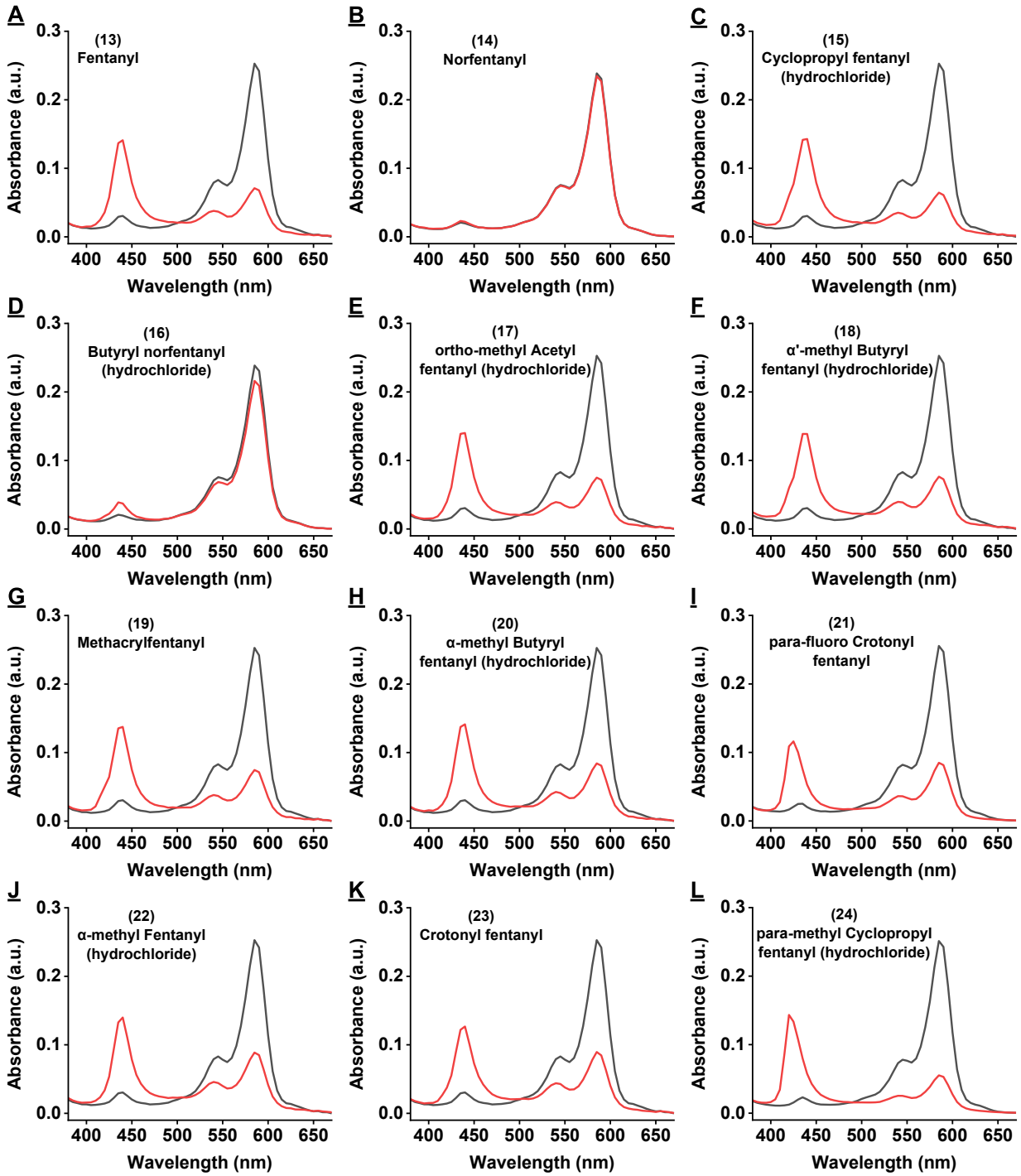

Figure S31. Absorbance spectra from the X-732-91C dye displacement assay with MF2-mut and fentanyl analogs (**A**) 13, (**B**) 14, (**C**) 15, (**D**) 16, (**E**) 17, (**F**) 18, (**G**) 19, (**H**) 20, (**I**) 21, (**J**) 22, (**K**) 23, and (**L**) 24. The red and black curves respectively indicate data for samples with and without ligand.

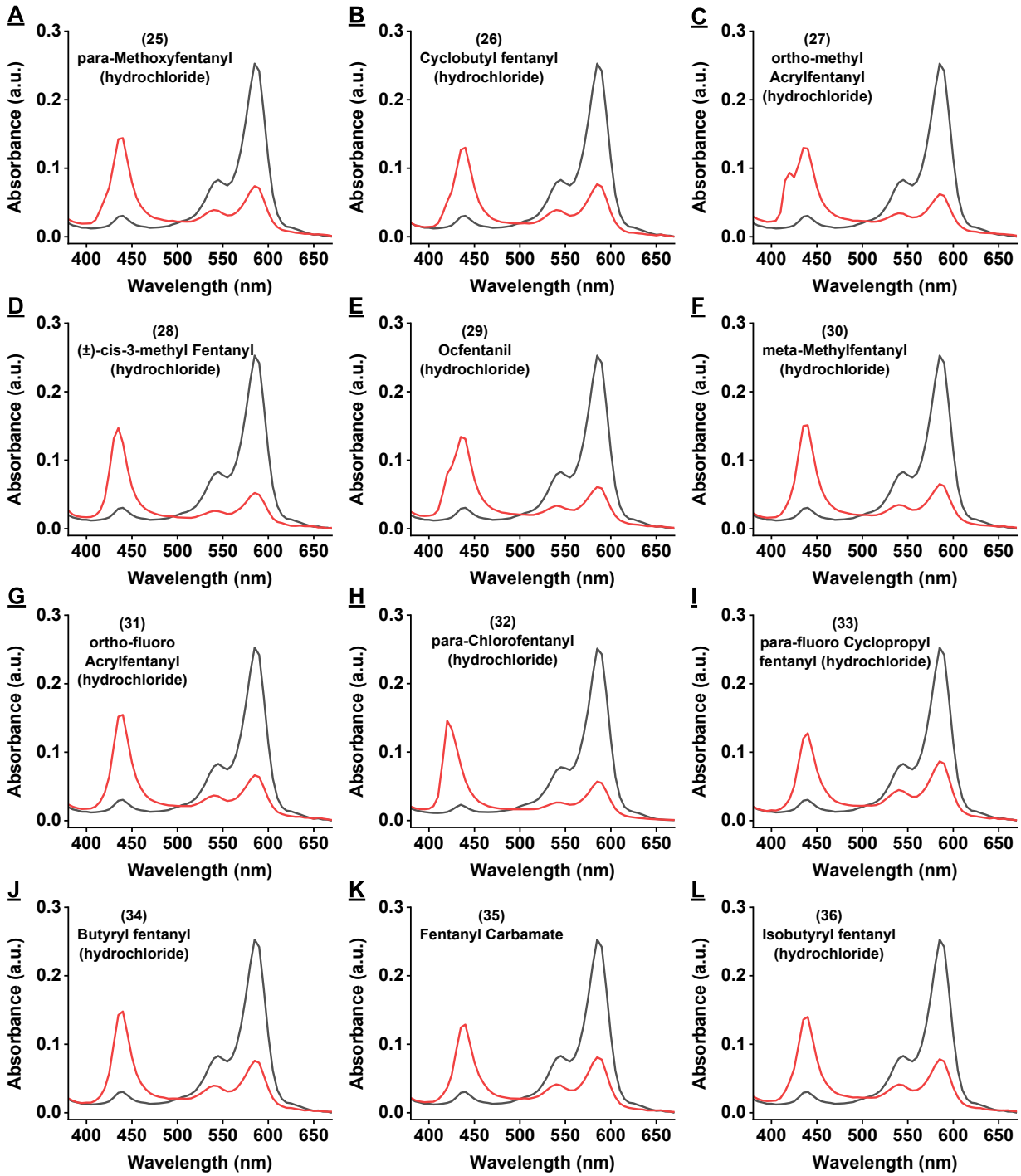

Figure S32. Absorbance spectra from the X-732-91C dye displacement assay with MF2-mut and fentanyl analogs (**A**) 25, (**B**) 26, (**C**) 27, (**D**) 28, (**E**) 29, (**F**) 30, (**G**) 31, (**H**) 32, (**I**) 33, (**J**) 34, (**K**) 35, and (**L**) 36. The red and black curves respectively indicate data for samples with and without ligand.

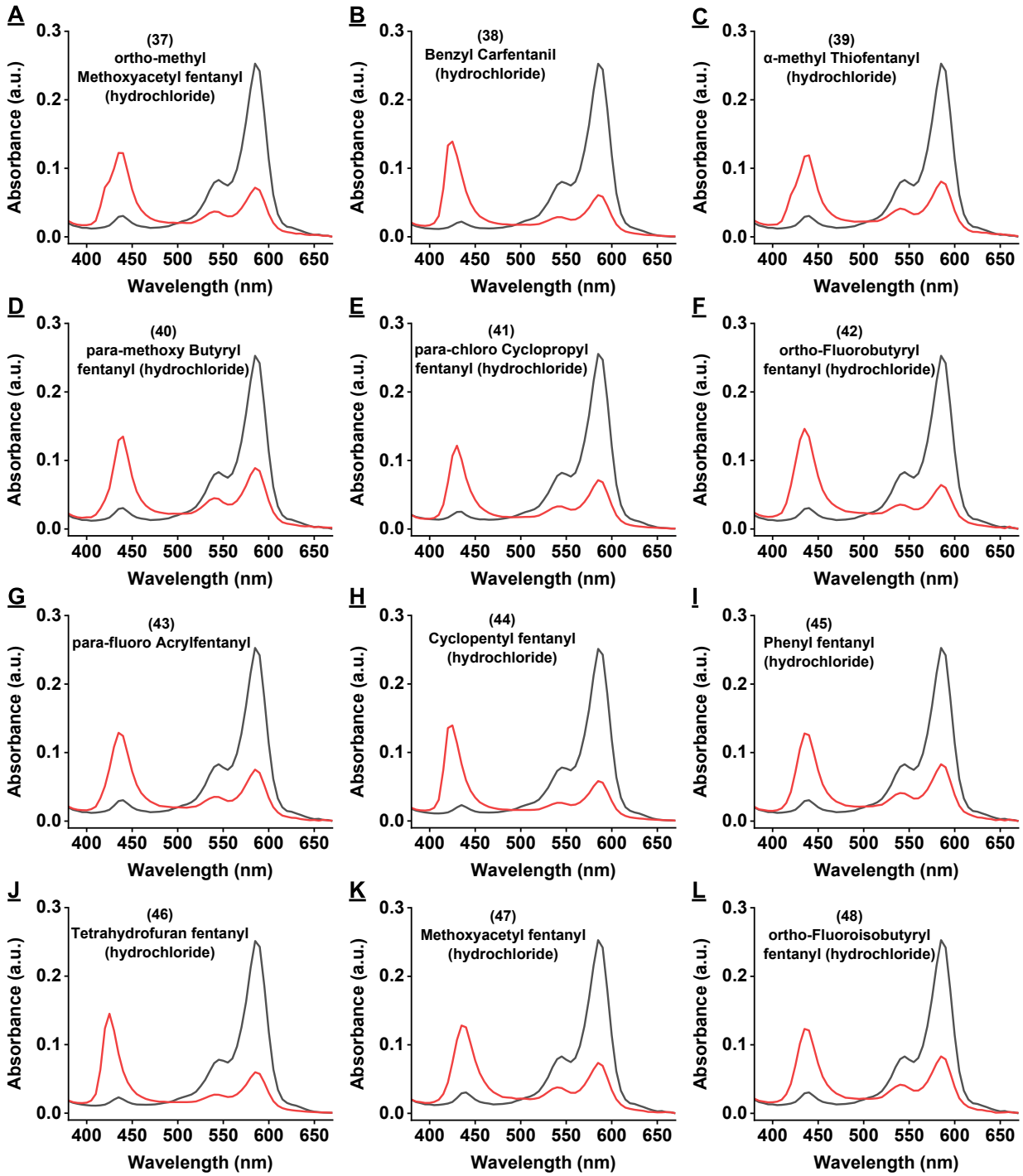

Figure S33. Absorbance spectra from the X-732-91C dye displacement assay with MF2-mut and fentanyl analogs (**A**) 37, (**B**) 38, (**C**) 39, (**D**) 40, (**E**) 41, (**F**) 42, (**G**) 43, (**H**) 44, (**I**) 45, (**J**) 46, (**K**) 47, and (**L**) 48. The red and black curves respectively indicate data for samples with and without ligand.

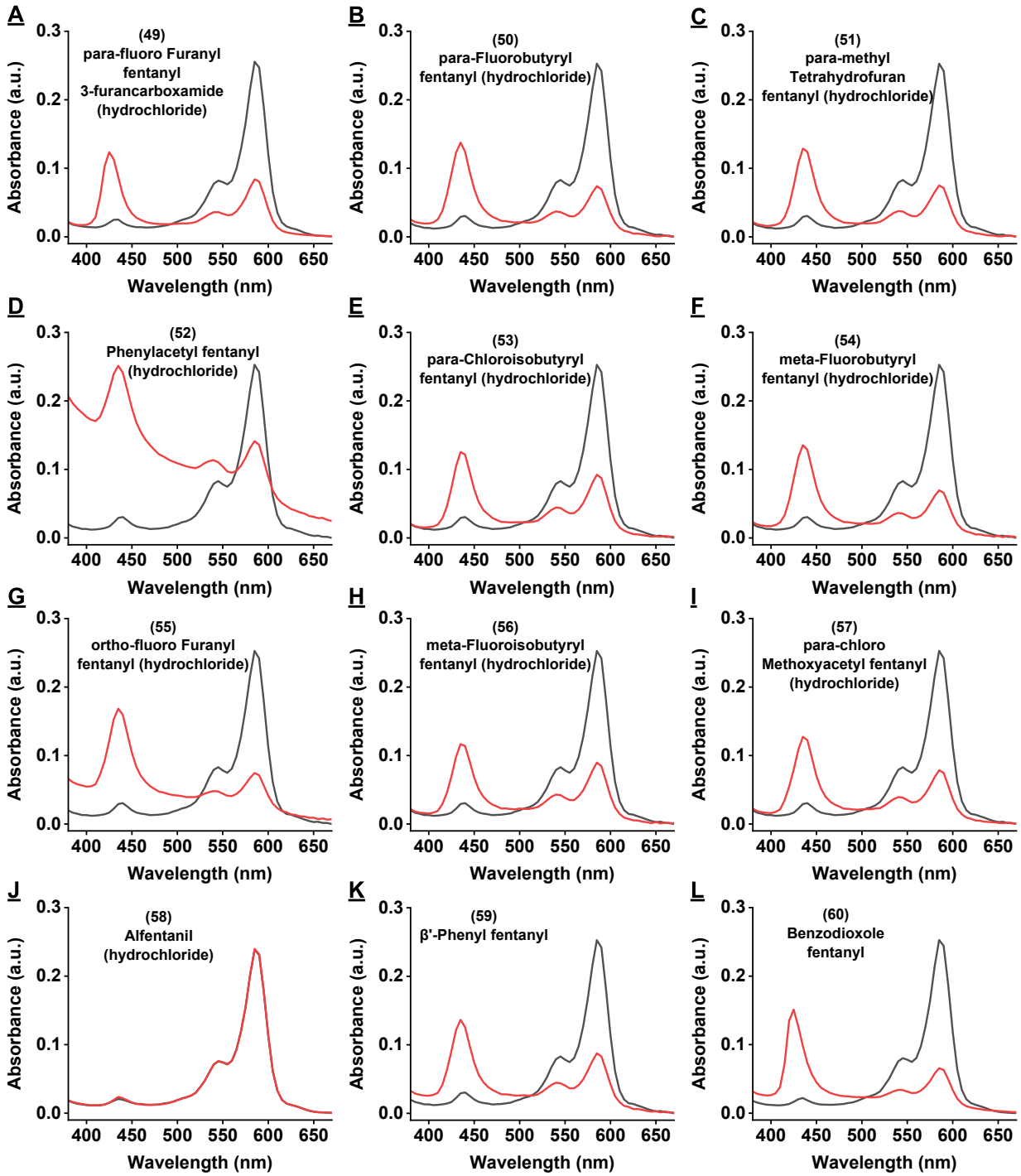

Figure S34. Absorbance spectra from the X-732-91C dye displacement assay with MF2-mut and fentanyl analogs (**A**) 49, (**B**) 50, (**C**) 51, (**D**) 52, (**E**) 53, (**F**) 54, (**G**) 55, (**H**) 56, (**I**) 57, (**J**) 58, (**K**) 59, and (**L**) 60. The red and black curves respectively indicate data for samples with and without ligand.

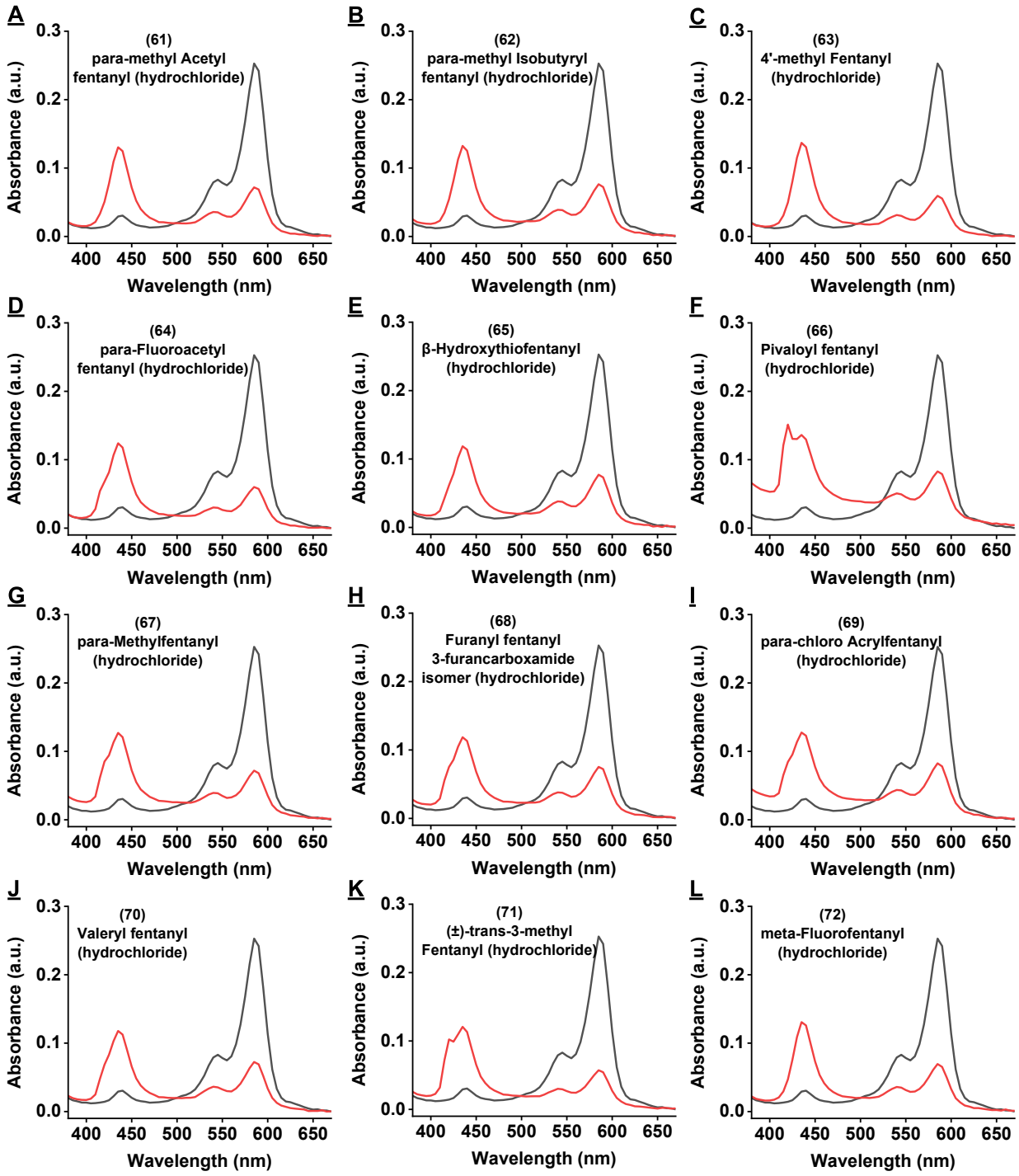

Figure S35. Absorbance spectra from the X-732-91C dye displacement assay with MF2-mut and fentanyl analogs (**A**) 61, (**B**) 62, (**C**) 63, (**D**) 64, (**E**) 65, (**F**) 66, (**G**) 67, (**H**) 68, (**I**) 69, (**J**) 70, (**K**) 71, and (**L**) 72. The red and black curves respectively indicate data for samples with and without ligand.

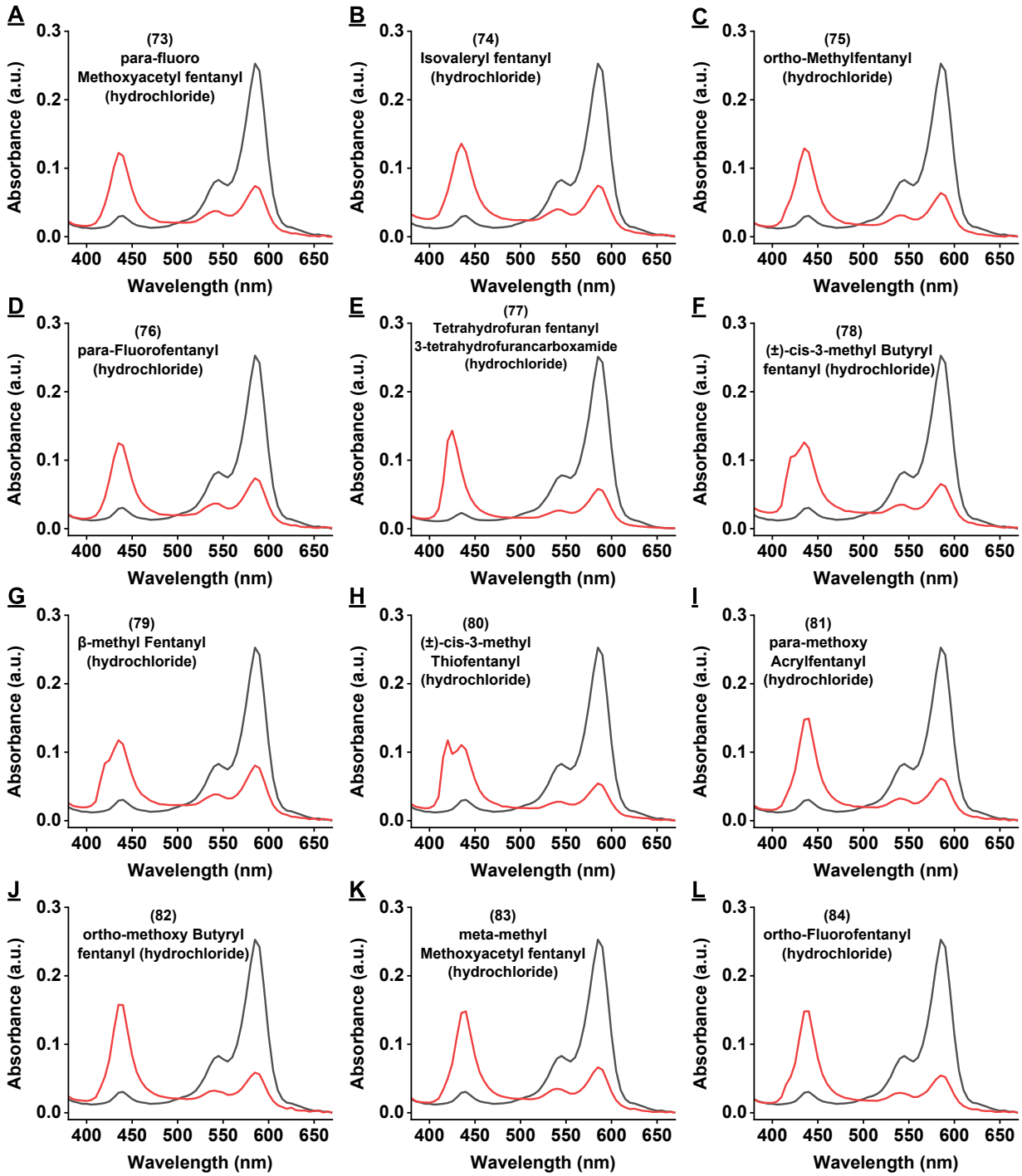

Figure S36. Absorbance spectra from the X-732-91C dye displacement assay with MF2-mut and fentanyl analogs (**A**) 73, (**B**) 74, (**C**) 75, (**D**) 76, (**E**) 77, (**F**) 78, (**G**) 79, (**H**) 80, (**I**) 81, (**J**) 82, (**K**) 83, and (**L**) 84. The red and black curves respectively indicate data for samples with and without ligand.

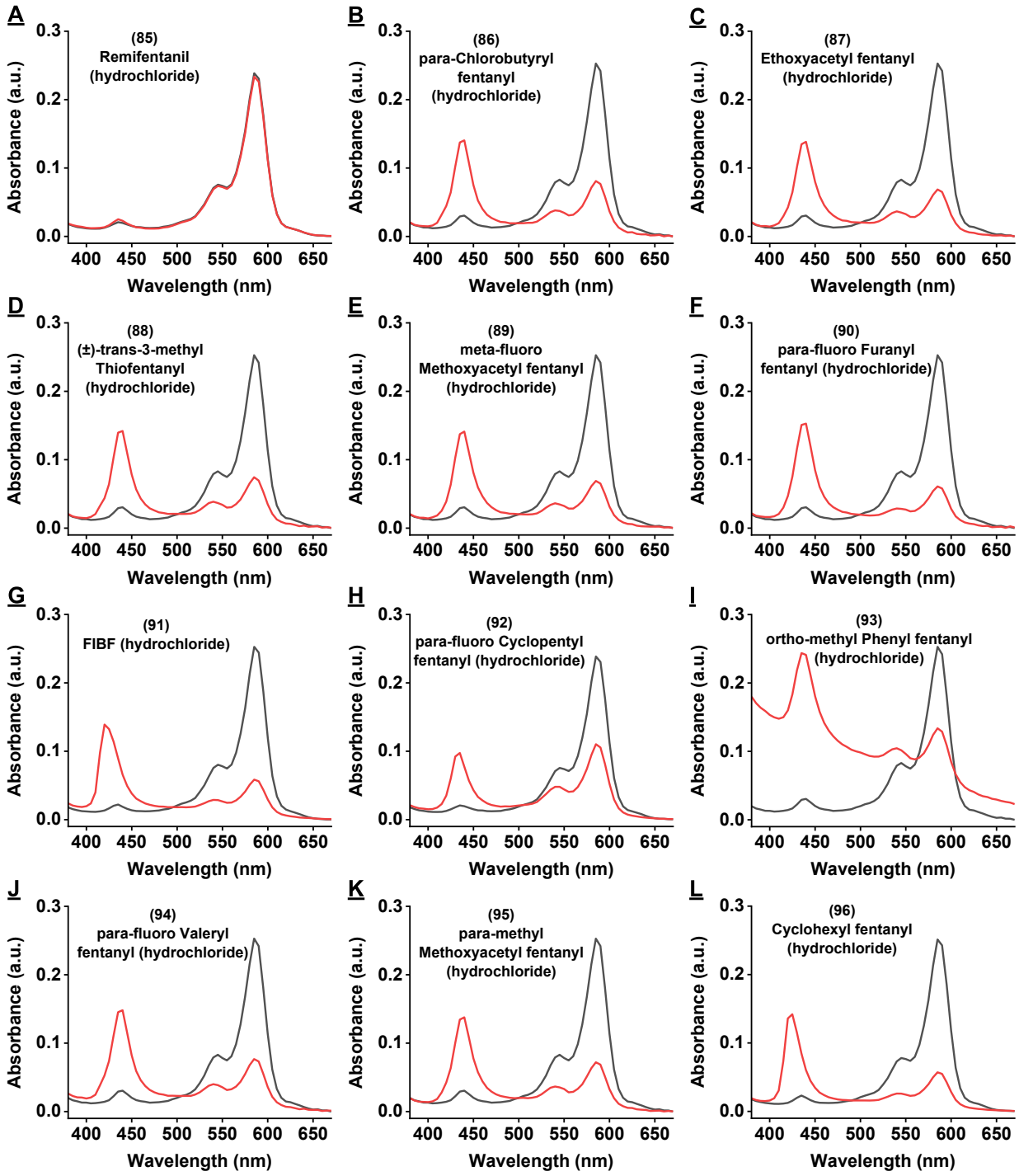

Figure S37. Absorbance spectra from the X-732-91C dye displacement assay with MF2-mut and fentanyl analogs (**A**) 85, (**B**) 86, (**C**) 87, (**D**) 88, (**E**) 89, (**F**) 90, (**G**) 91, (**H**) 92, (**I**) 93, (**J**) 94, (**K**) 95, and (**L**) 96. The red and black curves respectively indicate data for samples with and without ligand.

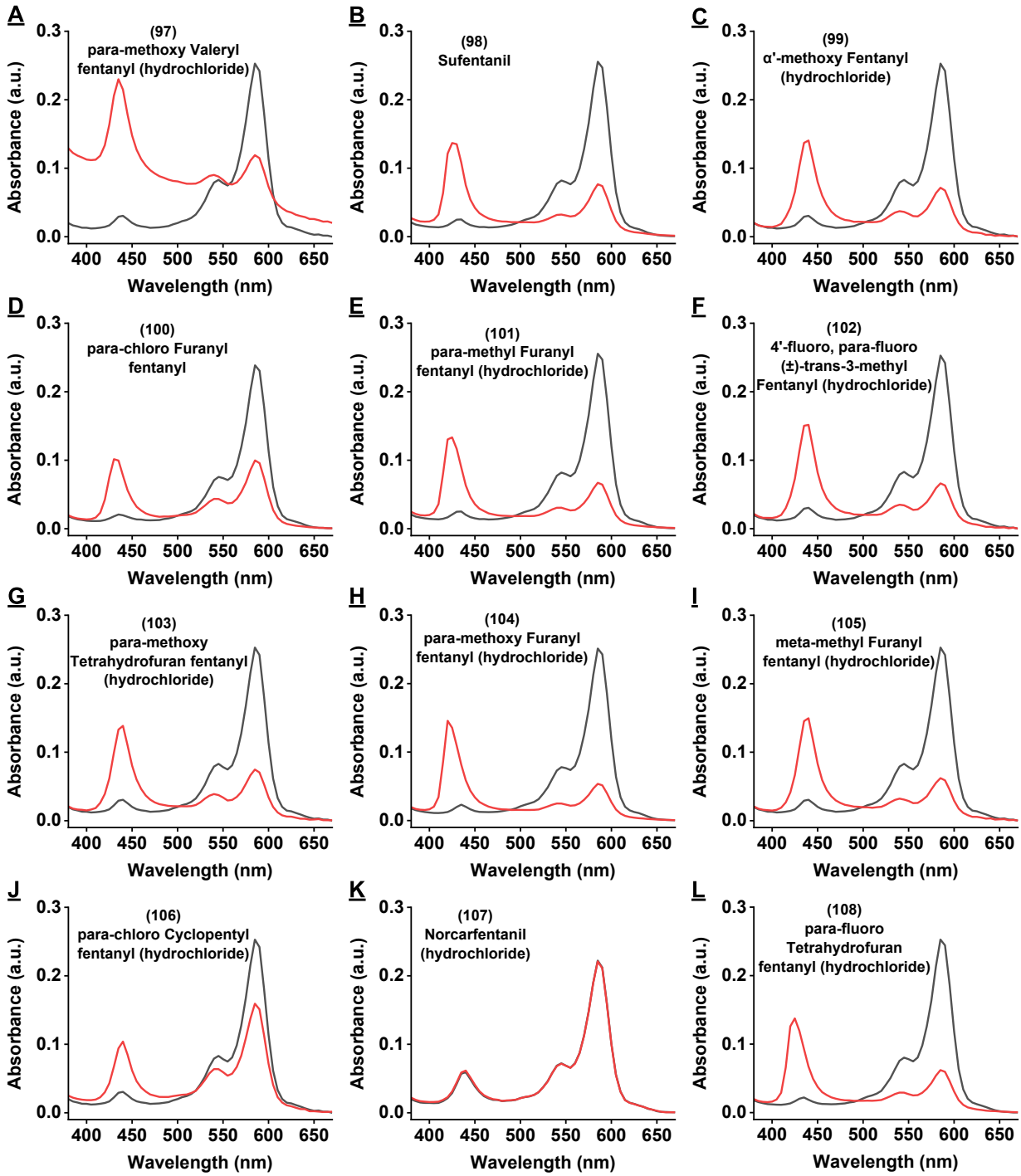

Figure S38. Absorbance spectra from the X-732-91C dye displacement assay with MF2-mut and fentanyl analogs (**A**) 97, (**B**) 98, (**C**) 99, (**D**) 100, (**E**) 101, (**F**) 102, (**G**) 103, (**H**) 104, (**I**) 105, (**J**) 106, (**K**) 107, and (**L**) 108. The red and black curves respectively indicate data for samples with and without ligand.

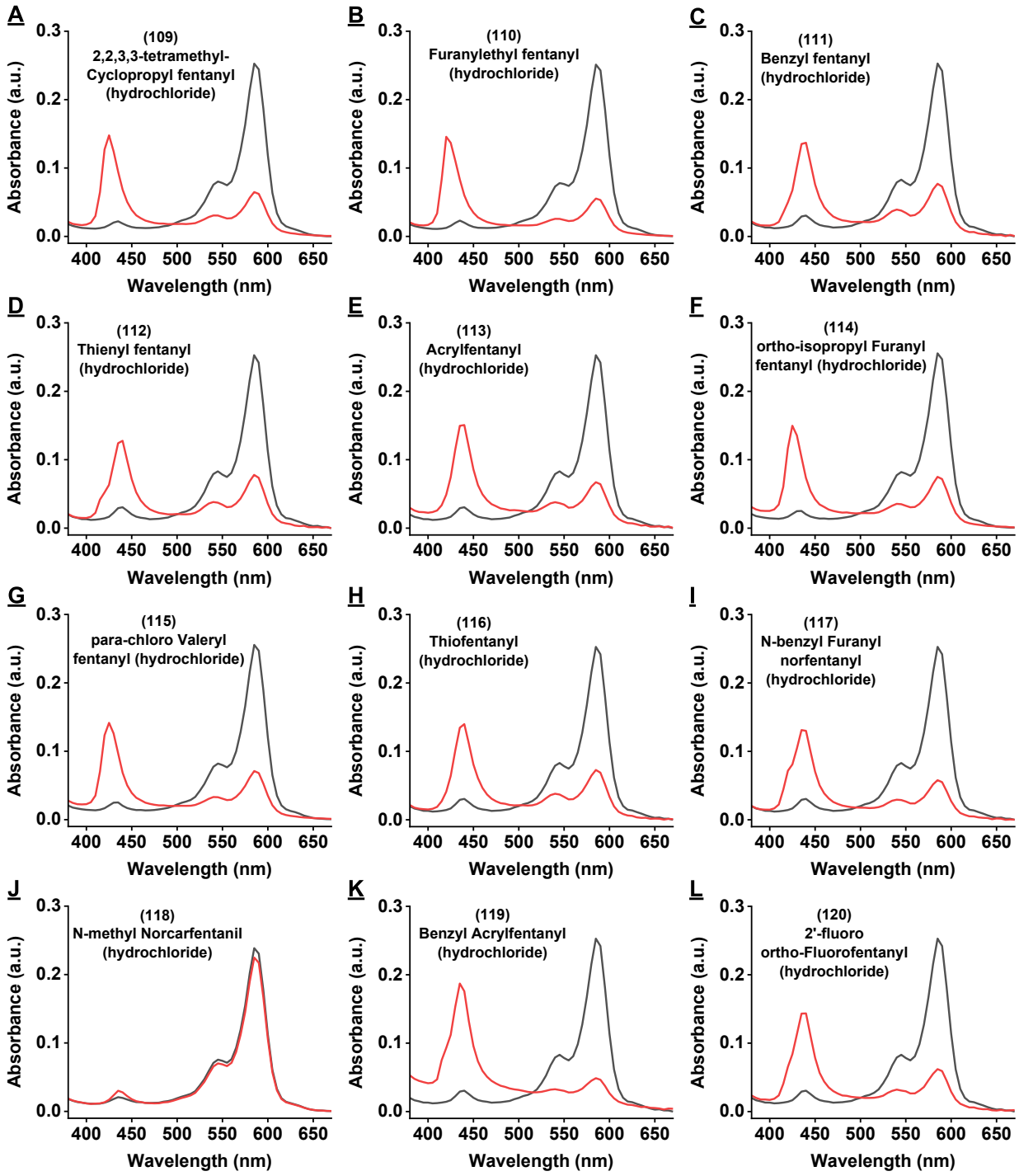

Figure S39. Absorbance spectra from the X-732-91C dye displacement assay with MF2-mut and fentanyl analogs (**A**) 109, (**B**) 110, (**C**) 111, (**D**) 112, (**E**) 113, (**F**) 114, (**G**) 115, (**H**) 116, (**I**) 117, (**J**) 118, (**K**) 119, and (**L**) 120. The red and black curves respectively indicate data for samples with and without ligand.

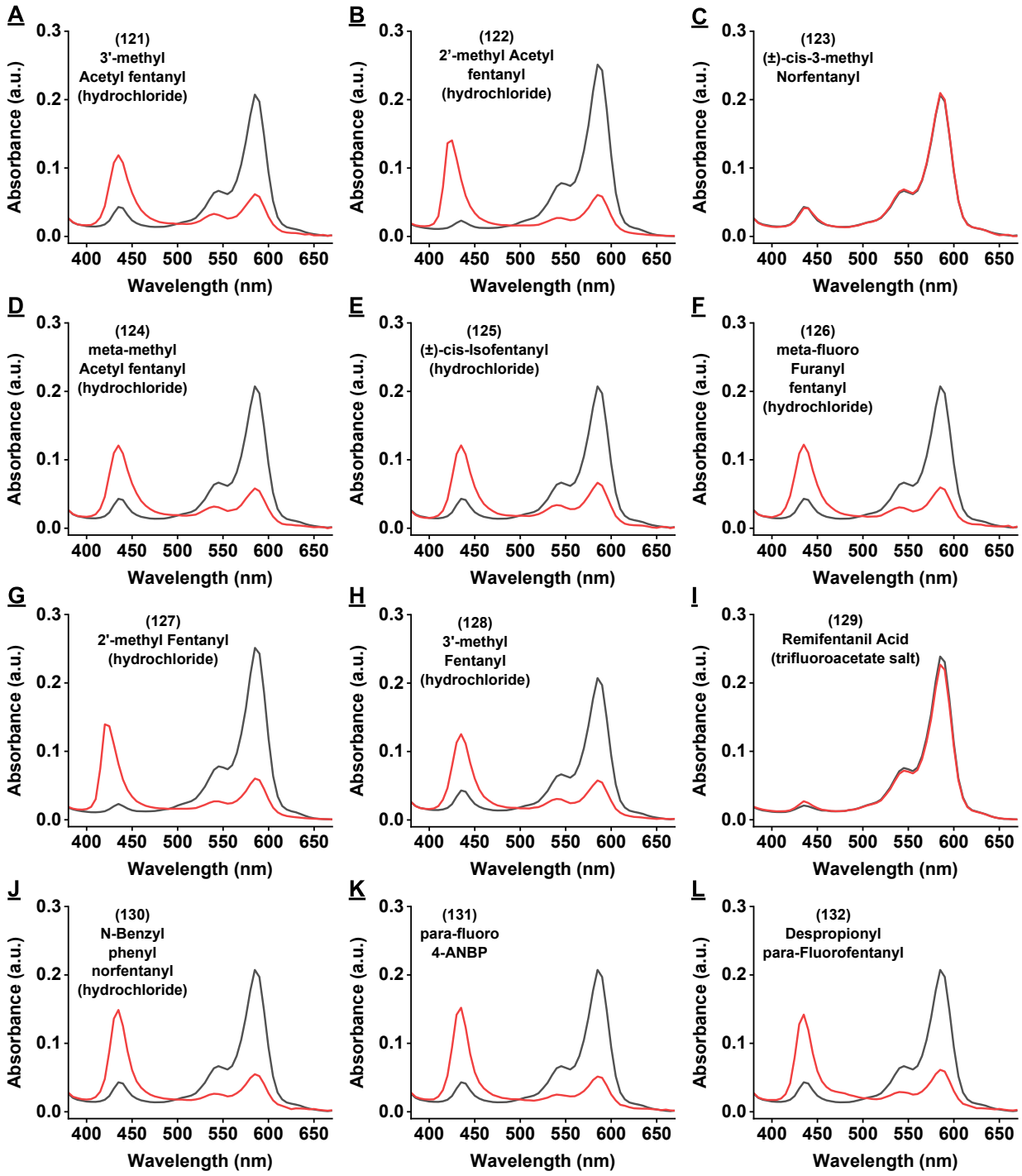

Figure S40. Absorbance spectra from the X-732-91C dye displacement assay with MF2-mut and fentanyl analogs (**A**) 121, (**B**) 122, (**C**) 123, (**D**) 124, (**E**) 125, (**F**) 126, (**G**) 127, (**H**) 128, (**I**) 129, (**J**) 130, (**K**) 131, and (**L**) 132. The red and black curves respectively indicate data for samples with and without ligand.

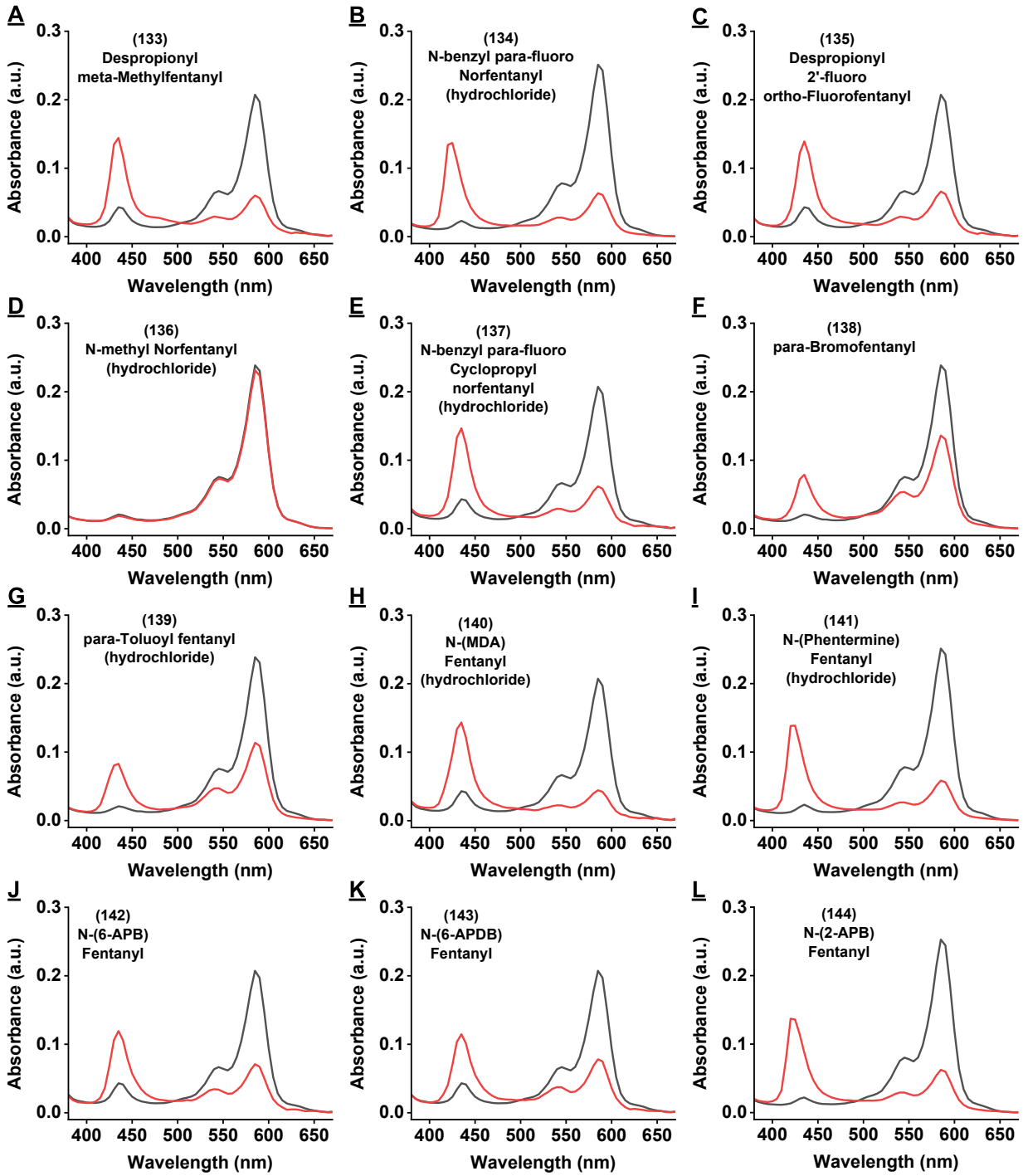

Figure S41. Absorbance spectra from the X-732-91C dye displacement assay with MF2-mut and fentanyl analogs (**A**) 133, (**B**) 134, (**C**) 135, (**D**) 136, (**E**) 137, (**F**) 138, (**G**) 139, (**H**) 140, (**I**) 141, (**J**) 142, (**K**) 143, and (**L**) 144. The red and black curves respectively indicate data for samples with and without ligand.

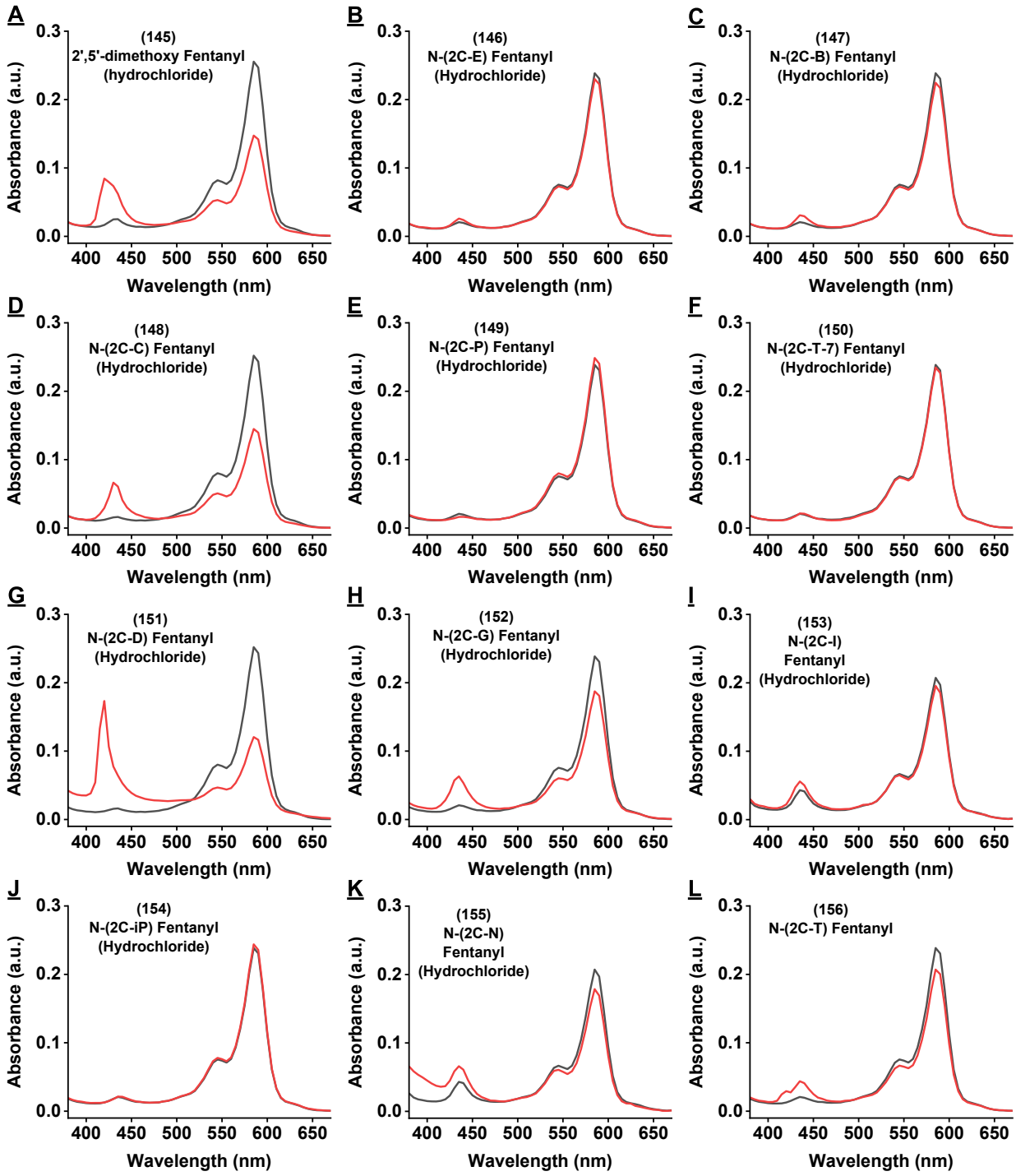

Figure S42. Absorbance spectra from the X-732-91C dye displacement assay with MF2-mut and fentanyl analogs (**A**) 145, (**B**) 146, (**C**) 147, (**D**) 148, (**E**) 149, (**F**) 150, (**G**) 151, (**H**) 152, (**I**) 153, (**J**) 154, (**K**) 155, and (**L**) 156. The red and black curves respectively indicate data for samples with and without ligand.

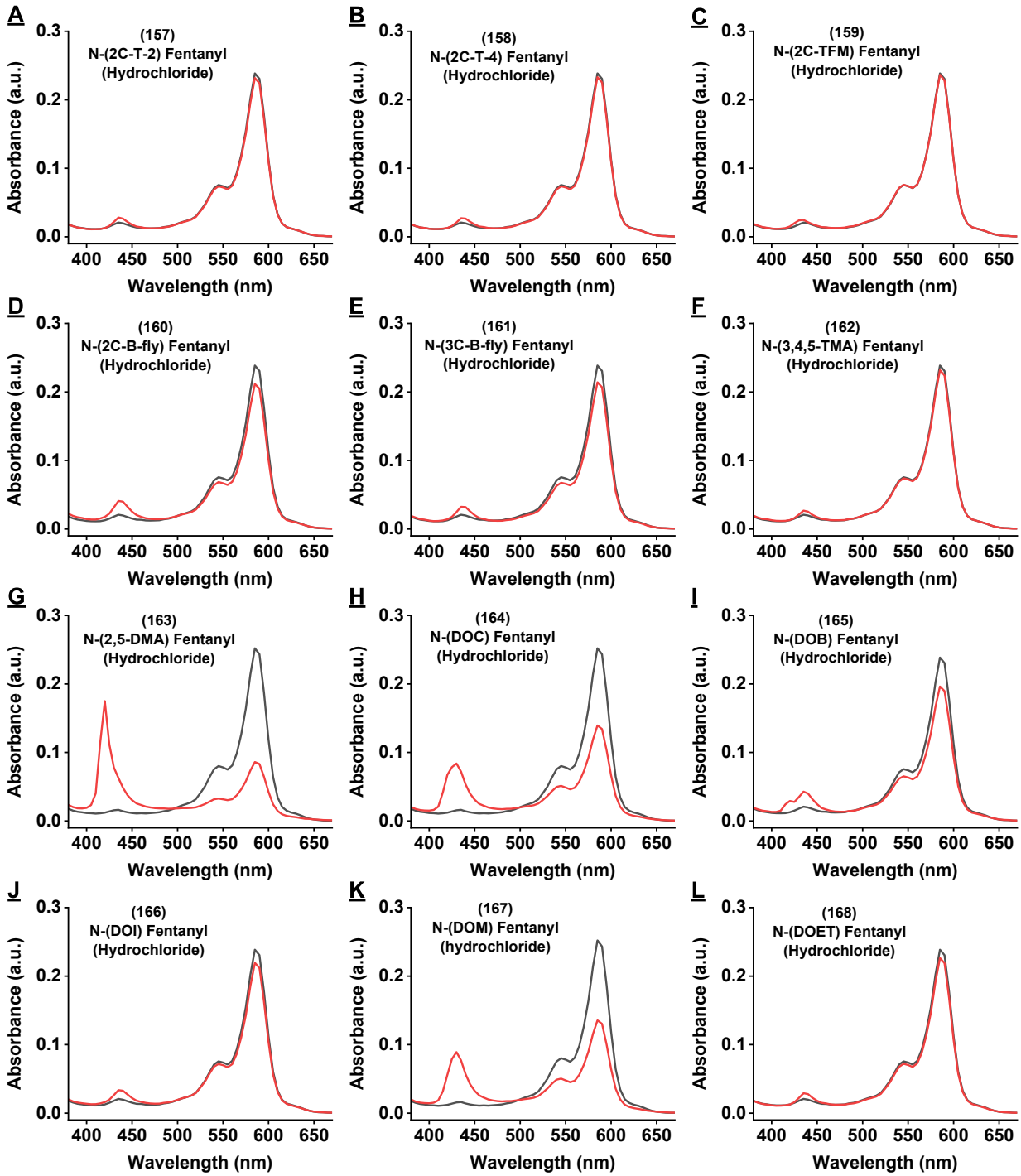

Figure S43. Absorbance spectra from the X-732-91C dye displacement assay with MF2-mut and fentanyl analogs (**A**) 157, (**B**) 158, (**C**) 159, (**D**) 160, (**E**) 161, (**F**) 162, (**G**) 163, (**H**) 164, (**I**) 165, (**J**) 166, (**K**) 167, and (**L**) 168. The red and black curves respectively indicate data for samples with and without ligand.

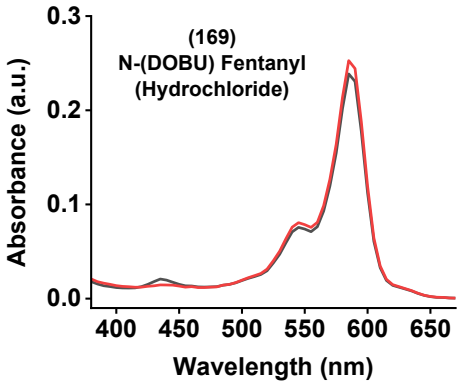

Figure S44. Absorbance spectra from the X-732-91C dye displacement assay with MF2-mut and fentanyl analog 169. The red and black curves respectively indicate data for samples with and without ligand.

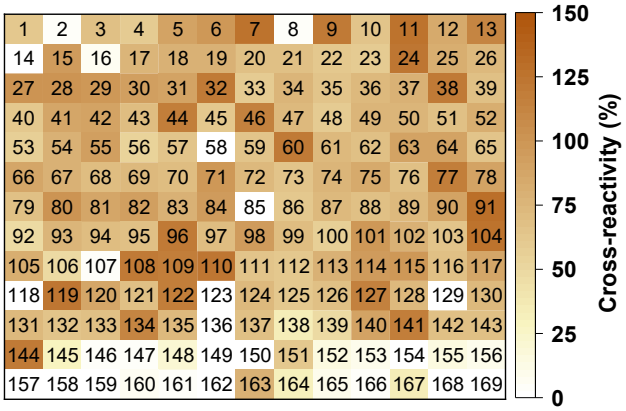

Figure S45. Cross-reactivity of fentanyl analogs to the aptamer-based dye-displacement assay. Analog cross-reactivity was calculated relative to the response yielded by 100 µM cis-3-methyl fentanyl.

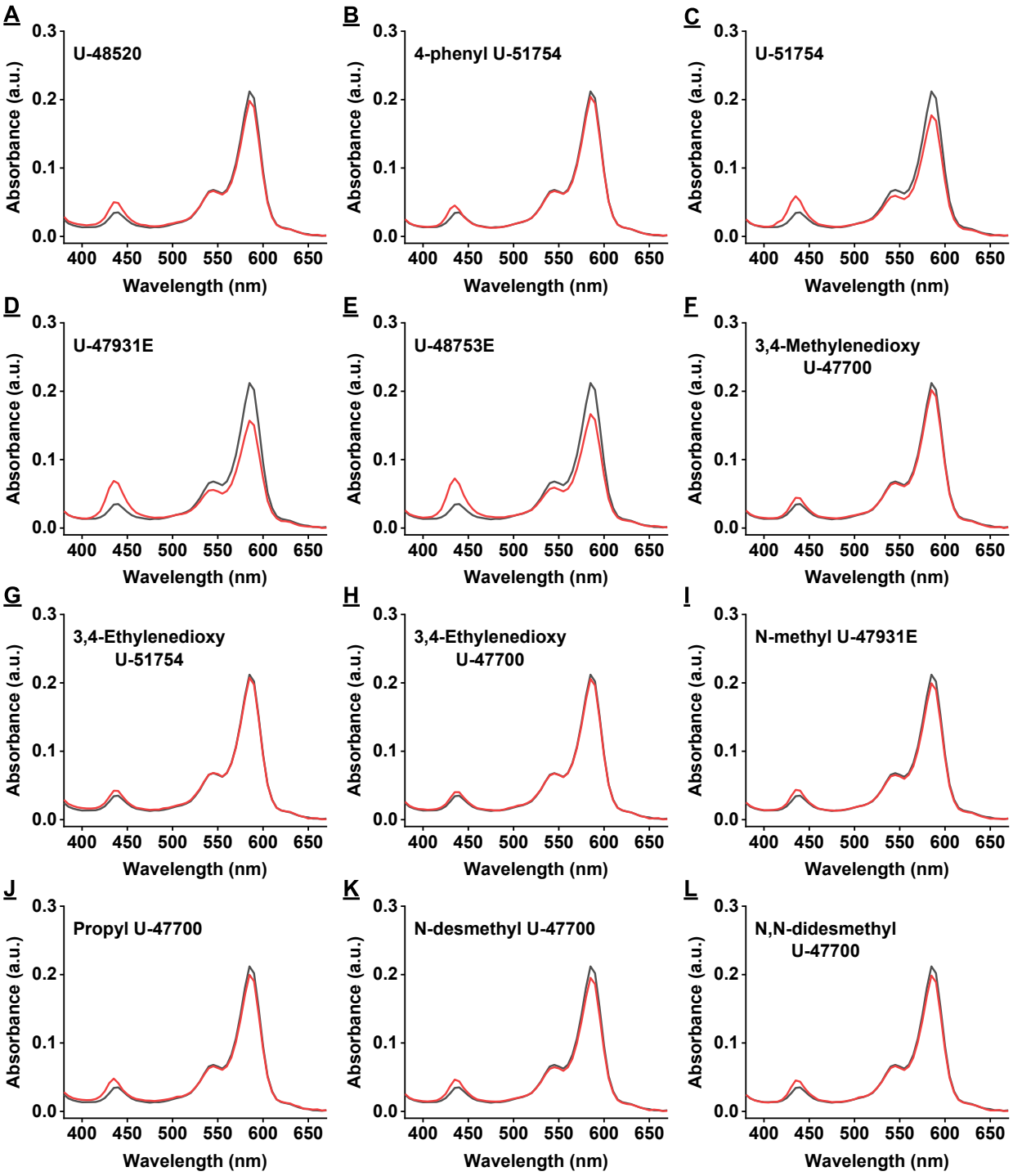

Figure S46. Absorbance spectra from the X-732-91C dye displacement assay with MF2-mut and the U-47700-derived synthetic opioids (**A**) U-48520, (**B**) 4-phenyl U-51754, (**C**) U-51754, (**D**) U-47931E, (**E**) U-48753E, (**F**) 3,4-methylenedioxy U-47700, (**G**) 3,4-ethylenedioxy U-51754, (**H**) 3,4-ethylenedioxy U-47700, (**I**) N-methyl U-47931E, (**J**) propyl U-47700, (**K**) N-desmethyl U-47700, and (**L**) N,N-didesmethyl U-47700. The red and black curves respectively indicate data for samples with and without ligand.

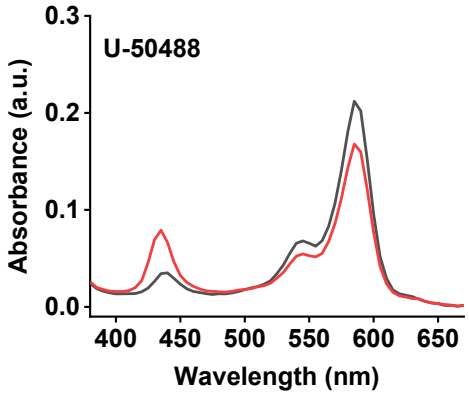

Figure S47. Absorbance spectra from the X-732-91C dye displacement assay with MF2-mut and the synthetic opioid U-50488. The red and black curves respectively indicate data for samples with and without ligand.

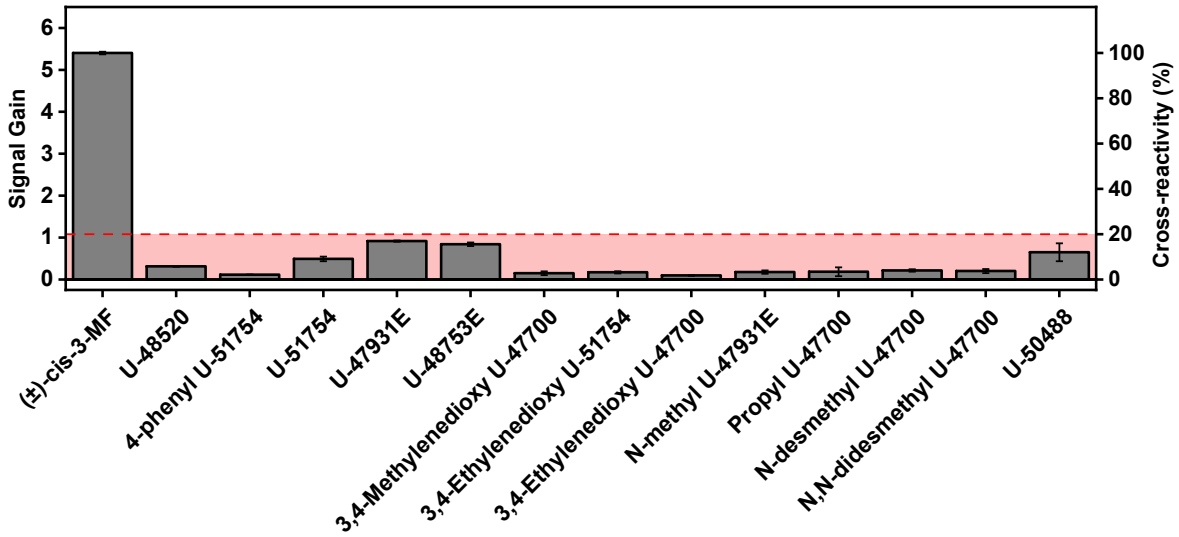

Figure S48. Sensor response to 100 µM (±)-cis-3-methyl fentanyl; 100 µM U-48520, U-47931E, and U-48753E; 25 µM 4-phenyl U-51754; or 50 µM of the other nine U-47700-related interferents we tested in this work.

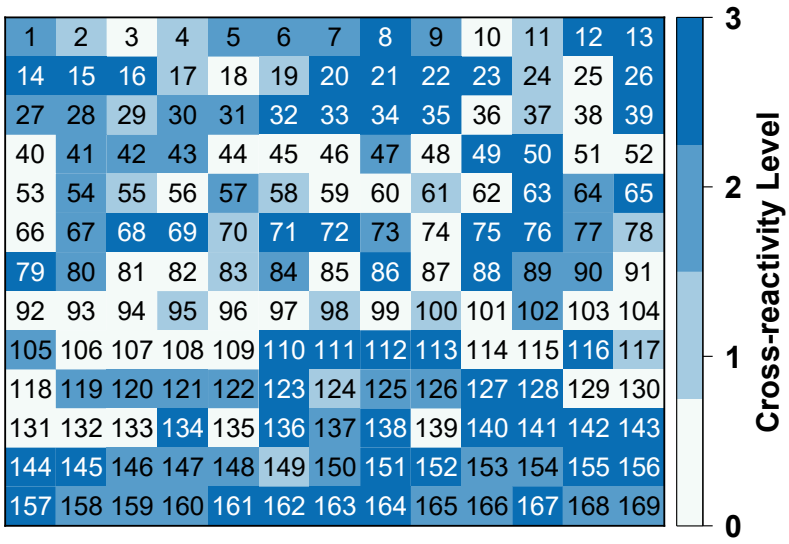

Figure S49. Reactivity heatmap of the DanceSafe lateral-flow immunoassay to fentanyl and 168 fentanyl analogs based on previously published results.[4] Cross-reactivity levels 0–3 indicate no detection, 20,000 ng/mL, 2,000 ng/mL, and 200 ng/mL and limits of detection, respectively.

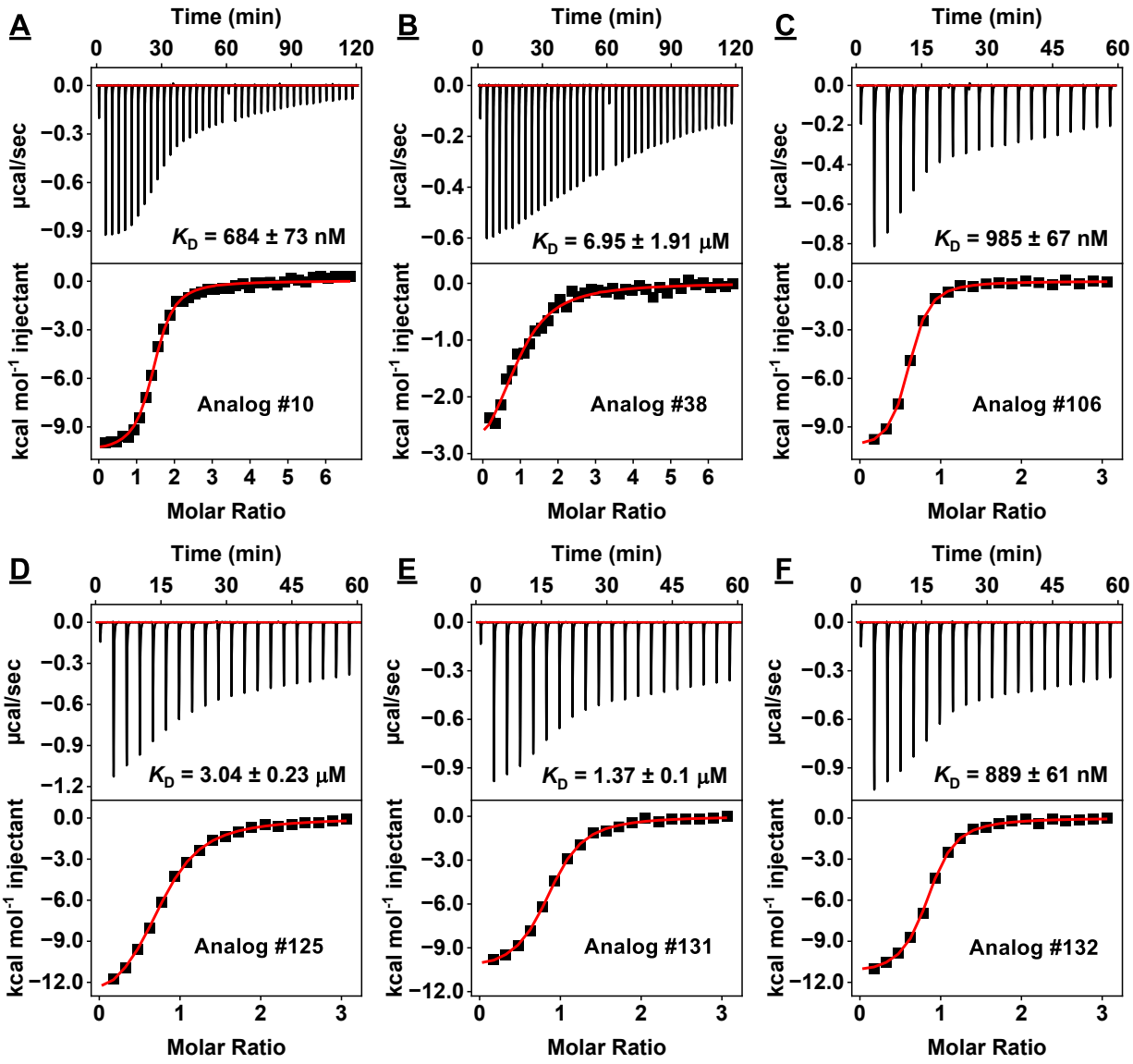

Figure S50. Determining the binding affinity of MF2-mut aptamer to fentanyl analogs using isothermal titration calorimetry (ITC). Top panels display the heat generated from each titration of MF2-mut into (**A**) analog #10, (**B**) analog #38, (**C**) analog #106, (**D**) analog #125, (**E**) analog #131, and (F) analog #132, respectively. Bottom panels show the integrated heat of each titration after correcting for the heat of dilution of the titrant.

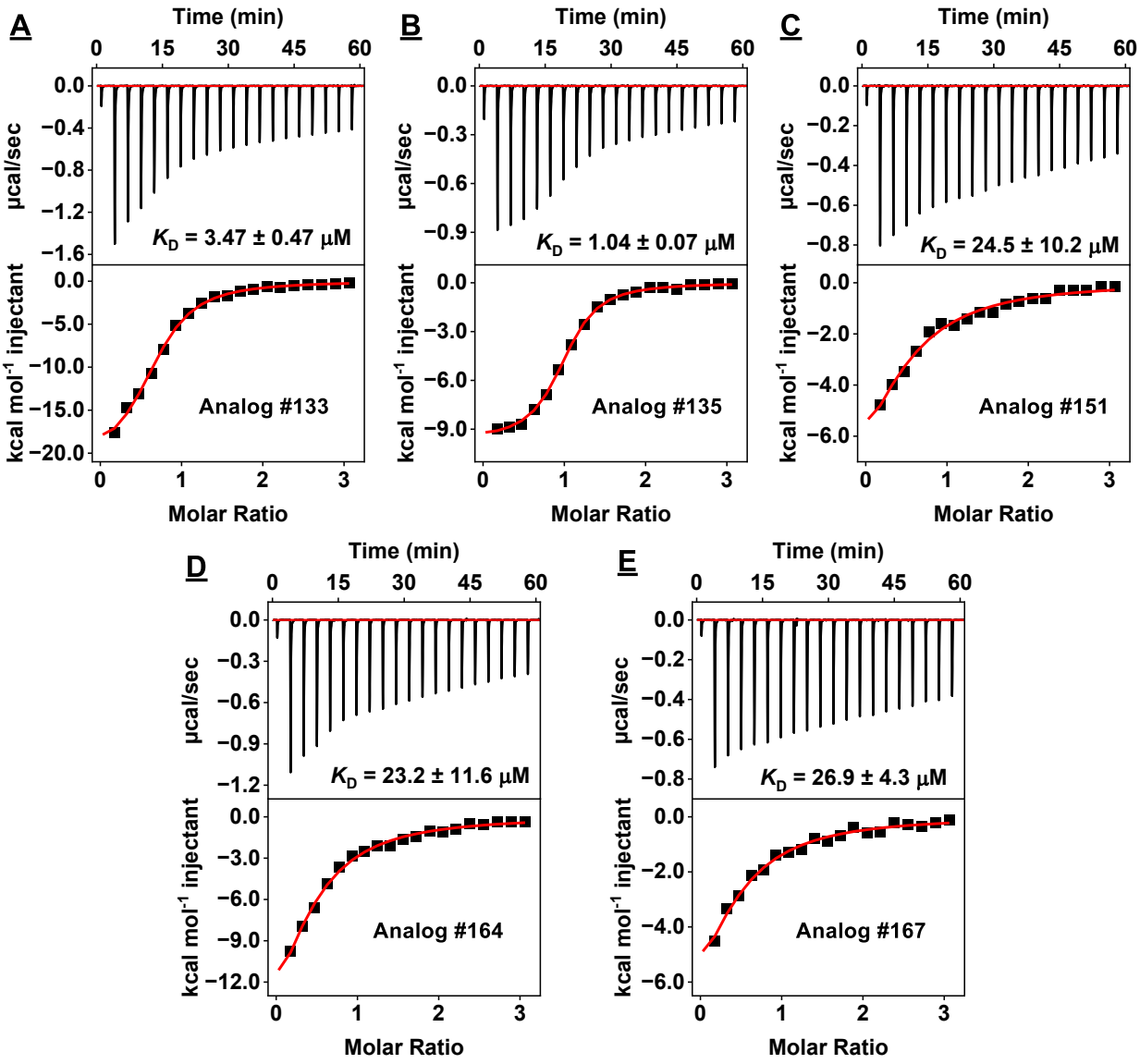

Figure S51. Determining the binding affinity of MF2-mut aptamer to fentanyl analogs using isothermal titration calorimetry (ITC). Top panels display the heat generated from each titration of MF2-mut into (**A**) analog #133, (**B**) analog #135, (**C**) analog #151, (**D**) analog #164, and (**E**) analog #167, respectively. Bottom panels show the integrated heat of each titration after correcting for the heat of dilution of the titrant.

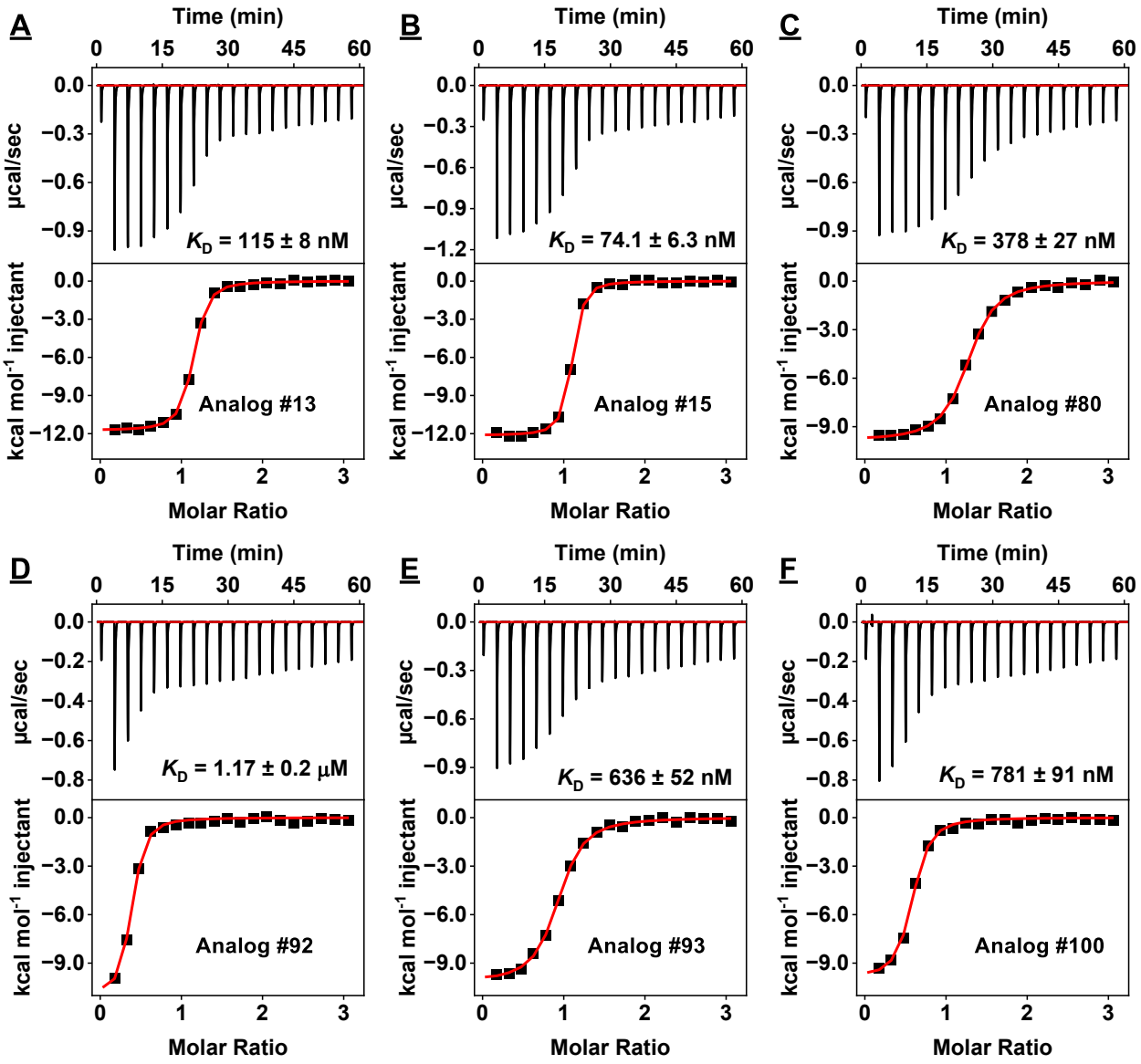

Figure S52. Determining the binding affinity of MF2-mut aptamer to fentanyl analogs using isothermal titration calorimetry (ITC). Top panels display the heat generated from each titration of MF2-mut into (**A**) analog #13, (**B**) analog #15, (**C**) analog #80, (**D**) analog #92, (**E**) analog #93 and (F) analog #100, respectively. Bottom panels show the integrated heat of each titration after correcting for the heat of dilution of the titrant.

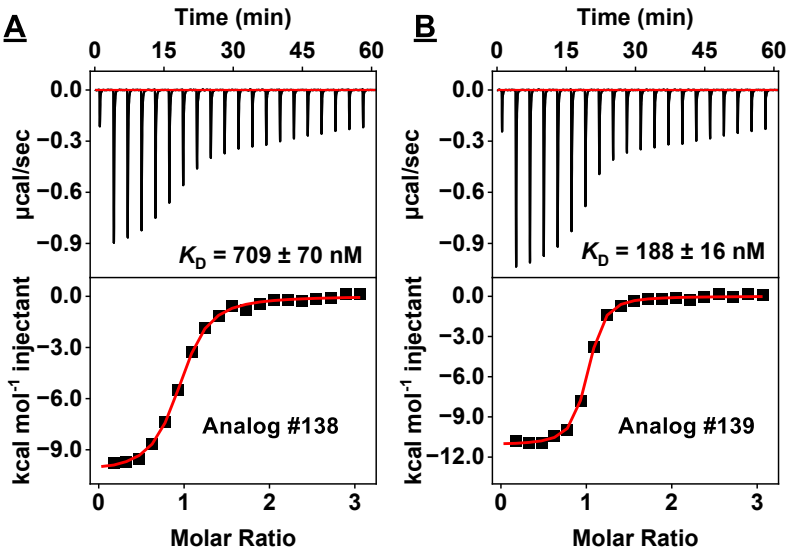

Figure S53. Determining the binding affinity of MF2-mut aptamer to fentanyl analogs using isothermal titration calorimetry (ITC). Top panels display the heat generated from each titration of MF2-mut into (**A**) analog #138 and (**B**) analog #139, respectively. Bottom panels show the integrated heat of each titration after correcting for the heat of dilution of the titrant.

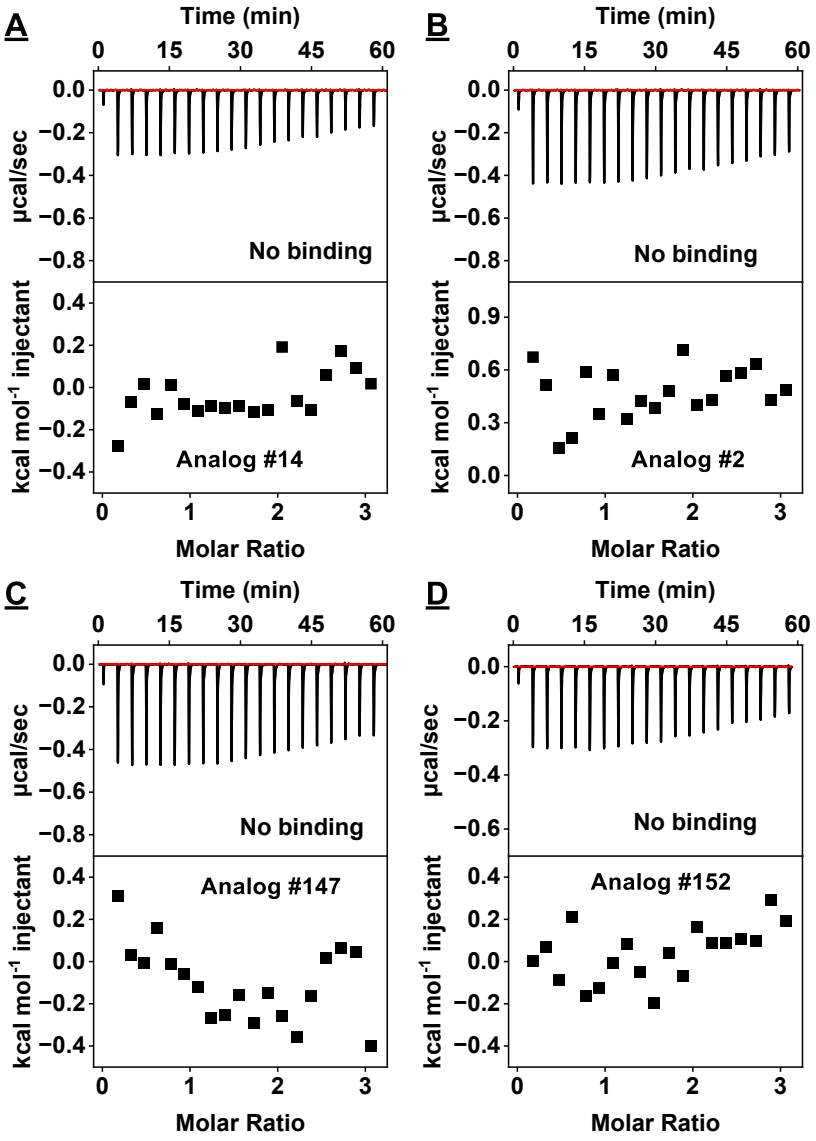

Figure S54. Determining the binding affinity of MF2-mut aptamer to fentanyl analogs using isothermal titration calorimetry (ITC). Top panels display the heat generated from each titration of MF2-mut into (**A**) analog #14 and (**B**) analog #2, (**C**) analog #147, and (**D**) analog #152, respectively. Bottom panels show the integrated heat of each titration after correcting for the heat of dilution of the titrant.